Department of Exploration Geophysics
School of Resource Science & Technology

Effects of Fractures on Seismic Waves in Poroelastic Formations

Miroslav Brajanovski

This thesis is presented as part of the requirements for
the award of the Degree of Doctor of Philosophy
of
Curtin University of Technology

February 2004

Declaration

This thesis contains no material which has been accepted for the award of any other degree or diploma in any university.

To the best of my knowledge and belief this thesis contains no material previously published by any other person except where due acknowledgment has been made.

Signature: _

Date: _

To my parents,
and their parents before them…

Acknowledgements

I would like to sincerely thank my supervisor, Professor Boris Gurevich, for the friendship and inspiration, as well as academic guidance throughout the duration of my PhD study.

I have greatly appreciated collaborating with Michael Schoenberg and thank him for the valuable discussions, useful advice, and his professional help.

I also wish to express my gratitude to Peter Hatherly and acknowledge the financial support provided by the Cooperative Research Centre for Mining Technology and Equipment (CMTE).

I record my appreciation to Gracjan Lambert for his help with numerical modeling (Chapter 6).

Finally, I wish to thank all my friends for their support.

Contents

List of Figures

Abstract

Naturally fractured reservoirs have attracted an increased interest of exploration and production geophysics in recent years. In many instances, natural fractures control the permeability of the reservoir, and hence the ability to find and characterize fractured areas of the reservoir represents a major challenge for seismic investigations. In fractured and porous reservoirs the fluid affects elastic anisotropy of the rock and also causes significant frequency dependent attenuation and dispersion. In this study we develop a mathematical model for seismic wave attenuation and dispersion in a porous medium in a porous medium with aligned fractured, caused by wave induced fluid flow between pores and fractures.

In this work fractures in the porous rock are modelled as very thin and highly porous layers in a porous background. Dry highly porous materials have low elastic moduli; thus dry skeleton of our system contains thin and soft layers, and is described by linear slip theory. The fluid saturated rock with high-porosity layers is described by equations of poroelasticity with periodically varying coefficients. These equations are analyzed using propagator matrix approach commonly used to study effective properties of layered systems. This yields a dispersion equation for a periodically layered saturated porous medium taking into account fluid communication between pore spaces of the layers. Taking in this dispersion equation a limit of small thickness for high-porosity layers gives the velocity and attenuation as a function of frequency and fracture parameters.

The results of this analysis show that porous saturated rock with aligned fractures exhibits significant attenuation and velocity dispersion due to wave induced fluid flow between pores and fractures. At low frequencies the material properties are equal to those obtained by anisotropic Gassmann theory applied to a porous material

with linear-slip interfaces. At high frequencies the results are equivalent to those for fractures with vanishingly small normal slip in a solid (non-porous) background. The characteristic frequency of the attenuation and dispersion depends on the background permeability, fluid viscosity, as well as fracture density and spacing.

The wave induced fluid flow between pores and fractures considered in this work has exactly the same physical nature as so-called squirt flow, which is widely believed to by a major cause of seismic attenuation. Hence, the present model can be viewed as a new model of squirt-flow attenuation, consistent with Biot's theory of poroelasticity.

The theoretical results of this work are also limited by the assumption of periodic distribution of fractures. In reality fractures may be distributed in a random fashion. Sensitivity of our results to the violation of the periodicity assumption was examined numerically using reflectivity modelling for layered poroelastic media. Numerical experiments for a random distribution of fractures of the same thickness still show surprisingly good agreement with theoretical results obtained for periodic fractures. However this agreement may break down if fracture properties are allowed to vary from fracture to fracture.

The results of this thesis show how to compute frequency dependences of attenuation and velocity caused by wave induced fluid flow between pores and fractures. These results can be used to obtain important parameters of fractured reservoirs, such as permeability and fracture weakness, from attenuation measurements. The major requirement for the success of such an approach is that measurements must be made in over a relatively broad frequency range.

1 Introduction

1.1 Natural fractures in rocks

1.1.1 Geological formation of fractures

Naturally fractured reservoirs have attracted an increased interest of exploration and production geophysics in recent years. In many instances, natural fractures control the permeability of the reservoir, and hence the ability to find and characterize fractured areas of the reservoir represents a major challenge for seismic investigations. Natural fractures influence the permeability of the reservoir; therefore the ability to find and characterize fractured areas of the reservoir represents a major challenge for modern seismic investigations.

The formation of natural fractures arises from geological processes of physical deformation or diagenesis, which induce strains exceeding the maximum strength of the rock. Main processes responsible for the formation of fractures are listed by Landes (1959) as: structural deformation arising from folding and faulting, deep and rapid erosion of overburden that allows uplift and expansion of depth pressured rocks, volume reduction caused by dewatering of shales, cooling of igneous rocks, or desiccation in sedimentary rocks, paleokarstification and solution collapse, release of high pore fluid pressure in sedimentary strata and meteorite impacts that cause complex, highly brecciate, fracture systems.

Geologically fractures are classified as tectonic, regional or diagenetic. Tectonic fractures can occur as a result of some local tectonic event, such as faulting or folding processes. Fractures due to faulting normally form as a result of the regional stresses that caused the faulting, not the faulting process itself. On the other hand, fractures

caused by folding, form as a result of the actual folding process, and not the regional stresses. These fractures are the most important type of fractures for petroleum exploration because they are associated with the actual hydrocarbon production.

Regional fractures do not depend on local structures and are initiated by surface forces. They tend to develop over large areas of the earth's crust in an orthogonal pattern. Regional fractures have very little variation in orientation, no offset across the fracture plane, and are always perpendicular to major bedding surfaces. Therefore the presence of regional fractures enables fluid flow.

Diagenetic fractures form due to diagenetic changes in the host rock, including desiccation, syneresis, thermal gradients and mineral phase changes, and are initiated by body forces rather than surface forces.

The stress applied during these geological processes induces strain. Strain is considered to be any change in the original size or shape of the rock caused by the stress applied to the rock. The actual response of a rock to stress is dependent on pressure (depth), temperature, competence and rate of deformation (strain rate). Low levels of stress induce elastic (linear) deformation and the rocks original shape is recovered once the stress is removed. This linear relationship between stress and strain is defined by Hooke's law, but it no longer holds at levels of stress higher than the elastic limit of the rock. Therefore, when stress applied is higher than the elastic limit of the rocks plastic deformation (change in shape or size that is not recovered once the stress is removed) can arise. However, although plastic deformation can decrease the strain above the plastic yield point, most rocks do not undergo a plastic yield phase and once, the external stress exceeds the maximum or rupture strength of the rock, defined by the yield point, the rock will suffer a brittle failure and fracture. Once the rock fractures there is a sudden decrease in the effective stress. If the rock

moves along the fracture, the stress continues to decrease as the rock undergoes brittle deformation. Rocks usually fracture at strains of 10^{-3} to 10^{-4}.

Three dimensional stress fields are resolved in three orthogonal directions, the principal axes of stress, denoted as σ_3, σ_2, σ_1 for maximum, intermediate and minimum normal stress respectively. Along the principal axes of stress, normal stresses are at a maximum while shear stresses are zero. Rocks fail along planes at angles of 45 degrees or less to the axis of maximum stress σ_3. Since σ_3 is usually perpendicular to the earth's surface, most natural fractures are sub-vertical to vertical.

1.1.2 Fracture properties and morphology

The porosity and permeability of rock formations can be of two general types, primary or secondary. Primary porosity and permeability is caused by the open spaces in the rock that existed at its formation. Fracture porosity and permeability is described as secondary as it occurred after the deposition and have no direct relation to the form of the sedimentary particles.

Permeability is the capability of a rock to transmit fluids. Many factors are involved in the relative permeability of rocks. In general, coarser grained sedimentary rocks are more permeable. The permeability of fractures depends on both fracture morphology and the scale of measurement. The presence of uncemented and open fractures increases the secondary permeability, and hence total permeability, of a rock. Fractures held open by partial mineralization can reach apertures over 0.2 mm wide (Aguilera 1998).

Fracture morphology relates to the characteristics of fracture surfaces and fracture fill. Fracture morphology can be described as open, deformed, mineral filled or vuggy (Nelson 2001).

Open fractures are uncemented and have no secondary mineralization or alteration of the original fracture surface. Fracture width is usually very small and fracture porosity is a fraction of a percent. Open fractures increase permeability parallel to the fracture strike but have negligible effect perpendicular to the fracture strike.

Deformed fractures include gouge filled fractures and slickenside fractures. Gouge is a finely abraded material that results from sliding motion along shear fractures in friable rock, which reduces fracture permeability. A slickenslide is a polished fracture surface resulting from frictional sliding along a fault plane, which can increase fracture permeability parallel to the fracture but decrease permeability perpendicular to the fracture. Deformed fractures can cause permeability anisotropy in an otherwise isotropic reservoir.

Mineral filled fractures are filled, or partially filled, with post fracture formation mineralization. Completely filled fractures form impermeable barriers that inhibit fluid flow. Partially filled fractures can increase hydrocarbon recovery because the secondary mineralization holds the fractures open during production.

Vuggy fractures result from acidic water percolating through fractures. Vuggy fractures usually remain open during production and have irregular and rounded shapes that can significantly increase reservoir porosity and permeability.

1.1.3 Fractured reservoirs

Natural fractures are present in most reservoirs, although the degree of fracturing is related to stress, host rock properties, pore fluid composition and pressure, and thermal history. Fracturing affects competent rock, such as cemented sandstones and carbonates, more than incompetent rock, such as shale and evaporates. High quality reservoir rocks are usually competent with high yield points.

The production of hydrocarbon reservoirs depends on the fluid flow within the reservoir. In many cases, the density and orientation of natural fractures controls the permeability of the reservoir. To efficiently deplete fractured reservoirs, the theoretical model to describe the effect of fractures on permeability and reserve distribution needs to be designed.

Natural fractures can have a positive, neutral or negative effect on permeability and fluid flow. The effect of fractures on reservoir productivity depends on the lithology and fabric of the host rock, and the density, orientation and morphology of the fractures. Fracture porosity and permeability are more significant in regions of higher fracture density.

Open fractures increase the permeability and porosity of a reservoir, increasing the volume of interconnecting pores and allowing fluid migration into and within the reservoir. Open fractures significantly increase permeability in the direction parallel to fracture strike. Fractures orientated parallel to the maximum principal normal stress are usually open for uninhibited fluid flow. Vertical fractures can form fluid migration pathways from generating source beds to traps, increasing reservoir charge in the region of fracturing. With increasing compressive stress, the decreasing aperture of fractures oriented perpendicular to the stress axis leads to a decrease in permeability both parallel and perpendicular to the stress. For flow parallel to the maximum horizontal stress direction, this is a consequence of the finite length of the fractures, flow in fractures perpendicular to the stress direction being required to connect fractures oriented parallel to the stress direction (Sayers 1990).

Closed fractures form impermeable barriers that inhibit fluid flow and cause permeability anisotropy. The heterogeneous distribution of charge in anisotropic reservoirs with closed fractures, results in more unproductive wells and limited hydrocarbon

recovery.

Fractures can alternate between open and closed following precipitation of solutions in the fractures, or changes in stress. Open fractures usually close during production unless held open by partial mineralization.

Fractured reservoirs can be classified according to the effect of the fracture system on reservoir quality. Relating the porosity and permeability contributions of the matrix and the fractures, Nelson (2001) describes four types of fractured reservoirs.

I. Fracture system contributes reservoir storage, porosity and permeability.

II. Matrix contributes reservoir storage and porosity. Fracture system contributes required permeability to an otherwise unproductive reservoir.

III. Matrix contributes reservoir storage, porosity and permeability. Fracture system contributes additional permeability to a productive reservoir.

IV. Fracture system forms impermeable barriers, inhibit fluid flow and cause reservoir anisotropy. Fractures contribute no additional porosity or permeability.

Fractures increase reservoir quality in fractured reservoir types I to III, but decrease it in fractured reservoir type IV. In Type I and II reservoirs, reserves are stored in the fractures or require fractures to be recovered from a region of the matrix. A variation in fracture density has big effect on production distribution as a small proportion of wells produce most of the reserves. These reservoirs have more unproductive wells. In Type III & IV reservoirs, reserves are stored in the dominant matrix. A variation in fracture density has little effect on production distribution as most wells produce an equal proportion of the reserves. Type III and IV reservoirs have fewer unproductive wells.

To characterize reservoirs with natural fractures, we require expressions relating the elastic properties of the reservoir rock to the properties of the fractures and fluid. Efficient primary and secondary production depends on detecting fractures and determining their effect on fluid flow and reserve distribution in reservoirs. Unproductive wells are often drilled on the assumption that reserves are homogeneously distributed and controlled only by the matrix. To deplete the inhomogeneous distribution of reserves in fractured reservoirs, the effect of fractures on permeability must be accounted for. The effect of fractures on permeability depends on their density, orientation and fill. If these fracture properties and geometry of fractures can be determined using seismic methods, than thanks to the advanced drilling technology lateral wells can be drilled across open fractures and in areas of high fracture density and permeability.

1.2 Seismic measurements and interpretation

Acoustic and elastic waves are extensively used in the oil and gas industry to image subsurface down to a few kilometers and obtain information about geological structures and sedimentary rocks. Measurement techniques using waves comprise surface seismic, vertical seismic profiling (VSP), cross-well tomography, sonic logging and ultrasonic measurements in laboratory. These techniques use different sources of acoustic waves in different frequency ranges. Waves propagate through the formation (medium, rock) and are detected by the receivers in form of seismograms (traces, waveforms). Objective of all these techniques is to extract information in terms of rock properties from measured seismograms.

Surface seismic method is based on recording reflected waves from the interfaces between layers of different elastic properties (acoustic impedances). Sources are small dynamite explosions (or air-gun explosions in marine seismic) producing waves in

frequency range 10-100 Hz. From the arrival times of reflected waves velocities of layers and depth of interfaces are extracted. Also amplitudes of signals as a function of offset (distance between source and receiver) are used in data processing. Basic assumption of these methods is that given geological formation corresponds to a given signature in seismogram, so lithology information of sedimentary rocks can be obtained doing inversion of measured data.

VSP method is used in areas with boreholes, in which receivers are placed while sources remain on the surface. This allows higher frequencies of signals, up to 400 Hz. Putting sources and receivers in boreholes allows cross-hole measurements up to the frequency of 1 kHz and the use of inversion technique called tomography. Resolution depends on frequency and is of order of 1 m for cross-hole methods and 20 m for surface seismic.

Finally, sonic (2-100 kHz) and ultrasonic (up to 10 MHz) borehole logging techniques allow to investigate reservoir with much higher resolution down to the pore scale. These techniques also have the smallest depth of investigations, and therefore can only be used in boreholes in the method known as sonic logging. This method is based on measured refracted waves propagating along the boreholes. This method is used to estimate porosity, and differentiate different formations.

Classical processing and interpretation of measurements using all these methods which cover a wide range of frequencies, traditionally were mostly applied to delineate rock interfaces to evaluate structures that might contain hydrocarbons. These methods did not take into account frequency dependent phenomena such as dispersion, assuming that all geological formations can be represented by a linear elastic solid. Word 'elastic' means that portion of medium deformed by an external force will completely return to its undeformed state after force was removed. This process of

deformation is reversible. 'Linear' means that relation between stress and strain is linear. It is known that linear elastic continuum is non-dispersive (velocity of waves does not depend on frequency). Effects of wave induced fluid flow were neglected. These methods are effective in imaging interfaces and faults on large scale, but relatively little use has been made of seismic waves for the determination of rock properties (such as permeability) directly from seismic waves, or for the direct detection of hydrocarbons.

In last two decades the oil industry have realized that major problem in reservoir evaluation and production is high complexity of many reservoirs. This complexity is related to the significant spatial heterogeneity of porosity, permeability, fracture density etc. Need to gain more knowledge of such complex reservoirs causes a shift in the use of acoustic signals and wide use of rock physics to relate seismic observations to rock properties. Since seismic waves respond to permeability, fracture density, orientation and fluid fill, they have the potential to characterize fractured reservoirs. So far mainly empirical relations between travel time and amplitude of seismic signals related to various rock properties have been used in interpretation. To better understand the influence of rock properties on recorded signals we are not only interested in travel times and amplitude variations but also in the attenuation caused by saturating fluids and frequency dependent response of medium to waves.

Prediction of the response of fractured reservoirs to seismic waves requires expressions relating the elastic properties of such reservoirs to to the properties of the background rock, parameters of fractures, and fluid properties. Such expressions are known for the case when the background (unfractured) rock is elastic. However when the background rock is itself porous and contains fluids, these expressions cannot be used as they would ignore the fluid flow between pores and fractures. Derivation of such expressions for porous media with aligned fractures is the main topic of this thesis.

Classical theory of seismic waves is based ont he theory of elasticity developed for continuous elastic solids. Reservoir rocks are porous media saturated with fluids, and thus require some modifications to the theory. The porous medium used as a model for rocks in this work is a composite containing two interconnected phases: solid matrix (skeleton) and saturating fluid. The dry skeleton of the rock is formed from grains that are in mutual elastic contact (consolidated grains). The dry skeleton as a whole is elastic. Saturating fluid is assumed to be a viscous and compressible fluid and can flow through voids between grains (pores) or micro flow ducts. Microscopic heterogeneity of such a medium causes very complex macroscopic behavior that is sensitive to variations of skeleton structure (micro cracks) or fluid content.

Norris (1993) illustrated the complexity of the problem by the different characteristic lengths associated with wave propagation in a saturated porous medium. The characteristic length associated with the wave itself is a wavelength ranging from 1 cm to 100 m. For a typical water saturated sandstone at frequency 100 Hz, the wavelength is 30 m. The characteristic length associated with the skeleton is average pore radius, which for the given example is 6×10^{-7} m, or average width of the flow channels. In a fractured formation the important length is average fracture distance (spacing) and thickness. The lengths associated with viscosity and fluid flow related to channels and fractures are frequency dependent skin depth and diffusion length, which for the given example, are 5×10^{-5} m and 6×10^{-2} m respectively. The frequency at which skin depth is equal to average pore radius is called the "Biot's critical frequency". Fluid flow has different character for frequencies higher and lower than this critical frequency. For frequencies lower than the critical frequency, fluid flow can be approximated to be laminar. In this case the constitutive relation connects only fluid

pressure and loading stress with displacements of the solid and fluid, and does not contain any time dependency in explicit form. In this work all considered frequencies will be assumed to be lower than Biot's critical frequency.

Many works have been already done on general problems of wave propagation in porous homogeneous and inhomogeneous media. The effect of a saturating fluid on the elastic properties of a porous rock is described by the Gassmann (1951) equation. An assumption of the Gassmann equation is that the dry and saturated porous rocks are statistically isotropic and pore pressure of the fluid is constant, which means that this is a quasi-static or low frequency approximation. Gassmann equation gives saturated elastic moduli as an explicit function of measurable quantities, which are the moduli of dry skeleton, grain material and fluid, and porosity.

Kosten and Zwikker (1941) were the first to obtain a complete set of equations describing wave propagation including simultaneous average fluid and solid motions of a porous material. They postulated that for each phase (solid and fluid), the average time rate of momentum is equal to sum of the average pressure gradients, and frictional (dissipative) force caused by viscous fluid motion is proportional to the relative velocity between solid part and fluid. Frenkel (1944) provided more detailed analysis of the stress-strain (constitutive) relation in terms of divergence of stress (symmetric tensor), rather than gradient of pressure (tensor with zeros out of diagonal), to allow for shear (transverse) waves. In addition, all of these theories predicted the existence of two types of dilatational (longitudinal) waves, one controlled mainly by the compressibility of the skeleton (this wave corresponds to the usual P wave in seismology and is called the "fast wave"), and the other controlled mainly by the fluid and is called the "slow wave".

Biot (1956a,b, 1962) developed a similar set of coupled equations, and thanks to

his comprehensive analysis as well as the many papers he authored on this topic, the entire subject of porous-media acoustics become known as a "Biot theory". Biot derived wave equations in statistically isotropic and homogeneous porous medium by postulating the validity of Euler-Lagrange equation and taking average solid and fluid (relative to the solid) displacements as generalized coordinates. Approximating small displacements due to the wave (adiabatic approximation), kinetic energy and strain free energy were taken to be quadratic functions of these generalized coordinates, as well as dissipative potential. Biot noted that, for the fast wave compression of skeleton and fluid occur in phase, while for the slow wave they occur out of phase.

Since Biot modelled porous a rocks as a homogeneous medium, Biot theory underestimates attenuation and dispersion of elastic waves in real rocks, especially those with thin cracks or fractures. Real reservoir rocks are spatially very heterogeneous at different scales. For example a typical reservoir may be composed of horizontal sedimentary layers with vertical fractures of different properties. Inhomogeneities in fluid saturated rocks change overall fluid flow and permeability, and cause additional attenuation of elastic waves, which is the central topic of this work.

Many mechanisms have been have been proposed to exaplain attenuation of elastic waves in rocks. The mechanism which is believed to be most significant in heterogeneous porous formations is the so called "squirt-flow" mechanism associated with fluid flow across the interfaces between inhomogeteities (Mavko and Nur, 1975; Jones, 1986; Murphy et al., 1986). The squirt-flow mechanism arises from the incident wave inducing gradients of fluid pore pressure across the interfaces between regions of different poroelastic properties. On the other hand, these disturbances of pressure cause fluid flow from more compliant regions to stiffer regions. This meachanism has been studied in detail for layered porous media when significant attenuation arises due to fluid flow from more complaint into less compliant layers (White et al., 1975; Nor-

ris, 1993; Gurevich and Lopatnikov, 1995; Gelinsky et al., 1998; Shapiro and Müller, 1999).

In particular when a reservoir is permeated by a regular system of open fractures, an elastic wave propagating in this reservoir will deform the fractures more than the outside formation. Thus the fluid will squeese from more compliant fractures into the less compliant pores of the surrounding rock and vice versa. Such a wave induced flow of the viscous pore fluid will in turn cause energy dissipation, resulting in attenuation and dispersion of the propagating wave.

The objective of this study is to develop a mathematical model for the "squirt-flow" mechanism of seismic wave attenuation and dispersion in a porous medium caused by the presence of aligned fractures.

1.4 Methodology

Analysis of wave propagation in porous fractured media can be developed by generalizing the theory of wave propagation in elastic fractured media. Wave propagation in an elastic medium containing aligned fractures have been anaysed by several approaches. Two approaches most widely used in seismic are the penny-shaped crack model and the linear slip model.

In penny-shaped crack model, fractures are modelled as isolated strongly oblate spheroids (Hudson 1981 , Nishizawa 1982). The radii and the distances between adjacent fractures are assumed to be small compared to the wavelength, and the interaction between fractures is usually neglected. Hudson's theory predicts elastic anisotropy due to the presence of fluid-filled or empty cracks.

In the linear slip model fractures are considered as imperfectly bonded interfaces

inside the rock, that is surfaces across which the displacement is not necessarily continuous (Schoenberg, 1980; Schoenberg and Douma, 1988). The word "linear" means that at the interface between background and fracture, displacement is discontinuous but linearly related to the traction. The linear slip model is valid for wavelength much larger than fracture spacing. Linear slip interface arises, for instance, as the limit of a thin infinite parallel plane, highly compliant, soft layer embedded in a solid matreial. In this theory the effect of fractures on elastic properties of a material is described through only two effective parameters called normal and tangential excess compliances.

The models developed for elastic media with fractures are not directly applicable to fluid-saturated porous rocks, since they are not elastic materials. Instead we will model fractures in porous rocks as thin layers with high porosity. Dry highly porous materials have low elastic moduli; thus dry skeleton of our system will contain thin and soft layers, and could be described by linear slip theory. The fluid saturated rock with high-porosity layers can be described by equations of poroelasticity with periodically varying coefficients. These equations can be analyzed using propagator matrix approach commonly used to study effective properties of layered systems. This will lead to a dispersion equation for a periodically layered saturated porous medium taking into account fluid communication between pore spaces of the layers. Taking in this dispersion equation a limit of small thickness for high-porosity layers will give the velocity and attenuation as a function of frequency and fracture parameters.

1.5 Thesis organization

The structure of the thesis is as follows. In Chapter 2 we review some basic elastodynamic equations and physical laws for elastic and poroelastic materials. In Chapter 3

a layered periodic poroelastic medium is analyzed using propagator matrix approach. Eigenvalue representation for propagator matrix gives expressions for effective compressional velocity modulus for periodic poroelastic medium. Chapter 4 we derive an asymptotic model for saturated rocks with fractures represented as a limiting case of thin highly porous layers. Frequency dependent attenuation and velocity dispersion are analyzed for different fracture permeability and fracture weakness. In Chapter 5 expressions for low and high frequency limiting moduli for a poroelastic fractured medium are derived. We show the equivalence between low frequency modulus derived from iso-stress condition and from frequency dependent expression of Chapter 4. Comparison of the theoretical results with numerical simulations obtained using reflectivity algorithm is presented in Chapter 6. The conclusions and recommendations based on this research are given in Chapter 7.

2 Elements of elasticity and poroelasticity

2.1 Fundamental equations of theory of elasticity

2.1.1 Strain and stress

A poroelastic medium is assumed to be a composite of two interconnected phases: the solid elastic skeleton, and the viscous fluid which fills the pores of the skeleton. In this chapter the elastic solid and fluid are initially considered separately; then the results are integrated in an analysis of the porous composite as a whole.

Mechanics of both solid bodies and fluids regard these substances as continuous media described using principles of continuum physics. The smallest possible elementary volume (EV) of such a medium taken to represent such a continuous medium is assumed to be much larger than intermolecular distance. Since theory of elasticity is considered on a macroscopic scale, this intermolecular distance can be regarded as infinitely short.

When a force or stress is applied to a elastic body, it induces deformation or strain (a change of shape and volume) in the body. This deformation can be described by the displacement of a point in the body $\mathbf{u} = \mathbf{r}' - \mathbf{r}$, which is defined as the difference in position vectors of that point before $\mathbf{r}$ and after $\mathbf{r}'$ the force was applied. Displacement is a vector field quantity and in general is a function of position and time. A more comprehensive mathematical description of the deformation is given by the change in squared distance due to the deformation between two adjacent points in the continuum (Landau and Lifshitz, 1986). The squared distance is used because it is scalar quantity representing the metrics of vector space, and is invariant with respect to the choice of the coordinate system. Using index summation conventions,

the squared distance between two neighboring points before dl and after dl' stress induced deformation is given in an orthogonal Cartesian reference system $\{x_i\}$ by

$$dl^2 = dx_i^2,\ dl'^2 = dx_i'^2 = (dx_i + du_i)^2. \tag{1}$$

Substituting the total differential of displacement $du_i = (\partial u_i/\partial x_k)dx_k$ into (1) gives

$$dl'^2 = dl^2 + 2\frac{\partial u_i}{\partial x_k}dx_i dx_k + \frac{\partial u_i}{\partial x_k}\frac{\partial u_i}{\partial x_m}dx_k dx_m. \tag{2}$$

The second term on the RHS of (2) can be written in symmetrical form because summation is taken over both indices i and k. The indices i and m in the third term can also be interchanged because summation is taken over all indices . This gives

$$dl'^2 = dl^2 + \left(\frac{\partial u_i}{\partial x_k} + \frac{\partial u_k}{\partial x_i} + \frac{\partial u_m}{\partial x_k}\frac{\partial u_m}{\partial x_i}\right)dx_i dx_k = dl^2 + 2\varepsilon_{ik}dx_i dx_k, \tag{3}$$

where the factor

$$\varepsilon_{ik} = \frac{1}{2}\left(\frac{\partial u_i}{\partial x_k} + \frac{\partial u_k}{\partial x_i} + \frac{\partial u_m}{\partial x_k}\frac{\partial u_m}{\partial x_i}\right) \tag{4}$$

is called the strain tensor. Since the strain tensor is symmetrical, it has real eigenvalues and orthogonal eigenvectors (principal axes). If the strain tensor is diagonalized in the vicinity of some reference point, equation (3) can be rewritten as

$$dl'^2 = (\delta_{ik} + 2\varepsilon_{ik})\, dx_i dx_k = \sum_{i=1}^{3}\left(1 + 2\varepsilon^{(i)}\right)dx_i^2,$$

where $\varepsilon^{(i)}$ are the principal values of strain and δ_{ik} is Kronecker's symbol. There are three independent strains in the corresponding principal directions in the sum. Then $dx_i' = \sqrt{(1 + 2\varepsilon^{(i)})}dx_i$, and the relative extension in principal direction $(dx_i' - dx_i)/dx_i$ is equal to $\sqrt{(1 + 2\varepsilon^{(i)})} - 1$.

The elastic waves used in seismic exploration cause small displacements, and consequently small strains. The quadratic term in the expression for the strain tensor (4) is a second order term in displacement and can be neglected in comparison with other two terms, reducing the strain tensor to

$$\varepsilon_{ik} = \frac{1}{2}\left(\frac{\partial u_i}{\partial x_k} + \frac{\partial u_k}{\partial x_i}\right). \tag{5}$$

For small displacements, $\sqrt{(1+2\varepsilon^{(i)})} - 1 \approx \varepsilon^{(i)}$, therefore the volume of the body after deformation can be approximated as $dV' = dV \sum\limits_{i=1}^{3}\left(1+\varepsilon^{(i)}\right)$. Neglecting higher order terms, the sum of the diagonal components of strain tensor $\mathrm{tr}\,\boldsymbol{\varepsilon}$ is equal to the relative volume change of the body,

$$\varepsilon_{ii} = \mathrm{tr}\,\boldsymbol{\varepsilon} = \frac{dV' - dV}{dV},$$

which is one of the invariants of the strain tensor.

When a stress induced deformation occurs, the body is no longer in a state equilibrium because of the change in shape and volume. The new arrangement of molecules in the body results in internal forces, which try to restore the body to the original state of equilibrium. Molecular forces have a very short range of action, of the same order of magnitude as distance between the molecules. Therefore, for any chosen EV of volume V surrounded by the surface S, the forces inside EV cancel according to Newton's third law, and the forces exerted on it by surrounding parts act only on the surface of EV. The three volumetric components of the resultant of all internal forces can be written as the divergence of some tensor σ_{ik} which is called the stress tensor

$$f_i = \frac{\partial}{\partial x_k}\sigma_{ik}, \tag{6}$$

or in vector form as

$$\mathbf{f} = \operatorname{div} \boldsymbol{\sigma} = \boldsymbol{\nabla}\boldsymbol{\sigma}.$$

The volume integral representing the resultant of body forces in EV can be transformed into an integral over its closed surface using Gauss's formula,

$$\int\limits_V f_i dV = \int\limits_V \frac{\partial}{\partial x_k}\sigma_{ik} dV = \oint\limits_S \sigma_{ik} n_k dS,$$

where n_k is a component of unity vector orthogonal to the infinitesimal surface dS oriented in the outward direction. A positive sign for the force $\sigma_{ik} n_k dS$ corresponds to the situation where force is exerted on EV from surrounding parts, i.e. from the outside, while a negative sign describes internal forces of EV acting on the surface.

The angular momentum of the force $\mathbf{f} \times \mathbf{r}$ exerted on EV forms an antisymmetric stress tensor of rank two. The resultant angular momentum of the whole EV is

$$M_{ik} = \int\limits_V \left(f_i x_k - f_k x_i\right) dV \ .$$

Substituting f_i from equation (6) for angular momentum we get

$$M_{ik} = \int\limits_V \left(\frac{\partial \sigma_{im}}{\partial x_m} x_k - \frac{\partial \sigma_{km}}{\partial x_m} x_i\right) dV \ ,$$

or

$$M_{ik} = \int\limits_V \left[\frac{\partial}{\partial x_m}\left(\sigma_{im} x_k\right) - \frac{\partial}{\partial x_m}\left(\sigma_{km} x_i\right)\right] dV - \int\limits_V \left(\sigma_{im}\frac{\partial x_k}{\partial x_m} - \sigma_{km}\frac{\partial x_i}{\partial x_m}\right) dV \ .$$

The first volume integral on the right transforms into the surface integral because it is divergency of some tensor, so that

$$M_{ik} = \oint_S (\sigma_{im} x_k - \sigma_{km} x_i)\, n_m dS - \int_V \left(\sigma_{im} \frac{\partial x_k}{\partial x_m} - \sigma_{km} \frac{\partial x_i}{\partial x_m} \right) dV.$$

or, using orthogonality of Cartesian coordinates $\partial x_k / \partial x_m = \delta_{km}$,

$$M_{ik} = \oint_S (\sigma_{im} x_k - \sigma_{km} x_i)\, n_m dS - \int_V (\sigma_{ik} - \sigma_{ki})\, dV.$$

In order for tensor M_{ik} to be an integral over surface alone, the second term representing angular momentum of forces f_i must be zero. This means that the stress tensor is symmetric.

2.1.2 Thermodynamical potentials

There are two types of relationships that describe the state of a medium, thermodynamical and constitutive, which are in direct connection with one another. If EV is deformed in such a way that displacement u_i changes by a small amount δu_i, then the total work done by the volume and surface forces applied on EV is

$$\delta R = \int_V f_i \delta u_i dV + \oint_S t_i \delta u_i dS, \tag{7}$$

where $t_i = \sigma_{ki} n_k$ is traction acting on elementary surface dS. Substituting traction into (7), and transforming the surface integral into a volume integral, gives

$$\delta R = \int_V \left[f_i \delta u_i + \frac{\partial}{\partial x_k} (\sigma_{ki} \delta u_i) \right] dV$$

or

$$\delta R = \int_V \left(f_i + \frac{\partial}{\partial x_k} \sigma_{ki} \right) \delta u_i dV + \int_V \sigma_{ki} \frac{\partial}{\partial x_k} \delta u_i dV. \tag{8}$$

To satisfy the condition of equilibrium (sum of surface and volume forces is zero), the first integral on the RHS of (8) must equal zero. Since the stress tensor is symmetric, the second integral becomes

$$\sigma_{ki}\frac{\partial}{\partial x_k}\delta u_i = \sigma_{ik}\frac{1}{2}\delta\left(\frac{\partial u_i}{\partial x_k} + \frac{\partial u_k}{\partial x_i}\right) = \sigma_{ik}\delta\varepsilon_{ik},$$

and the work done by internal stresses per unit volume is

$$\delta R = -\sigma_{ik}\delta\varepsilon_{ik}.$$

The first and second laws of thermodynamics yield expressions for internal energy, equal to the difference between the heat δQ acquired by the unit volume and work δR done by internal stresses,

$$dU = \delta Q - \delta R = TdS + \sigma_{ik}d\varepsilon_{ik},$$

where S is entropy and T is temperature. Quantities δQ and δR are not total differentials because their integrals depend on the path of integration in the space of thermodynamical parameters, while dU and dS are total differentials whose integrals depend only on the initial and final states. Entropy and strain components uniquely and completely describe internal energy. However entropy cannot be directly measured, therefore to convert from entropy to temperature, a thermodynamical potential called free energy is introduced by the tranformation $F = U - TS$. In differential form free energy is written as

$$dF = -SdT + \sigma_{ik}d\varepsilon_{ik}.$$

To describe the pure mechanical effect of deformation, it is useful to work with the strain-energy potential W (Aki and Richards, 1980), which is a function only of strain,

$$dW = \sigma_{ik}d\varepsilon_{ik}, \tag{9}$$

so that the stress tensor can be written as

$$\sigma_{ik} = \frac{\partial W}{\partial \varepsilon_{ik}}. \tag{10}$$

Internal heat generation generally comes from either heat sources within the Earth (e.g. radioactive materials) or energy conversion caused by frictional forces. However, in two common situations the heat transport contribution to the rate of change of internal energy can be neglected relative to deformation.

1) Quasi-static processes i.e. if the time scale of deformation is sufficiently long, heat will flow in order to equalize temperature and conditions will be isothermal. Such is the case for static deformation in the laboratory or in the long term deformation of Earth materials. In this case, free energy is used as the strain-energy potential W to define stress as an isothermal derivative of free energy over strain

$$\sigma_{ik} = \left(\frac{\partial F}{\partial \varepsilon_{ik}}\right)_T. \tag{11}$$

Traditionally, isothermal processes were used to define the elastic moduli in theory of elasticity.

2) Fast dynamic processes i.e. if the time scale of deformation is short enough, the thermal state has no time to adjust to the disturbance and the effect is comparable to thermal isolation. This is an adiabatic or isentropic state, appropriate for elastic wave propagation. In this case, internal energy is used as the strain-energy potential W to define stress as an adiabatic derivative of internal energy over strain

$$\sigma_{ik} = \left(\frac{\partial U}{\partial \varepsilon_{ik}}\right)_S. \tag{12}$$

Since the form of the internal energy function is different in these two cases, the mechanical response to deformation will also be different. For intermediate time-

scales, the roles of the deformation and thermal behavior are closely linked and need to be treated with continuum thermodynamics.

For any particular isotropic medium, we need to know how free energy depends on strain. Assuming small deformations of EV and isothermal processes, free energy can be expanded in a power series up to terms of second order in strain. Initial conditions are taken as no-strain no-stress conditions, which means that the linear term in the expansion of free energy is absent, see equation (11). Since free energy is a scalar, its lowest order term in strain must be a linear combination of the two quadratic scalar invariants of strain tensor: the squared sum of diagonal elements and the sum of squares of all components

$$F = F_0 + \frac{1}{2}\lambda(\varepsilon_{ii})^2 + \mu\varepsilon_{ik}^2. \tag{13}$$

In equation (13), F_0 is free energy of the undeformed body, and λ and μ are so called Lamé coefficients**.** The free energy of the undeformed body is not associated with any deformational processes, and therefore requires no further consideration. Since ε_{ii} is relative volume change, strain can be expressed as the sum of pure shear (constant volume, change in shape) and pure volumetric strain (change in volume, constant shape), to give a more physically intuitive expansion of the free energy

$$\varepsilon_{ik} = \left(\varepsilon_{ik} - \frac{1}{3}\delta_{ik}\varepsilon_{mm}\right) + \frac{1}{3}\delta_{ik}\varepsilon_{mm}. \tag{14}$$

Substituting the terms from equation (14) into the second order term of the expansion of free energy (13) gives (Landau and Lifshitz, 1986)

$$F = \mu\left(\varepsilon_{ik} - \frac{1}{3}\delta_{ik}\varepsilon_{mm}\right)^2 + \frac{1}{2}K\varepsilon_{mm}^2, \tag{15}$$

where K is bulk modulus or incompressibility, and μ is shear modulus. The relation-

ship between the bulk modulus and Lamé coefficients can be derived by comparing equations (13) and (15),

$$K = \lambda + \frac{2}{3}\mu. \tag{16}$$

The total differential of free energy (15) for a constant temperature is

$$\begin{aligned} dF &= 2\mu\left(\varepsilon_{ik} - \frac{1}{3}\delta_{ik}\varepsilon_{mm}\right) d\left(\varepsilon_{ik} - \frac{1}{3}\delta_{ik}\varepsilon_{mm}\right) + K\varepsilon_{mm}d\varepsilon_{mm} \\ &= \left[K\varepsilon_{mm}\delta_{ik} + 2\mu\left(\varepsilon_{ik} - \frac{1}{3}\delta_{ik}\varepsilon_{mm}\right)\right] d\varepsilon_{ik}. \end{aligned}$$

Substituting the above equation into the stress relationship for isothermal processes (11) yields stress as a function of strain

$$\sigma_{ik} = K\varepsilon_{mm}\delta_{ik} + 2\mu\left(\varepsilon_{ik} - \frac{1}{3}\delta_{ik}\varepsilon_{mm}\right). \tag{17}$$

Equation (17) is known as Hooke's law, and is the linear constitutive relation for an isotropic elastic body for small deformations.

Free energy is so-called homogeneous function of second order in strain so that

$$\varepsilon_{ik}F'(\varepsilon_{ik}) = 2F,$$

where F' is the first derivative of free energy with respect to strain. Then from equation (11),

$$F = \frac{1}{2}\sigma_{ik}\varepsilon_{ik}.$$

From the symmetry of this relation with respect to stress and strain, and from the fact that strain is a linear superposition of the components of stress from Hooke's law, it can be shown that the following important relation is also valid,

$$\varepsilon_{ik} = \left(\frac{\partial F}{\partial \sigma_{ik}}\right)_T .$$

Hooke's law (17) defines stress strain relation for isothermal processes. As mentioned earlier, elastic waves at seismic frequencies can be considered adiabatic processes. Bulk modulus K is one of the so-called response functions of a thermomechanical system, which describes how the system responds to a change of parameters of state. Bulk modulus K in particular describes the change of volume V due to applied stress. The three other response functions introduced here are adiabatic bulk modulus K_{ad}, coefficient of thermal expansion for constant pressure α_p, and specific heat for constant pressure C_p. In general they are defined as

$$\frac{1}{K} = -\frac{1}{V}\left(\frac{\partial V}{\partial p}\right)_T , \ \frac{1}{K_{ad}} = -\frac{1}{V}\left(\frac{\partial V}{\partial p}\right)_S , \ \alpha_p = \frac{1}{V}\left(\frac{\partial V}{\partial T}\right)_p , \ C_p = \left(\frac{\partial Q}{\partial T}\right)_p , \quad (18)$$

where p = -σ_{ii} is pressure. The relationship between adiabatic and isothermal bulk moduli is

$$\frac{1}{K_{ad}} = \frac{1}{K} - \frac{TV\alpha_p^2}{C_p}.$$

The adiabatic and isothermal shear moduli are equivalent because pure shear strain does not result in any change of volume.

Deformation of EV due to elastic wave propagation causes oscillations of temperature inside the EV. However, this heat diffusion is a very slow process (thermal conductivity of the medium is assumed to be very small) in comparison to the period of the wave. Therefore the EV can be considered as an isolated thermodynamical reservoir over the time of one period i.e. the process is adiabatic. In this case, equation (12) is used to define stress and the adiabatic bulk modulus is used for the volumetric elastic

response of the medium.

2.1.3 Constitutive relations and equation of motion

For solid elastic bodies considered as crystals with certain symmetry, isothermal free energy of deformation (13) can be written in general form as

$$F = \frac{1}{2} c_{ikjl} \varepsilon_{ik} \varepsilon_{jl}. \tag{19}$$

Hook's law (17) can then be written in its most general form:

$$\sigma_{ik} = c_{ikjl} \varepsilon_{jl}, \tag{20}$$

where c_{ikjl} is called the elastic stiffness tensor, a fourth rank tensor with a total of 81components. However, the symmetry of strain and stress tensor implies that $c_{ikjl} = c_{iklj} = c_{kijl} = c_{kilj}$, and therefore only 36 of these components are actually independent. Since the free energy is scalar and a quadratic function of strain, and strain itself is symmetric, the additional symmetry constraint $c_{ikjl} = c_{jlik}$ further reduces the number of independent components to 21. This is the largest number of elastic stiffness components that is required to fully describe the most general form of the elastic tensor. Due to these constraints, Hooke's law can be rewritten in condensed notation as a second order symmetric Voigt matrix. Stress and strain tensors of rank two are reduced to 6×1 matrices of by the following rule

$$\sigma_{ik} \rightarrow \sigma_n, \ \varepsilon_{ik} \rightarrow \varepsilon_n,$$

where $n = i$ if $i = k$, and $n = 9 - (i + k)$ if $i \neq k$. Similarly, the stiffness tensor of rank four is transformed to a 6×6 matrix by the rule applied to pairs of indices

$$c_{ikjl} \rightarrow c_{nm},$$

where for sets of indices i, k, n and j, l, m the same rule is applied. In matrix form Hooke's law can then be written as

$$\begin{bmatrix} \sigma_1 \\ \sigma_2 \\ \sigma_3 \\ \sigma_4 \\ \sigma_5 \\ \sigma_6 \end{bmatrix} = \begin{bmatrix} c_{11} & c_{12} & c_{13} & c_{14} & c_{15} & c_{16} \\ c_{21} & c_{22} & c_{23} & c_{24} & c_{25} & c_{26} \\ c_{31} & c_{32} & c_{33} & c_{34} & c_{35} & c_{36} \\ c_{41} & c_{42} & c_{43} & c_{44} & c_{45} & c_{46} \\ c_{51} & c_{52} & c_{53} & c_{54} & c_{55} & c_{56} \\ c_{61} & c_{62} & c_{63} & c_{64} & c_{65} & c_{66} \end{bmatrix} \begin{bmatrix} \varepsilon_1 \\ \varepsilon_2 \\ \varepsilon_3 \\ 2\varepsilon_4 \\ 2\varepsilon_5 \\ 2\varepsilon_6 \end{bmatrix}. \tag{21}$$

The above stiffness matrix is symmetrical about the main diagonal, so that $c_{ik} = c_{ki}$. The number of 21 independent constants can be reduced even further if the medium exhibits some symmetry properties.

The most simple case is an isotropic body, which is fully described by only 2 constants, namely Lamé coefficients λ and μ. In this case, $c_{11} = c_{22} = c_{33} = \lambda + 2\mu$, $c_{12} = c_{13} = c_{23} = \lambda$, and $c_{44} = c_{55} = c_{66} = \mu$. All other elements of the stiffness matrix are zero.

The other particular case of symmetry considered throughout this work is so-called transverse isotropy (TI). An example of a medium with this type of symmetry is a finely layered or a medium with rotationally invariant parallel fractures with an axis of symmetry normal to the layering or fractures. For wavelengths much larger than layer thickness or fracture spacing, such a medium can be considered as an effective medium with TI symmetry. Five independent coefficients are required in order to fully

describe such a medium. If x_3 is the axis of symmetry, the elastic stiffness matrix of a TI medium can be written in the form

$$c_{ik} = \begin{bmatrix} c_{11} & c_{11}-2c_{66} & c_{13} & 0 & 0 & 0 \\ c_{11}-2c_{66} & c_{11} & c_{13} & 0 & 0 & 0 \\ c_{13} & c_{13} & c_{33} & 0 & 0 & 0 \\ 0 & 0 & 0 & c_{44} & 0 & 0 \\ 0 & 0 & 0 & 0 & c_{44} & 0 \\ 0 & 0 & 0 & 0 & 0 & c_{66} \end{bmatrix}. \tag{22}$$

From the expression for free energy (19), which is always positive, the elements of the stiffness matrix are additionally constrained according to

$$c_{66} > 0,\ c_{44} > 0,\ c_{33} > 0,\ \text{and}\ c_{33}(c_{11}-c_{66}) > c_{13}^2.$$

For the isotropic case, this yields

$$\mu > 0,\ \lambda + 2\mu > 0,\ (\lambda+2\mu)(\lambda+\mu) > \lambda^2,\ \lambda + \frac{2}{3}\mu \equiv K > 0.$$

The fact that the bulk modulus is always positive is consistent with our day to day experience, that is that when outside pressure $-dp > 0$ is applied to a body, its volume is reduced.

In a porous medium saturated with a viscous liquid or gas, all phases are interconnected, with the pores of the elastic solid serving as channel ducts for moving fluid. In order to describe the moving viscous continuum, an Eulerian approach is used

to combine the conservation of mass and the conservation of linear momentum, and thereby yield the equation of motion.

Conservation of mass in integral and differential form is

$$\frac{\partial}{\partial t}\int\limits_V \rho dV - \oint\limits_S \rho v_k n_k dS = 0$$

and

$$\frac{\partial \rho}{\partial t} + \operatorname{div}(\rho \mathbf{v}) = 0, \tag{23}$$

where v is the velocity field and ρ is the density field.

Conservation of linear momentum is written in the form

$$\frac{\partial}{\partial t}\int\limits_V \rho v dV + \oint\limits_S (\rho v_i) v_k n_k dS = \int\limits_V \rho g_i dV + \oint\limits_S \sigma_{ik} n_k dS.$$

Evaluating the LHS in differential form gives

$$\frac{\partial \rho}{\partial t} v_i + \rho \frac{\partial v_i}{\partial t} + \frac{\partial \rho}{\partial x_k} v_i v_k + \rho \frac{\partial v_i}{\partial x_k} v_i + \rho v_i \frac{\partial v_k}{\partial x_k} = \rho \left(\frac{\partial v_i}{\partial t} + v_k \frac{\partial v_i}{\partial x_k} \right) + v_i \left[\frac{\partial \rho}{\partial t} + \frac{\partial}{\partial x_k}(\rho v_k) \right]. \tag{24}$$

Finally, substituting equation (23) into equation (24) yields the equation of motion, or Euler equation,

$$\rho \left(\frac{\partial v_i}{\partial t} + v_k \frac{\partial v_i}{\partial x_k} \right) = \rho g_i + \frac{\partial \sigma_{ik}}{\partial x_k}. \tag{25}$$

When seismic waves propagate through a medium, the medium does not move as a whole. Furthermore, particle velocities due to wave propagation are also small, so the convective term in equation (25) (second term on the LHS), written in vectorial form as $(\mathbf{v}\nabla)\,\mathbf{v}$, is quadratic in small vector $\mathbf{v}$ and can be neglected in comparison to the inertial term. The gravity force g_i can also be neglected since it is assumed to be constant. Euler's equation (25) therefore reduces to

$$\rho \frac{\partial v_i}{\partial t} = \frac{\partial \sigma_{ik}}{\partial x_k}. \tag{26}$$

The balance law for linear momentum does not include any reference to the properties of the continuum. The full description of the mechanical and thermal properties of a material requires further information regarding the relationship between stress and strain. This is provided by a constitutive equation that gives a functional dependence between stress and strain, designed to agree with the observed behavior of the material subjected to the deformation.

Fluid in rest possesses only hydrostatic pressure p, but in a moving fluid, viscous forces are directly connected to the change of velocities of different parts of the fluid. In the case of a moving fluid, the total stress tensor has the form

$$\sigma_{ik} = -p\delta_{ik} + \sigma'_{ik},$$

where σ'_{ik} is the viscous stress tensor. Viscous forces arise when there are gradients of velocity. If these gradients are not too steep, then stress caused by viscous forces has a linear dependence on the derivatives of velocity over coordinates. Furthermore, if a volume of fluid rotates with constant angular velocity ω there is no internal friction and thus the viscous stress tensor has to be zero. Since $v = \omega \times r$ in this case, linear combinations of velocity gradients which have to be zero are $(\partial v_i/\partial x_k + \partial v_k/\partial x_i)$, and these symmetrical derivatives have to be elements of the viscous tensor. For $v = const$ all components not connected with $\partial v_i/\partial x_k$ have to vanish. So, the most general form of constitutive relation for viscous fluid (Landau and Lifshitz, 1987) is

$$\sigma_{ik} = -p\delta_{ik} + \widetilde{\eta}\frac{\partial v_m}{\partial x_m}\delta_{ik} + \eta\left(\frac{\partial v_i}{\partial x_k} + \frac{\partial v_k}{\partial x_i} - \frac{2}{3}\frac{\partial v_m}{\partial x_m}\delta_{ik}\right), \tag{27}$$

where $\widetilde{\eta}$ is bulk viscosity and η is shear viscosity, both of which are functions of

temperature and pressure. Combining equation (25), and equation (27), and ignoring gravity yields the equation of motion for a viscous continuum

$$\rho\left[\frac{\partial v_i}{\partial t}+v_k\frac{\partial v_i}{\partial x_k}\right]=-\frac{\partial}{\partial x_i}p+\frac{\partial}{\partial x_k}\left[\eta\left(\frac{\partial v_i}{\partial x_k}+\frac{\partial v_k}{\partial x_i}-\frac{2}{3}\frac{\partial v_m}{\partial x_m}\delta_{ik}\right)\right]+\frac{\partial}{\partial x_i}\left(\widetilde{\eta}\frac{\partial v_m}{\partial x_m}\right),$$

However, in many cases the change in viscosity is so small that it can be considered as a constant, in which case the previous equations can be written in vectorial form giving the well known Navier-Stokes equation

$$\rho\left(\frac{\partial \mathbf{v}}{\partial t}+(\mathbf{v}\nabla)\,\mathbf{v}\right)=-\text{grad }p+\eta\boldsymbol{\Delta}\mathbf{v}+\left(\widetilde{\eta}+\frac{1}{3}\eta\right)\text{grad div }\mathbf{v}, \tag{28}$$

Our daily experience tells us that liquids such as water are virtually incompressible fluids, that is div $\mathbf{v}\rightarrow\mathbf{0}$. For an incompressible Newtonian fluid the last term in the Navier-Stokes equation is zero. However, elastic waves cannot propagate in an incompressible fluid; so that in problems of elastic wave propagation fluid compressibility cannot be neglected. At each point in the fluid, the oscillatory motion of the wave causes perturbations of pressure p' and density ρ', which are small (but not negligible) in comparison with the values p_0 and ρ_0 for the nonperturbed state (state of equilibrium)

$$p=p_0+p',\ \rho=\rho_0+\rho'. \tag{29}$$

Substituting equation (29) into the mass conservation relation (23) gives

$$\frac{\partial \rho'}{\partial t}+\rho_0\text{div }\mathbf{v}=0. \tag{30}$$

For small velocities and induced stresses, Euler's equation can be written in terms of

pressure and density as

$$\frac{\partial v_i}{\partial t} = -\frac{\nabla\ p}{\rho} = -\frac{\nabla p'}{\rho_0}. \tag{31}$$

If the changes in pressure and density occur quick enough in comparison to the characteristic time of thermal diffusion, the process is adiabatic, and there is a simple linear thermodynamic relation between pressure and density

$$p' = \left(\frac{\partial p}{\partial \rho_0}\right)_S \rho'. \tag{32}$$

Substituting equation (32) into equation (30) gives

$$\frac{\partial p'}{\partial t} + \rho_0 \left(\frac{\partial p}{\partial \rho_0}\right)_S \text{div } \mathbf{v} = 0.$$

Representing velocity through a potential $\mathbf{v} = -grad\ \varphi$ from equation (31) we get

$$p' = -\rho_0 \frac{\partial \varphi}{\partial t}.$$

Substituting this result into equation (30) gives the wave equation for potential φ

$$\frac{\partial^2 \varphi}{\partial t^2} - c^2 \mathbf{\Delta} \varphi = 0,$$

where $c = \sqrt{(\partial p/\partial \rho_0)_S}$ is the velocity of the wave in the compressible fluid.

For waves in an elastic solid which are adiabatic processes, we can use Hooke's law by taking strain-energy potential W to be internal energy rather than free energy. Combining Hooke's law

$$\sigma_{ik} = c_{ikjl}\varepsilon_{jl},\ \varepsilon_{jl} = \frac{1}{2}\left(\frac{\partial u_j}{\partial x_l} + \frac{\partial u_l}{\partial x_j}\right),$$

with Euler equation gives

$$\rho\frac{\partial^2 u_i}{\partial t^2} = \frac{\partial}{\partial x_k}\frac{\partial}{\partial x_l}\left(c_{ikjl}u_j\right),$$

which for homogeneous medium (elements of stiffness tensor do not depend on position) gives the elastic wave equation

$$\rho\frac{\partial^2 u_i}{\partial t^2} = c_{ikjl}\frac{\partial^2 u_j}{\partial x_k \partial x_l}.$$

Solutions of this equation depend on the symmetry of the medium (or of the stiffness tensor).

It is useful here to show how strain-energy potential W can be expressed in terms of scalar invariants for an isotropic body. Assuming small disturbances of an elastic medium, we can express strain potential thorough scalar invariants limited to the quadratic terms. There are two independent scalars of second order, the square of the sum of diagonal elements, and the sum of the squares of all components of the strain tensor. From equation (10) the total derivative of the strain potential can be written as

$$dW = \frac{\partial W}{\partial \varepsilon_{ij}} d\varepsilon_{ij} = \sigma_{ij} d\varepsilon_{ij}. \tag{33}$$

Taking into account the stress-strain relation for an isotropic body, $\sigma_{ij} = \lambda \mathrm{tr}\ \boldsymbol{\varepsilon}\delta_{ij} + 2\mu\varepsilon_{ij}$, and integrating equation (33), gives

$$\begin{aligned} 2W &= 2\lambda \int \mathrm{tr}\ \boldsymbol{\varepsilon}\delta_{ij} d\varepsilon_{ij} + 2\mu \int 2\varepsilon_{ij} d\varepsilon_{ij} = \\ &= \lambda\left(\varepsilon_{11}^2 + \varepsilon_{22}^2 + \varepsilon_{33}^2 + 2\varepsilon_{11}\varepsilon_{22} + 2\varepsilon_{11}\varepsilon_{33} + 2\varepsilon_{22}\varepsilon_{33}\right) + 2\mu\left(\varepsilon_{ij}\varepsilon_{ij}\right). \end{aligned}$$

For a symmetric tensor $\varepsilon_{ij}\varepsilon_{ij} = tr\left(\boldsymbol{\varepsilon}^2\right)$ so that

$$2W = \lambda\left(\mathrm{tr}\boldsymbol{\varepsilon}\right)^2 + 2\mu \mathrm{tr}\left(\boldsymbol{\varepsilon}^2\right) = (\lambda + 2\mu) I_1^2 + \mu I_2 \tag{34}$$

where $I_1 = \mathrm{tr}\boldsymbol{\varepsilon}$ and $I_2 = 2\left[\mathrm{tr}(\boldsymbol{\varepsilon}^2) - I_1^2\right]$ are two second order, scalar invariants of the strain-energy potential W.

2.2 Equations of poroelasticity

2.2.1 Description of porous medium

Real rocks are complex heterogeneous materials whose adequate description presents a formidable challenge. In order to apply physical laws and develop analytical descriptions of physical processes in such materials, some simplifications of the model are needed. A theoretical macroscopic model of a porous medium was introduced by Biot based on a set of physically reasonable assumptions allowing microscopic details to be ignored, which gives very good predictions confirmed by experimental measurements.

In Biot's description, both solid and fluid phases are assumed to be interconnected. Solid grains are connected through the elastic grain contacts, fluid through the pore space and flow channels. Any isolated or sealed void space is considered a part of the solid. The medium is considered fully saturated by a single fluid. Thermal and chemical effects are neglected.

From the acoustical point of view, the wavelength of the propagating wave is much larger than the size of an individual pore or an elementary pore channel. Deformations due to the wave propagation are assumed to be small, which means the problem can be linearized.

The elementary volume EV is chosen to be larger than pore space scale, but smaller than wavelength, so continuum mechanics can be used, and the porous material is approximated by a two-phase continuum. The skeleton is assumed to be statistically isotropic so that as the EV moves throughout the medium, porosity does not change.

Rewriting the constitutive relations for an elastic solid (skeleton) (17) and a viscous fluid (27) in vector form, AND changing the order of spatial and time differential operators in the expression for the fluid stress tensor, we obtain

$$\boldsymbol{\sigma}_s = K_s \nabla \cdot \mathbf{u}\mathbf{I} + \mu \left(\nabla \mathbf{u} + \nabla \mathbf{u}^T - \frac{2}{3} \nabla \mathbf{u}\mathbf{I} \right), \tag{35}$$

$$\boldsymbol{\sigma}_f = K_f \left(1 + \frac{\widetilde{\eta}}{K_f} \frac{\partial}{\partial t} \right) \nabla \cdot \mathbf{U}\mathbf{I} + \eta \frac{\partial}{\partial t} \left(\nabla \mathbf{U} + \nabla \mathbf{U}^T - \frac{2}{3} \nabla \mathbf{U}\mathbf{I} \right), \tag{36}$$

where $\mathbf{u}$ is solid displacement, $\mathbf{U}$ is fluid displacement, K_s is solid bulk modulus, $K_f = -p/\left(\nabla \cdot \mathbf{U}\right)$ is fluid bulk modulus, p is hydrostatic pressure, and quantity

$$K_f \left(1 + \frac{\widetilde{\eta}}{K_f} \frac{\partial}{\partial t} \right) = K_f^* = -\frac{\mathrm{tr}\boldsymbol{\sigma}_f}{3\left(\nabla \cdot \mathbf{U}\right)}$$

is the fluid bulk viscosity operator, which defines total pressure in the fluid caused by wave propagation or any other time dependent deformation. The first term on the RHS of equation (36) is called equilibrium pressure, or in porous media, pore pressure. When considering time harmonic motion (wave) of type $\exp\left(-i\omega t\right)$ with angular frequency ω, the time derivative operator is replaced with $-i\omega$ in frequency domain.

Comparing the dynamic shear viscosity of the fluid with the shear modulus of the skeleton, Pride et al. (1992) showed that the ratio $\omega\eta/\mu$ for a soft skeleton ($\mu > 10^8$ Pa) filled with water ($\eta \simeq 10^{-3}$ Pa s), for frequencies up to 10^7 Hz, is of the order of magnitude 10^{-4}. This means that second term on the RHS of equation (36) can be neglected, and the effect of dynamic viscosity can be accounted for in energy balance through the dissipative potential**.**

In the same paper, Pride et al. also showed that the ratio of dynamic bulk viscosity

over the isothermal (static) fluid bulk modulus $\omega\widetilde{\eta}/K_f$ for frequency 10^6 Hz is of the order of magnitude 10^{-5} and 10^{-3} for water and air, respectively. Therefore, with the assumption of small velocities, the distribution of stress in the fluid is nearly hydrostatic.

2.2.2 Strain-energy potential for poroelastic medium

To derive equations of motion of then porous medium, we need an expression for energy potential in such a medium through displacements of solid and fluid. Assuming $\mathbf{U}$ is the mean displacement of fluid phase (average of the sum of displacements of fluid contained in EV and of the fluid which has left and has entered into this volume) and $\mathbf{u}$ is the displacement of the EV as a whole (equal to the solid phase displacement), the macroscopic fluid flow rate can be written as

$$dQ = \dot{\mathbf{w}} \cdot \mathbf{n} dS, \quad \mathbf{w} = \phi(\mathbf{U} - \mathbf{u}),$$

where $\mathbf{w}$ is additional fluid flow relative to the solid. For any macroscopic volume V with boundary S the relative increase of fluid volume ξ in the EV is defined as

$$\int_S \mathbf{w} \cdot \mathbf{n} dS = \int_V \text{div } \mathbf{w} \, dV \,, \quad \xi = -\text{div } \mathbf{w}. \tag{37}$$

The strain potential can be expressed as a function of the strain tensor of EV in the same way as for an elastic body, but requires additional terms describing the relative motion of the fluid (increase of fluid content in that volume). One part of the fluid pressure balances skeleton loading, while the other part is doing work displacing part of the fluid out of or into the EV. Similarly to how the differential of strain energy potential was defined in equation (33), for a porous medium this potential is a total

differential of the form

$$dW = \frac{\partial W}{\partial \varepsilon_{ij}} d\varepsilon_{ij} + \frac{\partial W}{\partial \xi} d\xi = \sigma_{ij} d\varepsilon_{ij} + p d\xi,$$

where σ_{ij} is total stress of bulk material and p is pore pressure induced by loading of the skeleton. Again assuming small disturbances and isotropy, W can be expanded in the quadratic terms only. This expansion involves two invariants for the solid strain tensor, I_1 and I_2, increase of fluid volume contents ξ^2, and a coupling term that balances compressibility of skeleton and fluid in contact

$$2W = (\lambda_c + 2\mu) I_1^2 + \mu I_2 - 2\alpha M I_1 \xi + M \xi^2. \tag{38}$$

In analogy to equation (34), coefficient λ_c is called saturated (undrained) Lamé coefficient**,** M is a parameter of dimension of bulk modulus, and α is so-called Biot-Willis effective stress coefficient (Biot and Willis, 1957). Equation (38) can be rewritten

$$\begin{aligned} 2W &= \lambda_c I_1^2 + 2\mu I_1^2 + 2\mu \mathrm{tr}\left(\boldsymbol{\varepsilon}^2\right) - 2\mu I_1^2 - 2\alpha M I_1 \xi + M \xi^2 \\ &= \lambda_c I_1^2 + 2\mu \mathrm{tr}\left(\boldsymbol{\varepsilon}^2\right) - 2\alpha M I_1 \xi + M \xi^2. \end{aligned} \tag{39}$$

Using equation (39), constitutive relations for a porous saturated medium can be constructed in the following way

$$\sigma_{ij} = \lambda_c \mathrm{tr}\boldsymbol{\varepsilon} \delta_{ij} + 2\mu \varepsilon_{ij} - \alpha M \xi \delta_{ij}, \quad p = M(-\alpha \mathrm{tr}\boldsymbol{\varepsilon} + \xi), \tag{40}$$

or

$$\sigma_{ij} = \lambda \mathrm{tr}\boldsymbol{\varepsilon} \delta_{ij} + 2\mu \varepsilon_{ij} - \alpha p \delta_{ij}, \quad \xi = \frac{p}{M} + \alpha \mathrm{tr}\boldsymbol{\varepsilon}, \tag{41}$$

where λ and K are so called dry moduli introduced by the relation

$$\lambda = \lambda_c - \alpha^2 M, \; K = K_c - \alpha^2 M. \tag{42}$$

Dry skeleton means that there is either no fluid at all, or fluid pressure is kept constant, the latter situation referred to as drained condition.

2.2.3 Gassmann relations

Equation (42) gives relationship between dry and saturated elastic moduli of the porous material, but requires expressions for parameters α and M.To derive such expressions, we consider two limiting cases (Bourbié et al., 1987).

1. If fluid can flow in and out of the rock freely, it is an open system with zero increment pore pressure, there is no resistance to solid displacement, and equation (41) gives

$$\bar{\sigma} \equiv -\frac{1}{3}\mathbf{tr}\ \boldsymbol{\sigma} = K\mathbf{tr}\ \boldsymbol{\varepsilon}.$$

In the presence of fluid motion, total strain has to be adjusted for the increase of fluid content in EV. From equations (41), the net matrix strain can be written as

$$\mathbf{tr}\ \boldsymbol{\varepsilon} - \xi = (1-\alpha)\mathbf{tr}\ \boldsymbol{\varepsilon} = -(1-\alpha)\frac{\bar{\sigma}}{K}. \tag{43}$$

Therefore

$$-(1-\alpha)\frac{\bar{\sigma}}{K} = -\frac{\bar{\sigma}}{K_g},$$

where K_g is the bulk modulus of the solid grain material. This gives the relation between dry (or drained) modulus K and grain modulus K_g:

$$K = (1-\alpha)K_g. \tag{44}$$

We see that Biot-Willis parameter α is a characteristic of the skeleton only, depending on the quality of grain contacts, and describes the relative weakness of the skeleton. From equation (43) it can be seen that for an open system α quantifies the change of fluid content due to the volumetric change of skeleton.

2. If fluid can't flow in or out of the rock, $\xi = 0$ and it is a closed system where pore

pressure is equal to the hydrostatic pressure

$$\bar{\sigma} = -\frac{1}{3}\mathbf{tr}\ \boldsymbol{\sigma} = p.$$

This pressure equilibrates skeleton loading and in terms of strain gives

$$-p = K_g \mathbf{tr}\ \boldsymbol{\varepsilon}.$$

From the expression for relative increase of fluid (37) and constitutive relation for porous medium (41) we have

$$\xi = -\phi div(\mathbf{U} - \mathbf{u}) = -\phi div\mathbf{U} + \phi \mathbf{tr}\ \boldsymbol{\varepsilon},$$

$$\frac{p}{M} = -\phi div\mathbf{U} - (\alpha - \phi)\mathbf{tr}\ \boldsymbol{\varepsilon}.$$

Furthermore, from the definition of adiabatic bulk modulus (second of equations (18)) with assumption of small deformations we get

$$-p = K_f \mathbf{div}\ \mathbf{U},$$

$$\frac{1}{M} = \frac{\alpha - \phi}{K_g} + \frac{\phi}{K_f}. \tag{45}$$

Equation (42) with α given by (42) (44) and M given by equation (45) is one form of Gassmann equation (Gassmann, 1951). Combining these three equations we can get another form of Gassmann equation:

$$K_c = \frac{\phi(\frac{1}{K_g} + \frac{1}{K_f}) + \frac{1}{K_g} - \frac{1}{K}}{\frac{\phi}{K}(\frac{1}{K_g} + \frac{1}{K_f}) + \frac{1}{K_g}(\frac{1}{K_g} - \frac{1}{K})}.$$

For the limiting case of zero porosity (bulk material is solid),

$$\alpha = \phi = 0, \quad K_g = K, \quad \text{and } M \to \infty,$$

whereas for the fluid case (porosity $\phi = 1$),

$$\alpha = \phi = 1,\ K = 0,\ \text{and } K_c = K_f = M.$$

2.2.4 Biot's equations of poroelasticity

Having derived constitutive equations (41) for the poroelastic medium, we now have to derive the equations of motion. For an elastic medium equation of motion (25) was derived from conservation of mass and conservation of momentum. Such an approach can also be used to derive equation of motion for a porous medium using spatial averaging of conservation equations for fluid and solid written on pore scale, see Pride et al. (1992). However, for a statistically homogeneous and isotropic porous medium it is possible to avoid the analysis on microscale altogether by using a macroscopic energy approach proposed by Biot (1956a, 1956b). This can be done by using the principle of minimal action so that the Lagrange function can be then expressed through the generalized coordinates. Due to the smallness of velocity, displacements, and ratio of linear characteristic dimension of EV over the wavelength of incident wave, it is possible to represent kinetic energy, strain energy and dissipative potential in quadratic form.

In the absence of dissipation, the porous continuum can be fully described by the Lagrange function $L(q_i, q_{i,t}, q_{i,k}, t)$, where q_i is i-th component of generalized coordinate $\mathbf{q}$, subscript written after comma denotes partial derivative with respect to time t or spatial coordinate x_k. Generalized coordinates $\mathbf{q}(x_k, t)$ are functions that describe the state of the system in particular point in space and time. These functions are the ones for which equations of motion are to be obtained. For instance, in elasticity generalized coordinates are usually chosen as displacements. For a porous medium we choose as generalized coordinates the bulk solid displacement $u_i = u_i(x_k, t)$ and relative fluid displacement $w_i = w_i(x_k, t)$. One of the most fundamental principles of physics, the principle of minimal action, stipulates that integral S, called action,

$$S = \int_{t_1}^{t_2} L(q_i, q_{i,t}, q_{i,k}, t)dt,$$

is minimal for motion of the system between positions (states) $q^{(1)}$ at the moment t_1 and $q^{(2)}$ at the moment t_2 (Landau and Lifshitz, 1976). This means that variation of action is zero

$$\delta S = \delta \int_{t_1}^{t_2} L(q_i, q_{i,t}, q_{i,k}, t)dt = \int_{t_1}^{t_2} \left(\frac{\partial L}{\partial q_i}\delta q_i + \frac{\partial L}{\partial q_{i,t}}\delta q_{i,t} + \frac{\partial L}{\partial q_{i,k}}\delta q_{i,k} \right) dt = 0.$$

Integrating the second and third terms by parts, and using the condition $\delta q_i(t_1) = \delta q_i(t_2) = 0$ which means that the initial and final positions of the system are exactly known, it is possible to derive the equation of motion in generalized coordinates

$$\frac{d}{dt}\frac{\partial L}{\partial q_{i,t}} + \frac{\partial}{\partial x_k}\frac{\partial L}{\partial q_{i,k}} - \frac{\partial L}{\partial q_i} = 0 \tag{46}$$

Furthermore, if L is not an explicit function of time, i.e. the medium properties do not change with time, conservation of energy occurs, and $L = K - W$, where K is kinetic energy and W is strain energy (or potential energy) defined by the relation (38).

The above approach has been written for the process without dissipation. Elastic waves in porous medium are, in general accompanied by dissipation due to the motion of the fluid relative to the solid. Dissipative force is a function of relative velocity only, and for small velocities just the linear term is sufficient, and dissipative potential D can be written in quadratic form

$$D = \frac{\eta}{2\kappa} w_{i,t}^2$$

where κ is permeability. In the presence of dissipation, equation (46) becomes

$$\frac{d}{dt}\frac{\partial L}{\partial q_{i,t}} + \frac{\partial}{\partial x_k}\frac{\partial L}{\partial q_{i,k}} - \frac{\partial L}{\partial q_i} = -\frac{\partial D}{\partial q_{i,t}}. \tag{47}$$

Viscous force is then $F_i = \partial D/\partial w_{i,t}$, which can be also written in the form

$$-\nabla p = \frac{\eta}{\kappa}\dot{\mathbf{w}}. \tag{48}$$

Equation (48), known as a Darcy law shows that relative fluid velocity in a porous medium is proportional to pressure gradient.

Kinetic energy can be expanded to quadratic terms in generalized coordinates:

$$2K = \rho_u u_{i,t} u_{i,t} + 2\rho_{uw} u_{i,t} w_{i,t} + \rho_w w_{i,t} w_{i,t} \tag{49}$$

where $\rho_u = \rho = (1-\phi)\rho_g + \phi\rho_f$ is average bulk density, with ρ_g and ρ_f as the densities of the grain material and fluid respectively. Coefficients ρ_{uw} and ρ_w are two new parameters with the dimension of density, whose physical meaning will be explained below.

Equation (49) shows that kinetic energy depends only on particle velocities. In turn, potential energy of deformations depends on spatial derivatives of displacements (strain), and dissipative potential depends only on relative velocity. Thus equation (47) reduces to

$$\frac{d}{dt}\frac{\partial K}{\partial q_{i,t}} + \frac{\partial}{\partial x_k}\frac{\partial W}{\partial q_{i,k}} - \frac{\partial W}{\partial q_i} = -\frac{\partial D}{\partial q_{i,t}}. \tag{50}$$

Substituting expressions for K, W, D in equation (50), yields two equations of motion known as Biot's equations of poroelasticity

$$\sigma_{ik,k} = \rho u_{i,tt} + \rho_{uw} w_{i,tt} \tag{51}$$

and

$$-p_{,i} = \rho_{uw} u_{i,tt} + \rho_w w_{i,tt} + \frac{\eta}{\kappa} w_{i,t} \ . \tag{52}$$

For a special case $w = 0$ and hence $U = u$, equation (52) yields

$$-p_{,i} = \rho_{uw} U_{i,tt}$$

which implies that $\rho_{uw} = \rho_f$. The density ρ_w is related to the drag force that is a result of the relative motion of the skeleton in viscous fluid (Landau and Lifshitz, 1987; Bourbié et al., 1987). It is proportional to ρ_f with a proportionality constant called tortuosity that depends on the geometry of the pore space. At low frequency, viscous forces are dominant and the inertial term can be neglected because the fluid moves together with the grains (small relative fluid velocity).

2.2.5 Biot's critical frequency

Since any porous medium is at least a two-phase composite, it is inherently heterogeneous with a spatial scale equal to the average pore radius or grain size. Assuming oscillatory fluid flow induced by the elastic wave propagation, and smooth variation of flow channel width, the presence of this spatial scale implies the existence of some critical frequency. The nature of the fluid flow is different for frequencies lower and higher than this critical Biot's frequency.

First consider an idealized case (Landau and Lifshitz, 1987) when an infinite solid yz plane oscillates with circular frequency ω in y direction. Viscous fluid occupies a volume $x > 0$. Velocity of the oscillating plane is $\dot{u} = \dot{u}_y = \dot{u}_0 \exp(-i\omega t)$. All components of the fluid and solid plane velocities are zero except for the y component. The boundary condition at $x = 0$ for the fluid velocity is $\dot{\mathbf{U}} = \dot{U}_y = \dot{u}_y$. According to

the symmetry of the problem, all quantities are functions of x and t only. The fluid is assumed to be nearly incompressible implying $\mathrm{div}\dot{\mathbf{U}} \simeq 0$. From here $\partial \dot{U}_x/\partial x = 0$, so that $\dot{U}_x = const$, and this constant is zero from the boundary condition. The convective term $\left(\dot{\mathbf{U}}\nabla\right)\dot{U}$ is also zero, and the Navier-Stokes equation (28) reduces to

$$\frac{\partial \dot{\mathbf{U}}}{\partial t} = -\frac{1}{\rho_f}\mathrm{grad}\ p + \frac{\eta}{\rho_f}\boldsymbol{\Delta}\dot{\mathbf{U}}.$$

For x component this gives $\partial p/\partial x = 0$, while for y component $\dot{U} \equiv \dot{U}_y$ we have

$$\frac{\partial \dot{U}}{\partial t} = \frac{\eta}{\rho_f}\frac{\partial^2 \dot{U}}{\partial x^2}. \tag{53}$$

Equation (53) is a 1-D diffusion equation whose solution is of the form $\dot{U} = \dot{u}_0 \exp i(kx - \omega t)$ and is automatically satisfied on the boundary. Substituting ansatz solution into equation (53) gives

$$i\omega = \frac{\eta}{\rho_f}k^2,\ k = \frac{1+i}{\delta},\ \delta = \sqrt{\frac{2\eta}{\omega\rho_f}},$$

where k is the wave number, and δ is a parameter called viscous skin depth. Finally, for the fluid velocity profile normal to the plane (in x direction) we have

$$\dot{\mathbf{U}} = \dot{u}_0 \exp\left(-\frac{x}{\delta}\right)\exp i\left(\frac{x}{\delta} - \omega t\right). \tag{54}$$

At the distance from the solid boundary equal to the skin depth ($x = \delta$), amplitude decreases e times, whereas for the same distance equal to the spatial period of wave ($x = 2\pi\delta$), amplitude decreases approximately 540 times.

The viscous skin depth parameter plays a fundamental role in various fluid flow problems. For instance, if fluid flows in a cylindrical pipe of diameter $l \ll \delta$, then viscous term dominates over the inertial term in Navier-Stokes equation (28), the fluid motion is quasi-stationary, and yields a so-called Poiseuille flow regime (Landau and Lifshitz, 1987). On the other hand, if $l \gg \delta$, then the inertial forces dominate

everywhere except for a thin skin layer near the pipe surface, and the oscillatory flow is similar to that in an inviscid fluid. For a porous medium the spatial parameter l can be taken as an average pore channel diameter or characteristic pore size. The frequency ω_B which yields viscous skin depth δ equal to $l/2$, i.e.,

$$\sqrt{\frac{2\eta}{\omega_B \rho_f}} = l/2 \tag{55}$$

is called Biot's characteristic frequency and plays fundamental role in dynamics of porous materials. Solving equation (55) for ω_B, we obtain

$$\omega_B = \frac{8\eta}{l^2 \rho_f}. \tag{56}$$

Pore space does not consist of cylindrical pipes, and thus parameter l provides only a characteristic size of the pore scale. For porous media equation (56) is usually written using the parameter of permeability κ which has dimension of the squared spatial length (Biot, 1956b):

$$\omega_B = \frac{\eta\phi}{\kappa\rho_f}.$$

Norris (1993) showed that pore space radius can be estimated using the formula $L_p \approx \sqrt{8F\kappa}$, where $F \approx 1/\phi^2$ is formation factor, ϕ is porosity and κ is permeability. For a sandstone with 20% porosity and permeability 0.2×10^{-8} cm^2 circular Biot's frequency $f_B = \omega_B/2\pi \approx 170$ kHz. In geophysics most field measurements are done at frequencies lower than the Biot's frequency. Dissipation of energy as a function of frequency has a maximum at Biot's critical frequency because whole fluid takes part in dissipation with maximal gradient of the velocity (Bourbié et al., 1987).

In this chapter we have outlined the basic principles of the theory of poroelasticity for macroscopically homogeneous porous materials, that is, the materials whose macroscopic properties (measured over EV) do not vary with spatial coordinates.

Real materials are usually macroscopically inhomogeneous. This makes the analysis of such materials much more complicated, since these materials have additional scale length parameters, which induce new relaxation processes. In the next chapter we analyze such phenomena for a simplest case of 1D inhomogeneous porous medium.

3 Layered porous media

The simplest example of macroscopically inhomogeneous porous medium is a layered porous medium, whose properties depend on one spatial coordinate, say z, only. The theory of layered porous media can be developed in analogy to the theory of layered fluid and solid media, which has found applications in many areas of geophysics (Brekhovskikh, 1981; Ewing, 1957; Aki and Richards, 1980). One of the main methods used to describe phenomena in layered media is matrix propagator method. In this method each layer is characterized by a certain matrix called system matrix, while the stack of layers as a whole is described by the so called propagator matrix obtained by multiplying the propagator matrices for each particular layer, which in turn depend on the system matrices. Elements of the propagator matrix are interference coefficients of reflection and transmission. Thus matrix propagator method can be used to compute reflected and transmitted wavefields in layered materials from the properties of individual layers. In addition, this method can also be used to obtain effective macroscopic elastic properties of thinly layered systems. This is the case for a finely layered medium when wavelength of the incident wave is at least one order of magnitude larger than thickness of the thickest layer (long wavelength limit). Multiplication of single propagator matrices gives an exact solution for the stack of layers, and this solution is equivalent to the one single propagator matrix representing the whole stack in approximation of an effective homogeneous medium. This means that the eigenvalues of the propagator matrix for the equivalent medium have to be equal to the eigenvalues of the matrix obtained by multiplication of the individual propagator matrices for each layer.

3.1 Poroelasticity equations in matrix form

Consider a one-dimensional periodic medium, with spatial period H, consisting of alternating layers of saturated poroelastic media 1 and 2 of thicknesses $h_1 H$ and $h_2 H$, so that $h_1 + h_2 = 1$. Layer interfaces are assumed to be parallel to xy plane. Each of the poroelastic layers is statistically isotropic and homogeneous, and is described by the constitutive relations (40) which can also be written in the form

$$\boldsymbol{\sigma} = \mathbf{L_s}\boldsymbol{\varepsilon} - \alpha M \xi \mathbf{I} \,, \qquad p = -\alpha M \varepsilon + M\xi, \tag{57}$$

where $\boldsymbol{\sigma}$ is total stress tensor, p is fluid pressure, $\boldsymbol{\varepsilon}$ is the solid strain tensor, $\varepsilon = \operatorname{tr}\boldsymbol{\varepsilon} = \boldsymbol{\nabla}\cdot\mathbf{u}$ ($\mathbf{u}$ is solid displacement), $\xi = -\boldsymbol{\nabla}\cdot\mathbf{w}$ ($\mathbf{w}$ is fluid displacement relative to the solid), M is pore space modulus defined by Gassmann relation (45), α is Biot's stress coefficient (44), $\mathbf{I}$ is the identity tensor and $\mathbf{L_s}$ is undrained (fluid saturated) stiffness tensor of the bulk material. In index notation, the first of equations (57) is

$$\sigma_{ij} = 2\mu\varepsilon_{ij} + (\lambda_s \varepsilon - \alpha M \xi)\delta_{ij} \,, \tag{58}$$

where λ_s is Lamé coefficient of the saturated porous material and μ is shear modulus.

Assume that a plane P-wave propagates in x, z plane with incident angle θ with respect to axis of symmetry z. From equations (57) and (58), we have

$$\begin{aligned}
\sigma_{xx} &= 2\mu\frac{\partial u_x}{\partial x} + \lambda_s\left(\frac{\partial u_x}{\partial x} + \frac{\partial u_z}{\partial z}\right) + \alpha M\left(\frac{\partial w_x}{\partial x} + \frac{\partial w_z}{\partial z}\right) \,, \\
\sigma_{zz} &= 2\mu\frac{\partial u_z}{\partial z} + \lambda_s\left(\frac{\partial u_x}{\partial x} + \frac{\partial u_z}{\partial z}\right) + \alpha M\left(\frac{\partial w_x}{\partial x} + \frac{\partial w_z}{\partial z}\right) \,, \\
\sigma_{xz} &= 2\mu\varepsilon_{xz} = \mu\left(\frac{\partial u_x}{\partial z} + \frac{\partial u_z}{\partial x}\right) \,, \\
-p &= \alpha M\left(\frac{\partial u_x}{\partial x} + \frac{\partial u_z}{\partial z}\right) + M\left(\frac{\partial w_x}{\partial x} + \frac{\partial w_z}{\partial z}\right) \,.
\end{aligned} \tag{59}$$

Assume also that pressure, stress and displacements are harmonic functions in time,

and harmonic functions in x defined by multiplicative factor $e^{i\omega(sx-t)}$, where s is a horizontal slowness. The derivatives over time and x then yield multiplication by $-i\omega$ and $-i\omega s$ respectively, so that only derivatives over z remain in the equations. The system of constitutive equations (59) can be expressed in the frequency domain using particle velocities rather than displacements as

$$-i\omega\sigma_{xx} = i\omega s\left(\lambda_s + 2\mu\right)\dot{u}_x + \lambda_s\frac{\partial \dot{u}_z}{\partial z} + \alpha M\frac{\partial \dot{w}_z}{\partial z} + i\omega s\alpha M\dot{w}_x \ , \tag{60}$$

$$-i\omega\sigma_{zz} = i\omega s\lambda_s\dot{u}_x + \left(\lambda_s + 2\mu\right)\frac{\partial \dot{u}_z}{\partial z} + \alpha M\frac{\partial \dot{w}_z}{\partial z} + i\omega s\alpha M\dot{w}_x \ , \tag{61}$$

$$-i\omega\sigma_{xz} = \mu\frac{\partial \dot{u}_x}{\partial z} + i\omega s\mu\dot{u}_z \ , \tag{62}$$

$$-i\omega\, p = -i\omega s\alpha M\dot{u}_x - \alpha M\frac{\partial \dot{u}_z}{\partial z} - M\frac{\partial \dot{w}_z}{\partial z} - i\omega s M\dot{w}_x \ , \tag{63}$$

where $\dot{u} \equiv \partial u/\partial t$, $\dot{w} \equiv \partial w/\partial t$.

Biot's equations of motion for the poroelastic medium (51) and (52) can be written in the form (Biot, 1962)

$$\frac{\partial \sigma_{ij}}{\partial x_j} = \frac{\partial}{\partial t}(\rho\dot{u}_i + \rho_f\dot{w}_i) \ , \tag{64}$$

$$-\frac{\partial p}{\partial x_i} = \frac{\partial}{\partial t}(\rho_f\dot{u}_i + m\dot{w}_i) + \frac{\eta}{\kappa}\dot{w}_i \ . \tag{65}$$

Writing equations (64) and (65) in the frequency domain for the 2D case gives

$$i\omega s\sigma_{xx} + \frac{\partial}{\partial z}\sigma_{xz} = -i\omega\rho\dot{u}_x - i\omega\rho_f\dot{w}_x \ , \tag{66}$$

$$i\omega s\sigma_{xz} + \frac{\partial}{\partial z}\sigma_{zz} = -i\omega\rho\dot{u}_z - i\omega\rho_f\dot{w}_z \ , \tag{67}$$

$$-i\omega sp = -i\omega\rho_f\dot{u}_x + \left(\frac{\eta}{\kappa} - i\omega m\right)\dot{w}_x \ , \tag{68}$$

$$-\frac{\partial}{\partial z}p = -i\omega\rho_f\dot{u}_z + \left(\frac{\eta}{\kappa} - i\omega m\right)\dot{w}_z \ , \tag{69}$$

where $\rho = (1-\phi)\rho_g + \phi\rho_f$ is average density of bulk material and $(\eta/\kappa - i\omega m)$ is Biot's visco-dynamic operator.

To write equations of poroelasticity in a matrix form, we define a symbolic 6-vector $\mathbf{b}$ as

$$\mathbf{b} = \begin{bmatrix} \dot{u}_z & \dot{w}_z & \sigma_{xz} & \sigma_{zz} & -p & \dot{u}_x \end{bmatrix}^T$$

of quantities that are continuous across the interface.

From the system of two equations (61) and (63)

$$(\lambda_s + 2\mu)\frac{\partial\dot{u}_z}{\partial z} + \alpha M\frac{\partial\dot{w}_z}{\partial z} = -i\omega\sigma_{zz} - i\omega s\lambda_s\dot{u}_x \ , \tag{70}$$

$$\alpha M\frac{\partial\dot{u}_z}{\partial z} + M\frac{\partial\dot{w}_z}{\partial z} = i\omega\, p - i\omega s\alpha M\dot{u}_x \ . \tag{71}$$

By solving system of equations (70) and (71), the z derivatives of $\dot{u}_z$ and $\dot{w}_z$ are calculated as

$$\frac{\partial\dot{u}_z}{\partial z} = -i\omega\frac{s\left(\lambda_s - \alpha^2 M\right)\dot{u}_x + \sigma_{zz} + \alpha p}{\lambda_s + 2\mu - \alpha^2 M} = -i\omega\frac{s\lambda\dot{u}_x + \sigma_{zz} + \alpha p}{L} \ , \tag{72}$$

$$\frac{\partial \dot{w}_z}{\partial z} = -i\omega \frac{2\mu s\alpha M \dot{u}_x - \alpha M \sigma_{zz} - (\lambda_s + 2\mu)\, p}{(\lambda_s + 2\mu - \alpha^2 M)\, M} = -i\omega \frac{2\mu s\alpha \dot{u}_x - \alpha \sigma_{zz} - \frac{C}{M} p}{L} \,, \quad (73)$$

where $C = \lambda_s + 2\mu$ is the saturated P-wave velocity modulus, $L = C - \alpha^2 M = \lambda + 2\mu$ is the dry P-wave velocity modulus, and $\lambda = \lambda_s - \alpha^2 M$ is the dry Lamé coefficient.

From equation (62)

$$\frac{\partial \dot{u}_x}{\partial z} = -i\omega \left(\frac{1}{\mu} \sigma_{xz} + s \dot{u}_z \right) \,, \quad (74)$$

and from equations (67) and (69)

$$\frac{\partial}{\partial z} \sigma_{zz} = -i\omega \rho \dot{u}_z - i\omega \rho_f \dot{w}_z - i\omega s \sigma_{xz} = -i\omega \left(\rho \dot{u}_z + \rho_f \dot{w}_z + s \sigma_{xz} \right) \,, \quad (75)$$

$$\frac{\partial}{\partial z} p = i\omega \rho_f \dot{u}_z + i\omega m \dot{w}_z - \frac{\eta}{\kappa} \dot{w}_z = -i\omega \left(-\rho_f \dot{u}_z - m \dot{w}_z - \frac{i\eta}{\omega \kappa} \dot{w}_z \right) \,. \quad (76)$$

Elimination of σ_{xx} from equations (60) and (66) yields

$$\frac{\partial \sigma_{xz}}{\partial z} = s\lambda_s \frac{\partial \dot{u}_z}{\partial z} + s\alpha M \frac{\partial \dot{w}_z}{\partial z} - i\omega \left(\rho - s^2 C \right) \dot{u}_x \,. \quad (77)$$

Substituting the z derivatives of $\dot{u}_z$ and $\dot{w}_z$, (72) and (73), into equation (77) gives

$$\begin{aligned}
\frac{\partial \sigma_{xz}}{\partial z} &= -i\omega \frac{s\lambda \dot{u}_x + \sigma_{zz} + \alpha p}{L} s\lambda_s - i\omega \frac{2\mu s\alpha \dot{u}_x - \alpha \sigma_{zz} - \frac{C}{M} p}{L} s\alpha M - i\omega \left(\rho - s^2 C \right) \dot{u}_x \\
&= -i\omega \left[\frac{s^2 \lambda \lambda_s + 2\mu s^2 \alpha^2 M + L\left(\rho - s^2 C\right)}{L} \dot{u}_x + \frac{s\left(\lambda_s - \alpha^2 M\right)}{L} \sigma_{zz} + \frac{s\alpha\lambda_s - s\alpha C}{L} p \right] \\
&= -i\omega \left[\frac{s^2 \left(\lambda\lambda_s + 2\mu\alpha^2 M - \lambda\lambda_s - 2\mu\lambda - 2\mu\lambda_s - 2\mu 2\mu\right) + L\rho}{L} \dot{u}_x + \frac{s\lambda}{L} \sigma_{zz} + \frac{-2\mu s\alpha}{L} p \right] \\
&= -i\omega \left[\frac{L\rho - 2\mu s^2 \left(\lambda + L\right)}{L} \dot{u}_x + \frac{s\lambda}{L} \sigma_{zz} - \frac{2\mu s\alpha}{L} p \right] \,. \quad (78)
\end{aligned}$$

Finally, we can now write all equations (72), (73), (78), (75), (76) and (74) in compact matrix form

$$\frac{\partial}{\partial z}\begin{bmatrix} \dot{u}_z \\ \dot{w}_z \\ \sigma_{xz} \\ \sigma_{zz} \\ -p \\ \dot{u}_x \end{bmatrix} = -i\omega \begin{bmatrix} 0 & 0 & 0 & \frac{1}{L} & \frac{-\alpha}{L} & \frac{s\lambda}{L} \\ 0 & 0 & 0 & \frac{-\alpha}{L} & \frac{1}{N} & \frac{2\mu s\alpha}{L} \\ 0 & 0 & 0 & \frac{s\lambda}{L} & \frac{2\mu s\alpha}{L} & \frac{L\rho - 2\mu s^2(\lambda+L)}{L} \\ \rho & \rho_f & s & 0 & 0 & 0 \\ \rho_f & \left(m + i\frac{\eta}{\omega\kappa}\right) & 0 & 0 & 0 & 0 \\ s & 0 & \frac{1}{\mu} & 0 & 0 & 0 \end{bmatrix} \begin{bmatrix} \dot{u}_z \\ \dot{w}_z \\ \sigma_{xz} \\ \sigma_{zz} \\ -p \\ \dot{u}_x \end{bmatrix} , \tag{79}$$

or,

$$\frac{\partial}{\partial z}\mathbf{b}(z) = -i\omega\mathbf{Q}(z)\mathbf{b}(z) , \tag{80}$$

where $N \equiv ML/C$. Matrix $\mathbf{Q}(z)$ is called the system matrix, whose elements are the material properties of a particular layer (constants in that layer). The continuity of the six-vector $\mathbf{b}(z)$ is assured across $z = const$ interfaces for open pore conditions (Deresiewicz and Skalak, 1963; Gurevich and Schoenberg, 1999).

3.2 Matrix propagator method for layered media

Equation (80) is a typical equation for layered media of different physical nature. The formal solution of equation (80) for a single layer between z_0 and z is

$$\mathbf{b}(z) = \exp\left[-i\omega\left(z - z_0\right)\mathbf{Q}\right]\mathbf{b}(z_0) \equiv \mathbf{P}\left(z - z_0\right)\mathbf{b}(z_0) , \tag{81}$$

where

$$\mathbf{P}\left(z - z_0\right) = \exp\left[-i\omega\left(z - z_0\right)\mathbf{Q}\right]$$

is called the propagator matrix in a straightforward analogy to the elastic case (Aki and Richards, 1980). The exponential of a matrix is defined by the relation (Lancaster, 1969)

$$\exp(\mathbf{Q}) = \sum_{0}^{\infty} \frac{\mathbf{Q}^m}{m!}, \tag{82}$$

so that

$$\mathbf{P}\left(z - z_0\right) = \sum_{m=0}^{\infty} \frac{\left[-i\omega\left(z - z_0\right)\right]^m \mathbf{Q}^m}{m!}.$$

In general, for a stack of k layers with thicknesses $h_j H$,the propagator matrix is

$$\mathbf{P}\left(\sum_{j=1}^{k} h_j H\right) = \prod_{j=k}^{1} \exp\left(-i\omega h_j H \mathbf{Q}_j\right) \ .$$

For the periodic medium considered in this work, a stack of n spatial periods with each period consisting of two layers, with $z_0 = 0$, equation (81) becomes

$$\mathbf{b}(nH) = \left[\exp\left(-i\omega h_2 H \mathbf{Q}_2\right) \exp\left(-i\omega h_1 H \mathbf{Q}_1\right)\right]^n \mathbf{b}(0) \equiv \left[\mathbf{P}_2\left(h_2 H\right) \mathbf{P}_1\left(h_1 H\right)\right]^n \mathbf{b}(0) \ .$$

On the other hand, in one homogeneous layer the vector $\mathbf{b}(z)$ in equation (80), can be written in terms of wave numbers i.e. slownesses,

$$\mathbf{b}(z) = \mathbf{b}(0) \exp ik_k z = \mathbf{b}(0) \exp i\omega s_k z \ ,$$

where index after k identifies the type of propagating plane wave. Substituting this solution into equation (80) gives

$$i\omega s_k \mathbf{b}(0) \exp i\omega s_k z = -i\omega \mathbf{Q}(z) \mathbf{b}(0) \exp i\omega s_k z \ ,$$

so that

$$\mp \mathbf{Q}(z) \mathbf{b}(0) = \pm s_k \mathbf{b}(0) \ ,$$

i.e. s_k are eigenvalues of the matrix $\mathbf{Q}$. This means that matrix $\mathbf{Q}$ can be represented as (Lancaster, 1969)

$$\mathbf{Q} = \mathbf{A}\mathbf{\Lambda}\mathbf{A}^{-1} \ , \tag{83}$$

where $\mathbf{\Lambda}$ is a diagonal matrix whose elements are eigenvalues of matrix $\mathbf{Q}$, and matrix $\mathbf{A}$ is composed of columns, the i^{th} column being the eigenvector associated with the i^{th} eigenvalue.

From the definition of propagator matrix (81) and equation (83), for a particular layer j ($j = 1, 2$) we have

$$\begin{aligned}\mathbf{P}_j &= \sum_{m=0}^{\infty} \frac{(-i\omega h_j H)^m}{m!} \left(\mathbf{A}_j \mathbf{\Lambda}_j \mathbf{A}_j^{-1}\right)^m \\ &= \sum_{m=0}^{\infty} \frac{(-i\omega h_j H)^m}{m!} \mathbf{A}_j \mathbf{\Lambda}_j \mathbf{A}_j^{-1} \cdot \mathbf{A}_j \mathbf{\Lambda}_j \mathbf{A}_j^{-1} \cdots \mathbf{A}_j \mathbf{\Lambda}_j \mathbf{A}_j^{-1} \\ &= \mathbf{A}_j \left(\sum_{m=0}^{\infty} \frac{(-i\omega h_j H)^m}{m!} \mathbf{\Lambda}_j^m \right) \mathbf{A}_j^{-1}.\end{aligned}$$

or

$$\mathbf{P}_j = \mathbf{A}_j \exp(-i\omega h_j H \mathbf{\Lambda}_j) \mathbf{A}_j^{-1}. \tag{84}$$

Note that since $\mathbf{\Lambda}_j$ is a diagonal matrix,

$$\det \mathbf{P}_j = \exp(\mathrm{tr}\mathbf{\Lambda}_j). \tag{85}$$

For wavelengths much larger than the spatial period of stratification, equivalent medium theory can be used. The system matrix $\mathbf{Q}^*$ of an equivalent homogeneous medium (one period of two layers) can be defined as

$$\exp\left(-i\omega H \mathbf{Q}^*\right) = \exp\left(-i\omega h_2 H \mathbf{Q}_2\right) \exp\left(-i\omega h_1 H \mathbf{Q}_1\right) = \mathbf{P}_2\left(h_2 H\right) \mathbf{P}_1\left(h_1 H\right) \equiv \mathbf{P}^*\left(H\right) \ . \tag{86}$$

For an equivalent medium containing two layers, equations (86) and (84) yield

$$\exp\left(-i\omega H \mathbf{Q}^*\right) = \mathbf{A}_2 \exp(-i\omega h_2 H \mathbf{\Lambda}_2) \mathbf{A}_2^{-1} \mathbf{A}_1 \exp(-i\omega h_1 H \mathbf{\Lambda}_1) \mathbf{A}_1^{-1}. \tag{87}$$

In equation (87), the RHS is the solution of equation (80) for the layered medium expressed through the parameters of each layer, and the LHS is the propagator matrix

for the pair of layers (one period) whose eigenvalues (corresponding to slownesses associated with matrix $\mathbf{Q}^*$) are as yet unknown. Each of these eigenvalues s_k^* is in turn related to a corresponding eigenvalue x_k of the matrix $\exp(-i\omega H\mathbf{Q}^*)$:

$$x_k = \exp(-i\omega H s_k^*). \tag{88}$$

Thus matrix $\exp(-i\omega H\mathbf{Q}^*)$ can be expressed in the form

$$\exp(-i\omega H\mathbf{Q}^*) = \mathbf{A}^* \exp(-i\omega H\mathbf{\Lambda}^*)(\mathbf{A}^*)^{-1}, \tag{89}$$

where $\mathbf{\Lambda}^*$ is diagonal matrix with elements s_k^*, and $\mathbf{A}^*$ is the corresponding matrix of eigenvectors. Since matrices on the left and right hand sides of equation (86) are equal, they must have the same eigenvalues. Therefore eigenvalues x_k of $\exp(-i\omega H\mathbf{Q}^*)$ must also be equal to the corresponding eigenvalues of the matrix $\mathbf{P}_2\mathbf{P}_1$

$$\det|\mathbf{P}_2\mathbf{P}_1 - x\mathbf{I}| = 0\ , \tag{90}$$

that is x_k are the roots of the characteristic polynomial $\det|\mathbf{P}_2\mathbf{P}_1 - x\mathbf{I}|$.

In this work, propagation of compressional waves is considered in the direction normal to the stratification because the effect of fluid flow on dispersion and attenuation is maximal in this direction. However before considering a layered poroelastic medium, we will first illustrate the use of the propagator matrix method for acoustic (or elastic) case.

3.3 Effective modulus for periodically layered elastic medium

One can consider an elastic medium as a limiting case of a porous medium with zero porosity. In this case $p = 0,\ \dot{\mathbf{w}} = \mathbf{0}$, and for normal incidence of compressional waves

(horizontal slowness $s = 0$), equation (79) reduces to

$$\frac{\partial}{\partial z}\begin{bmatrix} \dot{u} \\ \\ \sigma \end{bmatrix} = -i\omega \begin{bmatrix} 0 & \frac{1}{L} \\ \\ \rho & 0 \end{bmatrix} \begin{bmatrix} \dot{u} \\ \\ \sigma \end{bmatrix} , \tag{91}$$

or

$$\frac{\partial}{\partial z}\mathbf{b}(z) = -i\omega \mathbf{Q}(z)\mathbf{b}(z) ,$$

with

$$\mathbf{b} = \begin{bmatrix} \dot{u} & \sigma \end{bmatrix}^T ,$$

and

$$Q = \begin{bmatrix} 0 & \frac{1}{L} \\ \\ \rho & 0 \end{bmatrix}$$

where $\sigma = \sigma_{zz}$ and $\dot{u} = \dot{u}_z$. Equations (91) could of course be obtained directly from equation of motion (26) and constitutive equation (17) for elastic media. Then solving eigenvalue problem for $\mathbf{Q}$, we get eigenvalue and left and right eigenvector matrices

$$\mathbf{\Lambda} = \begin{bmatrix} \sqrt{\frac{\rho}{L}} & 0 \\ \\ 0 & -\sqrt{\frac{\rho}{L}} \end{bmatrix} , \ \mathbf{A} = \begin{bmatrix} \frac{1}{\sqrt{\rho L}} & \frac{-1}{\sqrt{\rho L}} \\ \\ 1 & 1 \end{bmatrix} , \ \mathbf{A}^{-1} = \frac{1}{2}\begin{bmatrix} \sqrt{L\rho} & 1 \\ \\ -\sqrt{L\rho} & 1 \end{bmatrix} .$$

Note that $tr(\Lambda) = 0$ and according to equation (84), $\det(P) = 1$. We aim to obtain effective parameters for a periodically alternating layers of two types: 1 and 2. For a single layer j $(j = 1, 2)$, the from equations (83) and (84), propagator matrix is

$$\mathbf{P}_j = \begin{bmatrix} \cos\left(\omega h_j H\sqrt{\frac{\rho_j}{L_j}}\right) & \frac{i}{\sqrt{\rho_j L_j}}\sin\left(\omega h_j H\sqrt{\frac{\rho_j}{L_j}}\right) \\ \\ i\sqrt{\rho_j L_j}\sin\left(\omega h_j H\sqrt{\frac{\rho_j}{L_j}}\right) & \cos\left(\omega h_j H\sqrt{\frac{\rho_j}{L_j}}\right) \end{bmatrix} .$$

According to equation (87), the product of propagator matrices for each layer $\mathbf{P}_2\mathbf{P}_1 = \mathbf{P}^*$ can be calculated. The elements of $\mathbf{P}^*$ are

$$
\begin{aligned}
P_{11}^{*} &= \cos\left(\omega h_1 H\sqrt{\frac{\rho_1}{L_1}}\right)\cos\left(\omega h_2 H\sqrt{\frac{\rho_2}{L_2}}\right) \\
&\quad -\frac{\sqrt{\rho_2 L_2}}{\sqrt{\rho_1 L_1}}\sin\left(\omega h_1 H\sqrt{\frac{\rho_1}{L_1}}\right)\sin\left(\omega h_2 H\sqrt{\frac{\rho_2}{L_2}}\right)\ , \\
P_{12}^{*} &= \frac{i}{\sqrt{\rho_2 L_2}}\cos\left(\omega h_1 H\sqrt{\frac{\rho_1}{L_1}}\right)\sin\left(\omega h_2 H\sqrt{\frac{\rho_2}{L_2}}\right) \\
&\quad +\frac{i}{\sqrt{\rho_1 L_1}}\cos\left(\omega h_2 H\sqrt{\frac{\rho_2}{L_2}}\right)\sin\left(\omega h_1 H\sqrt{\frac{\rho_1}{L_1}}\right)\ , \\
P_{21}^{*} &= i\sqrt{\rho_1 L_1}\cos\left(\omega h_2 H\sqrt{\frac{\rho_2}{L_2}}\right)\sin\left(\omega h_1 H\sqrt{\frac{\rho_1}{L_1}}\right) \\
&\quad +i\sqrt{\rho_2 L_2}\cos\left(\omega h_1 H\sqrt{\frac{\rho_1}{L_1}}\right)\sin\left(\omega h_2 H\sqrt{\frac{\rho_2}{L_2}}\right)\ , \\
P_{22}^{*} &= \cos\left(\omega h_1 H\sqrt{\frac{\rho_1}{L_1}}\right)\cos\left(\omega h_2 H\sqrt{\frac{\rho_2}{L_2}}\right) \\
&\quad -\frac{\sqrt{\rho_1 L_1}}{\sqrt{\rho_2 L_2}}\sin\left(\omega h_1 H\sqrt{\frac{\rho_1}{L_1}}\right)\sin\left(\omega h_2 H\sqrt{\frac{\rho_2}{L_2}}\right)\ .
\end{aligned}
$$

Note that $\mathrm{tr}(\mathbf{\Lambda}_j) = 0$ and according to equation (84), $\det(\mathbf{P}_j) = 1$ and $\det|\mathbf{P}_2\mathbf{P}_1| = 1$. Thus characteristic equation for $\mathbf{P}_2\mathbf{P}_1$ is,

$$
\lambda^2 - \left(P_{11}^{*} + P_{22}^{*}\right)\lambda + 1 = 0\ , \tag{92}
$$

so the eigenvalues depends only on $(P_{11}^{*} + P_{22}^{*})$ where

$$
\begin{aligned}
P_{11}^{*} + P_{22}^{*} &= 2\cos\left(\omega h_1 H\sqrt{\frac{\rho_1}{L_1}}\right)\cos\left(\omega h_2 H\sqrt{\frac{\rho_2}{L_2}}\right) \\
&\quad -\left(\frac{\sqrt{\rho_1 L_1}}{\sqrt{\rho_2 L_2}} + \frac{\sqrt{\rho_2 L_2}}{\sqrt{\rho_1 L_1}}\right)\sin\left(\omega h_1 H\sqrt{\frac{\rho_1}{L_1}}\right)\sin\left(\omega h_2 H\sqrt{\frac{\rho_2}{L_2}}\right)
\end{aligned} \tag{93}
$$

On the other hand $\mathbf{P}^{*}$ is equal to the propagator matrix for the whole spatial period of an equivalent medium, so from equation (89) we have

$$
\mathbf{P}^{*} = \mathbf{A}^{*}\exp(-i\omega H\mathbf{\Lambda}^{*})\left(\mathbf{A}^{*}\right)^{-1}, \tag{94}
$$

or

$$
\mathbf{P}^{*} = \begin{bmatrix} \cos\left(\omega H s^{*}\right) & \frac{i}{\sqrt{\rho^{*}L^{*}}}\sin\left(\omega H s^{*}\right) \\ i\sqrt{\rho^{*}L^{*}}\sin\left(\omega H s^{*}\right) & \cos\left(\omega H s^{*}\right) \end{bmatrix},
$$

where s^*, ρ^*, L^* are yet unknown slowness, density and P-wave modulus of the equivalent medium. Again, the eigenvalues of this matrix are defined by the sum of its diagonal elements,

$$P_{11}^* + P_{22}^* = 2\cos\left(\omega H s^*\right). \tag{95}$$

Slowness s^* for the equivalent medium can now be calculated by equating right-hand sides of equations (95) and (93). This gives

$$\begin{aligned} 2\cos\left(\omega H s^*\right) = & 2\cos\left(\omega h_1 H\sqrt{\frac{\rho_1}{L_1}}\right)\cos\left(\omega h_2 H\sqrt{\frac{\rho_2}{L_2}}\right) \\ & -\left(\frac{\sqrt{\rho_1 L_1}}{\sqrt{\rho_2 L_2}}+\frac{\sqrt{\rho_2 L_2}}{\sqrt{\rho_1 L_1}}\right)\sin\left(\omega h_1 H\sqrt{\frac{\rho_1}{L_1}}\right)\sin\left(\omega h_2 H\sqrt{\frac{\rho_2}{L_2}}\right) \end{aligned} \tag{96}$$

Equation (96) is an exact dispersion equation for a periodic system of alternating elastic layers. This equation was derived by Rytov (1956) using Floquet theorem for differential equations with periodic coefficients (Brillouin, 1963). To our knowledge the above derivation of the Rytov equation using matrix propagator method is new.

In general, equivalent slowness s^* is frequency dependent. For a finely layered medium $\omega s^* H \equiv \theta \ll 1$ (low frequency limit) equation (96) can be simplified using asymptotic expansion of sin and cosine for small argument. Then we have,

$$\omega^2 H^2 \left(s^*\right)^2 = \frac{1}{2}\omega^4 h_1^2 h_2^2 H^4 \frac{\rho_1}{L_1}\frac{\rho_2}{L_2} + \left(\frac{\sqrt{\rho_1 L_1}}{\sqrt{\rho_2 L_2}}+\frac{\sqrt{\rho_2 L_2}}{\sqrt{\rho_1 L_1}}\right) h_1 h_2 \omega^2 H^2 \sqrt{\frac{\rho_1}{L_1}}\sqrt{\frac{\rho_2}{L_2}}\,,$$

and neglecting term of $\mathcal{O}(\omega^4)$,

$$\left(s^*\right)^2 = h_1 h_2 \frac{\left(\rho_1 L_1 + \rho_2 L_2\right)}{L_1 L_2} = \rho^*\left(\frac{h_1}{L_1}+\frac{h_2}{L_2}\right)\,,$$

where $\rho^* = h_1\rho_1 + h_2\rho_2$ is the average density. For the effective P-wave modulus $L^* = \rho^*/\left(s^*\right)^2$ this yields

$$\frac{1}{L^*} = \frac{h_1}{L_1}+\frac{h_2}{L_2} = \left\langle\frac{1}{L}\right\rangle\,,$$

where angle brackets $\langle 1/L \rangle$ denote thickness weighted average of the quantity $1/L$, which is equal to Backus average (Backus, 1962) for compressional wave velocity modulus for normal incidence.

3.4 Effective modulus for periodically layered poroelastic medium

3.4.1 Properties for a single homogeneous layer

For a horizontally stratified poroelastic medium and normal incidence of compressional wave (horizontal slowness $s = 0$), the first order system of equations (79) can be written, in the frequency domain, as four differential equations for $\dot{u}$, $\dot{w}$, σ_{zz} and p in standard form (80)

$$\frac{\partial}{\partial z}\mathbf{b}(z) = -i\omega\mathbf{Q}\mathbf{b}(z)\ , \tag{97}$$

where now

$$\mathbf{b} \equiv \begin{bmatrix} \dot{u} \\ \dot{w} \\ \sigma_{zz} \\ -p \end{bmatrix}\ , \tag{98}$$

$$\mathbf{Q} \equiv \begin{bmatrix} 0 & 0 & \frac{1}{L} & -\frac{\alpha}{L} \\ 0 & 0 & -\frac{\alpha}{L} & \frac{1}{N} \\ \rho & \rho_f & 0 & 0 \\ \rho_f & \tilde{m} & 0 & 0 \end{bmatrix}\ , \tag{99}$$

and $\rho = (1-\phi)\rho_g + \phi\rho_f$ is the average density of the saturated material. All elements of the system matrix $\mathbf{Q}$ are combinations of material constants independent of frequency

except for the element $Q_{42} = \tilde{m} = m + i\eta/\omega\kappa$**.** This term combines two terms from the equations of motion (51) and (52) for the poroelastic medium in z direction (in other directions equations are trivial) which can be written in the form (Biot, 1962)

$$\begin{aligned}
&\frac{\partial \sigma_{zz}}{\partial z} = \frac{\partial^2}{\partial t^2}(\rho u + \rho_f w) \ , \\
&-\frac{\partial p}{\partial z} = \frac{\partial^2}{\partial t^2}(\rho_f u + m w) + \frac{\eta}{\kappa}\frac{\partial w}{\partial t} = \frac{\partial^2}{\partial t^2}\rho_f u + \frac{\partial}{\partial t}\left(\frac{\eta}{\kappa} + m\frac{\partial}{\partial t}\right) w \ ,
\end{aligned} \tag{100}$$

where

$$\left(\frac{\eta}{\kappa} + m\frac{\partial}{\partial t}\right) \rightarrow \frac{\eta}{\kappa}\left(1 - i\omega\frac{\kappa m}{\eta}\right) = \frac{\eta}{\kappa}\left(1 - i\frac{\omega}{\omega_B}\frac{\phi m}{\rho_f}\right) \tag{101}$$

is Biot's visco-dynamic operator in frequency domain. At frequencies much smaller than Biot's characteristic frequency $\omega_B = \eta\phi/\kappa\rho_f$, the second equation of motion (100) reduces to Darcy's law, and Biot's visco-dynamic operator becomes just a viscous operator

$$-\frac{\partial p}{\partial z} = \rho_f \frac{\partial}{\partial t}\dot{u} + \left(\frac{\eta}{\kappa} + m\frac{\partial}{\partial t}\right)\dot{w} = -i\omega\rho_f \dot{u} + \left(\frac{\eta}{\kappa} - i\omega m\right)\dot{w} \rightarrow \frac{\eta}{\kappa}\dot{w} \ . \tag{102}$$

Here and below we will assume that frequencies are much smaller than Biot's characteristic frequency and hence

$$\tilde{m} = i\eta/\omega\kappa.$$

An eigenvalue-eigenvector decomposition of system matrix $\mathbf{Q}$ for a single layer is $\mathbf{Q} = \mathbf{A}\mathbf{\Lambda}\mathbf{A}^{-1}$. Matrix $\mathbf{\Lambda}$ is a diagonal matrix whose diagonal elements, call them $\lambda_j,\ j = 1, 2, 3, 4$, are eigenvalues of $\mathbf{Q}$. Matrix $\mathbf{A}$ is the matrix whose columns are eigenvectors, the k^{th} column being the eigenvector associated with the k^{th} eigenvalue. Therefore $\mathbf{Q}^m = \mathbf{A}\mathbf{\Lambda}^m\mathbf{A}^{-1}$, and propagator matrix $\mathbf{P}\,(z - z_0)$ of equation (81) can be written in the form (84)

$$\mathbf{P}\,(z - z_0) = \sum_{m=0}^{\infty} \frac{\left[-i\omega\,(z - z_0)\right]^m}{m!}\mathbf{A}\mathbf{\Lambda}^m\mathbf{A}^{-1} = \mathbf{A}\exp(-i\omega\,(z - z_0)\,\mathbf{\Lambda})\mathbf{A}^{-1} \tag{103}$$

or

$$\mathbf{P}\left(z-z_0\right)=\mathbf{A}\begin{bmatrix} e^{-i\omega(z-z_0)\lambda_1} & 0 & 0 & 0 \\ 0 & e^{-i\omega(z-z_0)\lambda_2} & 0 & 0 \\ 0 & 0 & e^{-i\omega(z-z_0)\lambda_3} & 0 \\ 0 & 0 & 0 & e^{-i\omega(z-z_0)\lambda_4} \end{bmatrix}\mathbf{A}^{-1}\ . \qquad (104)$$

The eigenvalues of $\mathbf{Q}$ are determined as roots of the characteristic equation for $\mathbf{Q}$ which is a quadratic equation in λ^2:

$$\lambda^4-\frac{1}{L}\left[\tilde{m}\frac{C}{M}+\rho-2\alpha\rho_f\right]\lambda^2+\frac{\rho\tilde{m}-\rho_f^2}{LM}=0\ . \qquad (105)$$

This equation has exact solutions

$$\begin{aligned}\lambda_{\pm}^2 &= \frac{1}{2L}\left[\tilde{m}\frac{C}{M}+\rho-2\alpha\rho_f\pm\sqrt{\left(\tilde{m}\frac{C}{M}+\rho-2\alpha\rho_f\right)^2-4L\frac{\rho\tilde{m}-\rho_f^2}{M}}\ \right] \\ &= \frac{\tilde{m}C}{2LM}\left[1+\frac{M}{\tilde{m}C}(\rho-2\alpha\rho_f)\right]\left[1\pm\sqrt{1-\frac{4\rho LM}{\tilde{m}C^2}\frac{1-\frac{\rho_f^2}{\rho\tilde{m}}}{\left[1+\frac{M}{\tilde{m}C}(\rho-2\alpha\rho_f)\right]^2}}\ \right] \qquad (106)\end{aligned}$$

The solutions $\pm\lambda_+$ and $\pm\lambda_-$ correspond to the slownesses of four vertically propagating compressional waves (with displacements in the direction of propagation). To see which root corresponds to which wave, these roots can be evaluated as $\omega\to 0$, which is equivalent to letting $\tilde{m}$ be very large. In this limit the roots are given by

$$\lambda_{\pm}^2\approx\frac{\tilde{m}C}{2LM}\left[1\pm\sqrt{1-\frac{4\rho LM}{\tilde{m}C^2}}\right]\approx\frac{\tilde{m}C}{2LM}\left[1\pm\left(1-\frac{2\rho LM}{\tilde{m}C^2}\right)\right]\ ,$$

and finally "+" and "−" roots are

$$\lambda_+^2=\tilde{m}\frac{C}{LM}\sim\frac{\imath\eta C}{\omega\kappa LM}\ ,\qquad \lambda_-^2=\frac{\rho}{C}\ , \qquad (107)$$

Thus, for a homogeneous porous medium the solution (81) of equation (80) can be written as the sum of up and down propagating plane compressional waves with

slownesses $s_p = \lambda_-$ (fast wave) and $s_d = \lambda_+$ (slow wave), which in the low frequency limit is of diffusion nature. Therefore, we have

$$\mathbf{\Lambda} = \begin{bmatrix} s_p & 0 & 0 & 0 \\ 0 & -s_p & 0 & 0 \\ 0 & 0 & s_d & 0 \\ 0 & 0 & 0 & -s_d \end{bmatrix}$$

and

$$e^{i\omega(z-z_0)\mathbf{\Lambda}} = \begin{bmatrix} e^{i\omega(z-z_0)s_p} & 0 & 0 & 0 \\ 0 & e^{-i\omega(z-z_0)s_p} & 0 & 0 \\ 0 & 0 & e^{i\omega(z-z_0)s_d} & 0 \\ 0 & 0 & 0 & e^{-i\omega(z-z_0)s_d} \end{bmatrix}.$$

As can be seen from equation (103), eigenvectors of $\mathbf{Q}$ are also the eigenvectors of $\mathbf{P}$. The j^{th} eigenvector associated with a particular eigenvalue λ_j can be written as

$$\begin{bmatrix} \frac{1}{\lambda_j}\frac{\rho_f/M-\alpha\lambda_j^2}{\lambda_j^2-(\rho-\alpha\rho_f)/L} \\ \frac{C}{\lambda_j M}\frac{\lambda_j^2-\rho/C}{\lambda_j^2-(\rho-\alpha\rho_f)/L} \\ C\frac{\rho_f/M-\alpha\rho/C}{\lambda_j^2-(\rho-\alpha\rho_f)/L} \\ L \end{bmatrix}.$$

Therefore the matrix of eigenvectors $\mathbf{A}$ is exactly

$$\mathbf{A} = \begin{bmatrix} \frac{1}{s_p}\frac{\rho_f/M-\alpha s_p^2}{s_p^2-(\rho-\alpha\rho_f)/L} & -\frac{1}{s_p}\frac{\rho_f/M-\alpha s_p^2}{s_p^2-(\rho-\alpha\rho_f)/L} & \frac{1}{s_d}\frac{\rho_f/M-\alpha s_d^2}{s_d^2-(\rho-\alpha\rho_f)/L} & -\frac{1}{s_d}\frac{\rho_f/M-\alpha s_d^2}{s_d^2-(\rho-\alpha\rho_f)/L} \\ \frac{C}{s_pM}\frac{s_p^2-\rho/C}{s_p^2-(\rho-\alpha\rho_f)/L} & -\frac{C}{s_pM}\frac{s_p^2-\rho/C}{s_p^2-(\rho-\alpha\rho_f)/L} & \frac{C}{s_dM}\frac{s_d^2-\rho/C}{s_d^2-(\rho-\alpha\rho_f)/L} & -\frac{C}{s_dM}\frac{s_d^2-\rho/C}{s_d^2-(\rho-\alpha\rho_f)/L} \\ C\frac{\rho_f/M-\alpha\rho/C}{s_p^2-(\rho-\alpha\rho_f)/L} & C\frac{\rho_f/M-\alpha\rho/C}{s_p^2-(\rho-\alpha\rho_f)/L} & C\frac{\rho_f/M-\alpha\rho/C}{s_d^2-(\rho-\alpha\rho_f)/L} & C\frac{\rho_f/M-\alpha\rho/C}{s_d^2-(\rho-\alpha\rho_f)/L} \\ L & L & L & L \end{bmatrix} .$$

From the identity $L \equiv C - \alpha^2 M$, note that

$$\frac{\rho}{C} - \frac{\rho-\alpha\rho_f}{L} = \rho\left(\frac{1}{C}-\frac{1}{L}\right) + \frac{\alpha\rho_f}{L} = \frac{\alpha M}{L}\left[\frac{\rho_f}{M} + \frac{\rho}{\alpha M}\left(\frac{L}{C}-1\right)\right] = \frac{\alpha M}{L}\left[\frac{\rho_f}{M} - \frac{\alpha\rho}{C}\right] . \tag{108}$$

In order to simplify elements of eigenvectors we have to separate terms of the different dependence of ω in expressions for eigenvalues and then to see what terms can be neglected in low frequency limit. For the "+" root of equation (106),

$$\begin{aligned} \lambda_+^2 &\approx \tilde{m}\frac{C}{2LM}\left[1+\frac{M}{\tilde{m}C}(\rho-2\alpha\rho_f)\right]\left[1+\left(1-2\frac{\rho LM}{\tilde{m}C^2}+\mathcal{O}(\tilde{m}^{-2})\right)\right] = \\ &= \tilde{m}\frac{C}{LM}\left[1+\frac{M}{\tilde{m}C}(\rho-2\alpha\rho_f)\right]\left[1-\frac{\rho LM}{\tilde{m}C^2}+\mathcal{O}(\tilde{m}^{-2})\right] \approx \\ &\approx \tilde{m}\frac{C}{LM} + \frac{\rho\left(1-\frac{L}{C}\right)-2\alpha\rho_f}{L} + \mathcal{O}(\omega) = i\frac{\eta C}{\omega\kappa LM} + \frac{mC}{LM} + \frac{\alpha^2 M\rho}{LC} + \frac{2\alpha\rho_f}{L} + \mathcal{O}(\omega) . \end{aligned}$$

In the zero frequency limit, these eigenvalues give the phase slowness and decay of the Biot's slow wave. A similar calculation of the "−" root of equation (106) gives an expression for the fast wave. Finally, for low frequency (terms of the order of $\mathcal{O}(\omega^2)$ are neglected),

$$s_p^2 = \frac{\rho}{C} + \mathcal{O}(\omega) , \quad s_d^2 = i\frac{\eta C}{\omega\kappa LM}\left[1+\mathcal{O}(\omega)\right] \equiv i\frac{1}{\omega D}\left[1+\mathcal{O}(\omega)\right] , \tag{109}$$

where $D = \kappa LM/\eta C$ is the diffusion coefficient of dimension $[length^2/time]$. Using

equation (108), $\mathbf{A}$ can be written as

$$\mathbf{A} = \begin{bmatrix} \sqrt{\frac{C}{\rho}}\frac{L}{\alpha M} + \mathcal{O}(\omega) & -\sqrt{\frac{C}{\rho}}\frac{L}{\alpha M} + \mathcal{O}(\omega) & -\alpha\sqrt{-\imath\omega D}\,[1+\mathcal{O}(\omega)] & \alpha\sqrt{-\imath\omega D}\,[1+\mathcal{O}(\omega)] \\ 0 + \mathcal{O}(\omega) & 0 + \mathcal{O}(\omega) & \frac{C}{M}\sqrt{-\imath\omega D}\,[1+\mathcal{O}(\omega)] & -\frac{C}{M}\sqrt{-\imath\omega D}\,[1+\mathcal{O}(\omega)] \\ C\frac{L}{\alpha M} + \mathcal{O}(\omega) & C\frac{L}{\alpha M} + \mathcal{O}(\omega) & 0 + \mathcal{O}(\omega) & 0 + \mathcal{O}(\omega) \\ L & L & L & L \end{bmatrix}, \tag{110}$$

or in approximation neglecting terms of $\mathcal{O}(\omega)$,

$$\mathbf{A} = \begin{bmatrix} \sqrt{\frac{C}{\rho}}\frac{L}{\alpha M} & -\sqrt{\frac{C}{\rho}}\frac{L}{\alpha M} & -\alpha\sqrt{-\imath\omega D} & \alpha\sqrt{-\imath\omega D} \\ 0 & 0 & \frac{C}{M}\sqrt{-\imath\omega D} & -\frac{C}{M}\sqrt{-\imath\omega D} \\ C\frac{L}{\alpha M} & C\frac{L}{\alpha M} & 0 & 0 \\ L & L & L & L \end{bmatrix}. \tag{111}$$

Due to the simple structure of $\mathbf{A}$, it is straightforward to find that, to $\mathcal{O}(\omega)$,

$$\mathbf{A}^{-1} = \frac{1}{2}\begin{bmatrix} \sqrt{\frac{\rho}{C}}\frac{\alpha M}{L} & \sqrt{\frac{\rho}{C}}\frac{\alpha^2 M^2}{CL} & \frac{\alpha M}{CL} & 0 \\ -\sqrt{\frac{\rho}{C}}\frac{\alpha M}{L} & -\sqrt{\frac{\rho}{C}}\frac{\alpha^2 M^2}{CL} & \frac{\alpha M}{CL} & 0 \\ 0 & \frac{M}{C\sqrt{-\imath\omega D}} & -\frac{\alpha M}{CL} & \frac{1}{L} \\ 0 & -\frac{M}{C\sqrt{-\imath\omega D}} & -\frac{\alpha M}{CL} & \frac{1}{L} \end{bmatrix}. \tag{112}$$

Following equation (104), the propagator matrix can be found explicitly by matrix multiplication

$$\mathbf{P}(z-z_0) = \mathbf{A}e^{-i\omega(z-z_0)\mathbf{\Lambda}}\mathbf{A}^{-1} =$$

$$= \begin{bmatrix} \mathcal{C}_p & R\left[\mathcal{C}_p - \mathcal{C}_d\right] & -\imath\frac{1}{\sqrt{\rho C}}\mathcal{S}_p - \imath\frac{\alpha}{L}R\sqrt{-\imath\omega D}\mathcal{S}_d & \imath\frac{\alpha}{L}\sqrt{-\imath\omega D}\mathcal{S}_d \\ 0 & \mathcal{C}_d & \imath\frac{\alpha}{L}\sqrt{-\imath\omega D}\mathcal{S}_d & -\imath\frac{\alpha}{LR}\sqrt{-\imath\omega D}\mathcal{S}_d \\ -\imath\sqrt{\rho C}\mathcal{S}_p & -\imath\sqrt{\rho C}R\mathcal{S}_p & \mathcal{C}_p & 0 \\ -\imath\sqrt{\rho C}R\mathcal{S}_p & -\imath\sqrt{\rho C}R^2\mathcal{S}_p - \imath\frac{LR}{\alpha\sqrt{-\imath\omega D}}\mathcal{S}_d & R\left[\mathcal{C}_p - \mathcal{C}_d\right] & \mathcal{C}_d \end{bmatrix} \tag{113}$$

where dimensionless parameter $R = \alpha M/C$, and

$$\mathcal{C}_p \equiv \cos\omega\sqrt{\frac{\rho}{C}}\left(z - z_0\right),\ \mathcal{S}_p \equiv \sin\omega\sqrt{\frac{\rho}{C}}\left(z - z_0\right),$$
$$\mathcal{C}_d \equiv \cos\sqrt{\frac{\imath\omega}{D}}\left(z - z_0\right),\ \mathcal{S}_d \equiv \sin\sqrt{\frac{\imath\omega}{D}}\left(z - z_0\right).$$

Neglecting terms of $\mathcal{O}(\omega^2)$, the propagator matrix for a single layer is

$$\mathbf{P}(z - z_0) \approx \begin{bmatrix} 1 & 0 & -\imath\omega\frac{1}{L}\left(z - z_0\right) & \imath\omega\frac{\alpha}{L}\left(z - z_0\right) \\ 0 & 1 & \imath\omega\frac{\alpha}{L}\left(z - z_0\right) & -\imath\omega\frac{\alpha}{LR}\left(z - z_0\right) \\ -\imath\omega\rho\left(z - z_0\right) & -\imath\omega\rho R\left(z - z_0\right) & 1 & 0 \\ -\imath\omega\rho R\left(z - z_0\right) & \left[\frac{LM}{CD} - \imath\omega\rho R^2\right]\left(z - z_0\right) & 0 & 1 \end{bmatrix},$$

$$\mathbf{P}(z - z_0) \approx \begin{bmatrix} 1 & 0 & 0 & 0 \\ 0 & 1 & 0 & 0 \\ 0 & 0 & 1 & 0 \\ 0 & \frac{\eta}{\kappa}\left(z - z_0\right) & 0 & 1 \end{bmatrix} - \imath\omega\left(z - z_0\right)\begin{bmatrix} 0 & 0 & \frac{1}{L} & -\frac{\alpha}{L} \\ 0 & 0 & -\frac{\alpha}{L} & \frac{C}{ML} \\ \rho & \rho R & 0 & 0 \\ \rho R & \rho R^2 & 0 & 0 \end{bmatrix}. \tag{114}$$

To better understand the physical nature of parameters in matrices A and P we can derive the pore pressure induced by the incident wave (loading of the skeleton) in

adjacent layers, and consequently how fluid responds to the perturbation of pressure.

Using Gassmann relation (42) we can write constitutive relation (58) in terms of dry modulus λ:

$$\sigma_{ij} = 2\mu\varepsilon_{ij} + \left[(\lambda + \alpha^2 M)\varepsilon - \alpha(p + \alpha M\varepsilon)\right]\delta_{ij} \ .$$

Then, in our 1D case

$$\varepsilon = \frac{\sigma_{zz} + \alpha p}{L}. \tag{115}$$

When there is no fluid flow between layers $\xi = 0$, the second of equations (57) gives

$$\varepsilon = \frac{-p}{\alpha M}. \tag{116}$$

Combining the equations (115) and (116) yields

$$-p = \frac{\alpha M}{C}\sigma_{zz} = R\sigma_{zz} \ . \tag{117}$$

Now we can see that material parameter R connects the total stress in bulk material caused by the incident fast wave with the pore fluid pressure. More precisely, R defines magnitude of the fluid pore pressure induced by incident wave in each layer. Because pore pressure depends on properties of the layers, different pressure will be induced on different sides of an interface. In order to equilibrate pressure, fluid will move from the more compliant layer to the stiffer one (for positive loading of skeleton $\sigma_{zz} > 0$). On the macroscopic scale this type of fluid motion has the same nature as "squirt" flow (Mavko and Nur, 1975; Jones, 1986). Change of pressure in time and in direction normal to the interface is controlled by the diffusion equation which can be derived from the second and fourth equations in (97)

$$\frac{\partial \dot{w}_z}{\partial z} = -\frac{\alpha}{L}\frac{\partial \sigma_{zz}}{\partial t} - \frac{C}{LM}\frac{\partial p}{\partial t} \ , \tag{118}$$

$$-\frac{\partial p}{\partial z} = \frac{\eta}{\kappa}\dot{w} \ , \tag{119}$$

Differentiating equation (119) with respect to z and substituting $\partial \dot{w}_z/\partial z$ from equation (118) into equation (119), and neglecting the term containing σ_{zz} (rigid frame approximation) gives the diffusion equation for fluid pore pressure

$$\frac{\partial^2 p}{\partial z^2} = \frac{\eta C}{\kappa LM}\frac{\partial p}{\partial t} \ ,$$

where $\kappa LM/C\eta = D$ is the pressure diffusivity. Note that this is low frequency result since the first term in equation (118) was neglected assuming very slow time rate of total stress within the EV (practically constant stress). From the second equation of (109), the slowness of the slow wave is

$$s_d^2 = \frac{i}{\omega D} \ ,$$

so it is natural to use parameters $R,\ D$ and $N = ML/C$ (which plays a similar role in the slow wave slowness as the fast P-wave modulus C plays in the fast wave slowness). Furthermore, substituting the expression for slowness of the slow wave into ansatz solution of the diffusion equation gives

$$p = p_0 \exp\left(i\omega\sqrt{\frac{i}{\omega D}}z\right) = p_0 \exp\left(i\omega\frac{1+i}{\sqrt{2\omega D}}z\right) = p_0 \exp\left(-\sqrt{\frac{\omega}{2D}}z\right)\exp\left(i\sqrt{\frac{\omega}{2D}}z\right) \ .$$

By analogy with equation (54), quantity $\delta = \sqrt{2D/\omega}$ is the pressure skin depth or diffusion length, which defines the distance from the pressure disturbance (interface) at which the fluid has enough time to move and equilibrate pressure within half period of the incident wave. In wave terminology, diffusion length can be considered as "wavelength" of the slow wave. The ratio of diffusion length and layer half-width

defines the magnitude of the attenuation relaxation process, which is maximal when this ratio equals 1. As frequency increases, diffusion length shortens to very small distances, and in the high frequency case (wavelength of the slow wave is much smaller than thickness of layer), the fluid no longer moves. For a homogenous porous medium at low frequencies, attenuation due to fluid flow is negligible because diffusion length is very large in comparison with the only existing spatial scale (average pore space radius). However, in an inhomogeneous (e.g., layered) medium, attenuation can be significant; it is caused by the conversion of energy from fast into slow wave (squirt flow) which depends on the elastic contrast between the layers (described by the parameter R). In this case there is a new spatial scale responsible for dispersion, the average thickness of layers (inhomogeneities), which is much larger than pore radius, and causes another peak of attenuation at frequencies much lower than the Biot's characteristic frequency. This is the reason why measuring dispersion and attenuation can be used for estimation of permeability through the diffusion coefficient. In terms of the parameters $R,\ D$ and N, matrix $\mathbf{A}$ given by (111) is

$$\mathbf{A} = \begin{bmatrix} \frac{s_p}{\rho R} & -\frac{s_p}{\rho R} & -Rd\sqrt{-i\omega} & Rd\sqrt{-i\omega} \\ 0 & 0 & d\sqrt{-i\omega} & -d\sqrt{-i\omega} \\ R^{-1} & R^{-1} & 0 & 0 \\ 1 & 1 & 1 & 1 \end{bmatrix},$$

and for inverse matrix $\mathbf{A}^{-1}$

$$\mathbf{A}^{-1} = \frac{1}{2}\begin{bmatrix} \frac{\rho R}{s_p} & \frac{\rho R^2}{s_p} & R & 0 \\ -\frac{\rho R}{s_p} & -\frac{\rho R^2}{s_p} & R & 0 \\ 0 & \frac{1}{d\sqrt{-i\omega}} & -R & 1 \\ 0 & -\frac{1}{d\sqrt{-i\omega}} & -R & 1 \end{bmatrix},$$

where $d = \sqrt{D}/N$.

3.4.2 Periodic two - layers medium

From everyday experience it is known that when two sponges of different elastic properties are pressed together, the fluid will move from the more compliant sponge into the stiffer sponge. In the case of a layered medium a similar effect is expected, such that fluid will flow across the interface between different layers as a consequence of applying external stress to the medium.

Mathematically, this can be analyzed using the matrix propagator procedure outlined in section 3.2. In particular, effective slownesses of the fast and slow waves in a periodic system of alternating layers of types 1 and 2 can be derived as eigenvalues x_i, $i = 1..4$ of the matrix $\mathbf{P}_2\mathbf{P}_1$. Following equations (87) (88) (89) and (90), the characteristic polynomial $\det|\mathbf{P}_2\mathbf{P}_1 - x\mathbf{I}|$ of the matrix $\mathbf{P}_2\mathbf{P}_1$ can be written as

$$(x - x_1)(x - x_2)(x - x_3)(x - x_4) = x^4 + a_3x^3 + a_2x^2 + a_1x + a_0 ,$$

where

$$
\begin{aligned}
a_0 &= x_1 x_2 x_3 x_4, \\
a_1 &= -\left(x_1 x_2 x_3 + x_1 x_2 x_4 + x_1 x_3 x_4 + x_2 x_3 x_4\right) = -a_0 \left(\frac{1}{x_1} + \frac{1}{x_1} + \frac{1}{x_1} + \frac{1}{x_1}\right) , \\
a_2 &= x_1 x_2 + x_1 x_3 + x_1 x_4 + x_2 x_3 + x_2 x_4 + x_3 x_4 = \left(x_1 + x_2\right)\left(x_3 + x_4\right) + x_1 x_2 + x_3 x_4 , \\
a_3 &= -\left(x_1 + x_2 + x_3 + x_4\right) . \qquad (120)
\end{aligned}
$$

Because unknown eigenvalues s_k^* in equations (87) and (89) represent slownesses of fast and slow compressional waves in the equivalent medium, they appear in pairs of opposite signs

$$s_{1,2}^* = \pm s_p^* , \; s_{3,4}^* = \pm s_d^*,$$

or

$$x_{1,2} = \exp(\pm i\omega H s_p^*) , \; x_{3,4} = \exp(\pm i\omega H s_d^*) . \qquad (121)$$

Substituting (121) into equations (120) yields

$$
\begin{aligned}
a_1 &= -2\left[\cos(\omega H s_p^*) + \cos(\omega H s_d^*)\right] , \qquad (122) \\
a_2 &= 2\left[1 + 2\cos(\omega H s_p^*)\cos(\omega H s_d^*)\right] , \qquad (123) \\
a_0 &= 1 , \; a_1 = a_3 . \qquad (124)
\end{aligned}
$$

Solving the system of equations (122) (123) gives a quadratic equation whose roots are

$$\cos(\omega H s_{p,d}^*) = \frac{-a_1 \pm \sqrt{a_1^2 - 4\left(a_2 - 2\right)}}{4}. \qquad (125)$$

Effective slownesses can be obtained by writing out coefficients a_1 and a_2 of the characteristic polynomial for matrix $\mathbf{P}_2\mathbf{P}_1$. These coefficients are functions of frequency, material properties, and slownesses of fast and slow waves in layers 1 and 2. Since period H is assumed to be small compared to the wavelength of the fast wave in layers 1 and 2, as well the equivalent medium, slownesses s_{p1}, $s_{p2}$and s_p^* are assumed to be small. Thus a small parameter t can be introduced through the substitution $s_{p1} \to t s_{p1}$, $s_{p2} \to t s_{p2}$, $s_p^* \to t s_p^*$. The sign of the discriminant in equation (125) corresponding to the fast wave should be the one that gives $\cos(\omega H t s_p^*) \to 1$ as $t \to 0$. Substituting a_1 and a_2 into equation (125) shows that

$$\lim_{t\to 0}\cos(\omega H t s_p^*) = \frac{1}{4}\left[2\left(1+\cos\omega H s_d^*\right) \pm 2\sqrt{\left(1+\cos\omega H s_d^*\right)^2 - 4\cos\omega H s_d^*}\right] =$$
$$= \frac{1}{2}\left[1+\cos\omega H s_d^* \pm \sqrt{\left(1-\cos\omega H s_d^*\right)^2}\right] = 1,\ \cos\omega H s_d^* .$$

Thus "+" sign corresponds to slowness of the fast wave. From equation (125) the fast slowness can be expressed as a function of t

$$\cos(\omega H t s_p^*) = B(t), \tag{126}$$

where

$$B(t) = \frac{-a_1 - \sqrt{a_1^2 - 4(a_2-2)}}{4}.$$

Expanding a_1 and a_2 and cosine in a power series in t, equation (126) can be rewritten as

$$1 - \frac{1}{2}\left(\omega H t s_p^*\right)^2 = 1 + B_1 t + B_2 t^2 + \mathcal{O}(t^3), \tag{127}$$

where

$$B_1 = \lim_{t\to 0}\frac{1}{t}\left[B(t) - 1\right],$$
$$B_2 = \lim_{t\to 0}\frac{1}{t^2}\left[B(t) - 1 - tB_1\right].$$

Reverting to the original slownesses $ts_{p1} \to s_{p1}$, $ts_{p2} \to s_{p2}$, $ts_p^* \to s_p^*$ yields the desired equation for the effective slowness

$$\left(\omega H s_p^*\right)^2 = -2\left(B_1 + B_2\right). \tag{128}$$

Coefficients B_1 and B_2 are functions of frequency, more precisely functions of $\sqrt{\omega}$. To obtain explicit expressions for these coefficients they can be expanded in power series in $\sqrt{\omega}$, and up to the terms $\mathcal{O}(\omega^2)$. For coefficient B_2, the first term in $\sqrt{\omega}$ is of the order $\mathcal{O}(\omega^2)$, hence taking into account the average properties (density and velocity modulus) for one spatial period gives

$$B_2 = -\frac{1}{2}\omega^2\left(\rho_1 h_1 + \rho_2 h_2\right) H\left(\frac{h_1 H}{C_1} + \frac{h_2 H}{C_2}\right) = -\frac{1}{2}\omega^2 H^2\left(h_1\rho_1 + h_2\rho_2\right)\left(\frac{h_1}{C_1} + \frac{h_2}{C_2}\right),$$

or

$$B_2 = -\frac{1}{2}\omega^2 H^2 \rho^* \left\langle \frac{1}{C} \right\rangle . \tag{129}$$

Note that coefficient B_2 does not depend on slownesses of slow waves in layers, so it describes the quasi-elastic case where there is no fluid flow between layers. By comparing equation (129) with the equation (200), it can also be seen that $-2B_2/\omega^2 H^2$ is the high frequency slowness.

For B_1 we get

$$B_1 = \left[d_1 \sin(\omega h_1 H s_{d1}) \left(1 - \cos\left(\omega h_2 H s_{d2}\right)\right) + d_2 \sin(\omega h_2 H s_{d2}) \left(1 - \cos\left(\omega h_1 H s_{d1}\right)\right)\right] \times$$
$$\times \frac{\omega^2 H \left(\rho_1 h_1 + \rho_2 h_2\right) \left(R_2 - R_1\right)^2 d_1 d_2}{\sqrt{i\omega}\left[2 d_1 d_2 \left(\cos\left(\omega h_1 H s_{d1}\right) \cos\left(\omega h_2 H s_{d2}\right) - 1\right) - \left(d_1^2 + d_2^2\right) \sin(\omega h_1 H s_{d1}) \sin(\omega h_2 H s_{d2})\right]} . \tag{130}$$

Coefficient B_1 depends on slownesses of slow waves in layers but does not depend on slownesses of fast waves, which means it describes the frequency dependent ($\propto \omega^{-1/2}$) correction caused by fluid flow between layers. The expression for coefficient B_1 (130) can be rewritten as

$$B_1 = \frac{NUM}{DEN} \times \frac{\omega^2 H \left(\rho_1 h_1 + \rho_2 h_2\right) \left(R_2 - R_1\right)^2 d_1 d_2}{\sqrt{i\omega}} . \tag{131}$$

Replacing all cosines and sines with their half-angle representations, i.e. $\sin\theta = 2\sin\theta/2\cos\theta/2$ and $\cos\theta = \cos^2\theta/2 - \sin^2\theta/2$, and factorizing parts of the numerator and denominator of (131) gives

$$\begin{aligned}
NUM &= d_1 \sin(\omega h_1 H s_{d1}) \left(1 - \cos\left(\omega h_2 H s_{d2}\right)\right) + d_2 \sin(\omega h_2 H s_{d2}) \left(1 - \cos\left(\omega h_1 H s_{d1}\right)\right) \\
&= 4 d_1 \sin\left(\frac{\omega h_1 H s_{d1}}{2}\right) \cos\left(\frac{\omega h_1 H s_{d1}}{2}\right) \sin^2\left(\frac{\omega h_2 H s_{d2}}{2}\right) \\
&\quad + 4 d_2 \sin\left(\frac{\omega h_2 H s_{d2}}{2}\right) \cos\left(\frac{\omega h_2 H s_{d2}}{2}\right) \sin^2\left(\frac{\omega h_1 H s_{d1}}{2}\right) \\
&= 4 \sin\left(\frac{\omega h_1 H s_{d1}}{2}\right) \sin\left(\frac{\omega h_2 H s_{d2}}{2}\right) \\
&\quad \times \left[d_1 \sin\left(\frac{\omega h_2 H s_{d2}}{2}\right) \cos\left(\frac{\omega h_1 H s_{d1}}{2}\right) + d_2 \cos\left(\frac{\omega h_2 H s_{d2}}{2}\right) \sin\left(\frac{\omega h_1 H s_{d1}}{2}\right)\right] ,
\end{aligned}$$

and similarly for DEN,

$$\begin{aligned}
DEN &= 2d_1d_2\left(\cos\left(\omega h_1 H s_{d1}\right)\cos\left(\omega h_2 H s_{d2}\right)-1\right)-\left(d_1^2+d_2^2\right)\sin(\omega h_1 H s_{d1})\sin(\omega h_2 H s_{d2}) \\
&= -4d_1d_2\left[\sin^2\left(\frac{\omega h_1 H s_{d1}}{2}\right)\cos^2\left(\frac{\omega h_2 H s_{d2}}{2}\right)+\cos^2\left(\frac{\omega h_1 H s_{d1}}{2}\right)\sin^2\left(\frac{\omega h_2 H s_{d2}}{2}\right)\right] \\
&\quad -4\left(d_1^2+d_2^2\right)\sin\left(\frac{\omega h_1 H s_{d1}}{2}\right)\cos\left(\frac{\omega h_1 H s_{d1}}{2}\right)\sin\left(\frac{\omega h_2 H s_{d2}}{2}\right)\cos\left(\frac{\omega h_2 H s_{d2}}{2}\right) \\
&= -4\left[d_1\cos\left(\frac{\omega h_1 H s_{d1}}{2}\right)\sin\left(\frac{\omega h_2 H s_{d2}}{2}\right)+d_2\sin\left(\frac{\omega h_1 H s_{d1}}{2}\right)\cos\left(\frac{\omega h_2 H s_{d2}}{2}\right)\right] \\
&\quad \times\left[d_1\sin\left(\frac{\omega h_1 H s_{d1}}{2}\right)\cos\left(\frac{\omega h_2 H s_{d2}}{2}\right)+d_2\cos\left(\frac{\omega h_1 H s_{d1}}{2}\right)\sin\left(\frac{\omega h_2 H s_{d2}}{2}\right)\right] .
\end{aligned}$$

The ratio NUM/DEN is hence

$$\begin{aligned}
\frac{NUM}{DEN} &= \frac{4\sin\left(\frac{\omega h_1 H s_{d1}}{2}\right)\sin\left(\frac{\omega h_2 H s_{d2}}{2}\right)}{-4\left[d_1\cos\left(\frac{\omega h_2 H s_{d2}}{2}\right)\sin\left(\frac{\omega h_1 H s_{d1}}{2}\right)+d_2\sin\left(\frac{\omega h_2 H s_{d2}}{2}\right)\cos\left(\frac{\omega h_1 H s_{d1}}{2}\right)\right]} \\
&= -\frac{1}{d_1\cot\left(\frac{\omega h_2 H s_{d2}}{2}\right)+d_2\cot\left(\frac{\omega h_1 H s_{d1}}{2}\right)} .
\end{aligned}$$

Substituting this result back into (131) yields

$$B_1 = -\frac{\omega^2 H\left(\rho_1 h_1+\rho_2 h_2\right)\left(R_2-R_1\right)^2 d_1 d_2}{\sqrt{i\omega}\left[d_1\cot\left(\frac{\omega h_2 H s_{d2}}{2}\right)+d_2\cot\left(\frac{\omega h_1 H s_{d1}}{2}\right)\right]} .$$

In terms of average density for one spatial period, the previous equation becomes

$$-2B_1 = \frac{2\omega^2 H^2\rho^*\left(R_2-R_1\right)^2}{\sqrt{i\omega}H\left[\frac{N_2}{\sqrt{D_2}}\cot\left(\frac{\omega h_2 H s_{d2}}{2}\right)+\frac{N_1}{\sqrt{D_1}}\cot\left(\frac{\omega h_1 H s_{d1}}{2}\right)\right]} ,$$

and assuming that both layers are filled with the same fluid,

$$-2B_1 = \frac{2\omega^2 H^2\rho^*\left(R_2-R_1\right)^2}{\sqrt{i\omega\eta}H\left[\sqrt{\frac{N_1}{\kappa_1}}\cot\left(\sqrt{\frac{i\omega\eta}{\kappa_1 N_1}}\frac{h_1 H}{2}\right)+\sqrt{\frac{N_2}{\kappa_2}}\cot\left(\sqrt{\frac{i\omega\eta}{\kappa_2 N_2}}\frac{h_2 H}{2}\right)\right]} .$$

Remembering that on the LHS of equation (128) there is effective slowness for both layers,

$$\left(S_f^*\right)^2 = \left(\omega H s_f^*\right)^2 = \omega^2 H^2 \rho^* \frac{1}{C^*},$$

an equation for the effective velocity modulus of fast wave is finally found as

$$\frac{1}{C^*} = \left\langle \frac{1}{C} \right\rangle + \frac{2}{\sqrt{i\omega\eta}H} \frac{(R_1 - R_2)^2}{\sqrt{\frac{N_1}{\kappa_1}} \cot \sqrt{\frac{i\omega\eta}{\kappa_1 N_1}} \frac{h_1 H}{2} + \sqrt{\frac{N_2}{\kappa_2}} \cot \sqrt{\frac{i\omega\eta}{\kappa_2 N_2}} \frac{h_2 H}{2}}, \tag{132}$$

where h_1 and h_2 are volume fractions of the layers 1 and 2. This equation is the same as the one derived by Norris (1993) who used a different approach based on the Floquet theorem for differential equations with periodic coefficients (Brillouin, 1963).

4 Fractured porous media - dispersion and attenuation

In the previous chapter we have derived equations for equivalent properties, compressional wave dispersion and attenuation in periodically layered poroelastic media. In this chapter we will use those results to derive attenuation and dispersion in a porous medium with a periodic set of parallel fractures. A possibility to use results for layered media to characterize fractured media stems from analogy with the elastic case. Specifically, it has been shown that fractures in elastic media can be adequately described as thin highly compliant layers (Schoenberg, 1980). This description of fractured media has become known as linear slip theory. To better understand how this methodology can be extended and applied to porous and fractured rock, we will first review it for elastic fractured media.

4.1 Fractured elastic media - constitutive relation

Asymmetric stresses may cause rock to fracture, with such deformations commonly aligned with the dominant horizontal stress direction. At depth, due to lithostatic stress, sub-vertical or vertical fractures may open, which are of particular interest for hydrocarbon exploration because they increase overall permeability of a reservoir. Open fractures are likely to cause measurable seismic anisotropy, which has been observed in seismic data (Crampin, 1984). Seismic measurements showing azimuthal velocity anisotropy confirm the presence of near vertical aligned cracks or fractures. Vertical fractures of this type will act against the normal trend of depth-porosity reduction and enable exploration of deeper targets. This important fact attracted numerous researchers to study wave propagation in fractured rocks. Rigorous analysis and theoretical models which describe wave propagation in fractured media have been presented by a number of researchers, see e.g. Schoenberg (1980); Schoenberg

and Douma (1988); Hudson (1981); Nishizawa (1982); Thomsen (1995). In some of these studies, fractures are represented as ellipsoidal inclusions with low aspect ratio (Hudson, 1981; Nishizawa, 1982; Thomsen, 1995). However, real fractures do not have such defined idealized geometry, along their length they may have many points of contact and some minerals (calcite or quartz) may be deposited within the fractures causing stiffening. Consequently models of fractures with a fixed idealized shape may not be adequate.

With long wavelength approximation it is possible to describe fracturing in another phenomenological way. Intuitively it is clear that fractures make rock weaker, softer or more compliant, so it is logical to describe the qualitative influence of fractures through the constitutive relation that changes in the presence of fractures. In other words, from the point of view of (long) wave propagation it is important to see how the presence of fractures affects elastic moduli (note that usually we can assume that density is not affected by fracturing as they have infinitesimally small volume but large surface).

In this manner fractures can be considered as poorly bonded interfaces or thin layers filled with a material that is more compliant than the background. Schoenberg (1980) considers fractures either as planes of weakness with non-welded boundary condition, or as infinitely thin and highly compliant (soft) layers. These representations of fractures, called linear slip interfaces, are equivalent in the low frequency limit.

Displacements across linear slip interfaces are discontinuous. The linear slip theory uses linear relationships between the traction acting on interface and this discontinuity in displacement (slip) across the fractures. The slip is determined by the ratio of the stress on the fracture surface to the fracture specific stiffness. An assumption

of linear slip deformation is that the additional deformation of the background is the sum of slip across the fractures.

The linear slip model is only valid in the low frequency limit. At low frequencies, the displacement across a single fracture is relatively small compared to the total displacement over the wavelength. At higher frequencies, there are fewer fractures within the wavelength and the displacement across a single fracture is more significant. In the low frequency limit, the component of stress normal to the fractures, and the components of strain tangent to the fractures, are assumed to be constant over the wavelength. At higher frequencies however, seismic wave propagation in a rock with linear slip interfaces is dispersive, an effect not accounted for by linear slip theory (Schoenberg and Douma, 1988).

Sayers and Kachanov (1991) showed an elegant way to account for the effect of fracture "softness" in constitutive relation. If a rock contains fractures, then average strain over the elementary volume EV can be represented as strain of homogeneous background (with no fractures) plus additional strain caused by the fractures. Strain can be related to the average stress by the Hooke's law (20) which in compliances can be written in the form

$$\varepsilon_{ij} = s_{ijkl}\sigma_{kl}$$

where s_{ijkl} is the compliance tensor of the medium (inverse of the stiffness tensor). For the fractured medium, assuming infinitesimal volume of fractures (but a finite surface) and low frequency limit (constant stress over the EV), average the strain can be written as a sum of the strain in the background and fracture

$$\varepsilon_{ij} = s_{ijkl_b}\sigma_{kl} + \frac{1}{V}\int_V \varepsilon_{ij_f} dV.$$

where s_{ijkl_b} denotes compliance tensor of the background (unfractured) material and ε_{ij_f} is additional strain due to the presence of the fractures (Schoenberg and Sayers

1995). The second term on the RHS is transformed into a surface integral according to Gauss's theorem,

$$\frac{1}{V}\int\limits_V \varepsilon_{ij_f} dV = \frac{1}{2V}\int\limits_V \left(\frac{\partial}{\partial x_j}\left[u_i\right] + \frac{\partial}{\partial x_i}\left[u_j\right]\right) dV = \frac{1}{2V}\int\limits_S \left(\left[u_i\right] n_j + \left[u_j\right] n_i\right) dS,$$

where $[u_i] = u_i^+ - u_i^-$ denotes jump (discontinuity) in displacement and n_j denotes x_j component of the unit normal to the fracture plane. The assumption of linearity between this "slip" and stress acting on the interface allows the "fracture compliance tensor" $\mathbf{Z}$ to be introduced as

$$\frac{1}{V}\int\limits_{S_q} \left[u_i\right] dS = Z_{ir}\sigma_{rs}n_s \ .$$

For a set of aligned fractures with the same unit normal n_i , which do not interact with each other, the average strain caused by these fractures is

$$\begin{aligned}\varepsilon_{ij_f} &= \frac{1}{2V}\sum_q \int\limits_{S_q} \left(\left[u_i\right] n_j + \left[u_j\right] n_i\right) dS \equiv \frac{1}{2}\left(Z_{ir}\sigma_{rs}n_s n_j + Z_{jr}\sigma_{rs}n_s n_i\right) = \\ &= \frac{1}{2}\left(Z_{ir}\sigma_{rs}n_s n_j + Z_{jr}\sigma_{rs}n_s n_i\right) = \frac{1}{2}\left(Z_{ir}n_s n_j + Z_{jr}n_s n_i\right)\frac{\delta_{rk}\delta_{sl} + \delta_{rl}\delta_{sk}}{2}\sigma_{kl},\end{aligned}$$

which allows the compliance matrix associated with the fractures $s_{ijkl_f} = \varepsilon_{ij_f}\sigma_{kl}$ to be rewritten as

$$s_{ijkl_f} = \frac{1}{4}\left(Z_{ik}n_l n_j + Z_{jk}n_l n_i + Z_{il}n_k n_j + Z_{jl}n_k n_i\right) \ .$$

Then, the total compliance of a rock with an aligned fracture set can be written as

$$s_{ijkl} = s_{ijkl_b} + s_{ijkl_f} \ ,$$

which can be written in 6x6 matrix representation by analogy with (21) (Hsu and Schoenberg, 1993b; Schoenberg and Douma, 1988),

$$\mathbf{s} = \mathbf{s}_b + \mathbf{s}_f \ , \tag{133}$$

where $\mathbf{s}_b$ is the 6x6 compliance matrix of the isotropic background, and $\mathbf{s}_f$ is the 6x6 excess compliance matrix associated with the fractures. In a rotationally invariant fracture set, in which the fractures are aligned in the directions normal to the axis of symmetry x_3, there is no coupling between the normal displacement and shear stresses. The excess compliance associated with the fractures is given by the non-zero elements of the $\mathbf{s}_f$ matrix,

$$\mathbf{s}_f = \begin{bmatrix} 0 & 0 & 0 & 0 & 0 & 0 \\ 0 & 0 & 0 & 0 & 0 & 0 \\ 0 & 0 & Z_N & 0 & 0 & 0 \\ 0 & 0 & 0 & Z_T & 0 & 0 \\ 0 & 0 & 0 & 0 & Z_T & 0 \\ 0 & 0 & 0 & 0 & 0 & 0 \end{bmatrix} \ , \tag{134}$$

where Z_N is the excess normal compliance that relates normal displacements to normal stresses applied in the x_3 direction, and Z_T is the excess tangential compliance that relates tangential displacements and stresses in the x_2 and x_1 directions. The normal and tangential fracture compliances Z_N and Z_T implicitly handle the physical properties of the fractures including geometry, distribution and fracture fill.

The stiffness matrix (inverse of compliance matrix) of the isotropic elastic background

$\mathbf{c}_b = \mathbf{s}_b^{-1}$ is

$$\mathbf{c_b} = \begin{pmatrix} \lambda+2\mu & \lambda & \lambda & 0 & 0 & 0 \\ \lambda & \lambda+2\mu & \lambda & 0 & 0 & 0 \\ \lambda & \lambda & \lambda+2\mu & 0 & 0 & 0 \\ 0 & 0 & 0 & \mu & 0 & 0 \\ 0 & 0 & 0 & 0 & \mu & 0 \\ 0 & 0 & 0 & 0 & 0 & \mu \end{pmatrix}, \tag{135}$$

and the corresponding compliance matrix is

$$\mathbf{s_b} = \begin{pmatrix} \frac{\lambda+\mu}{(3\lambda+2\mu)\mu} & -\frac{1}{2}\frac{\lambda}{(3\lambda+2\mu)\mu} & -\frac{1}{2}\frac{\lambda}{(3\lambda+2\mu)\mu} & 0 & 0 & 0 \\ -\frac{1}{2}\frac{\lambda}{(3\lambda+2\mu)\mu} & \frac{\lambda+\mu}{(3\lambda+2\mu)\mu} & -\frac{1}{2}\frac{\lambda}{(3\lambda+2\mu)\mu} & 0 & 0 & 0 \\ -\frac{1}{2}\frac{\lambda}{(3\lambda+2\mu)\mu} & -\frac{1}{2}\frac{\lambda}{(3\lambda+2\mu)\mu} & \frac{\lambda+\mu}{(3\lambda+2\mu)\mu} & 0 & 0 & 0 \\ 0 & 0 & 0 & \frac{1}{\mu} & 0 & 0 \\ 0 & 0 & 0 & 0 & \frac{1}{\mu} & 0 \\ 0 & 0 & 0 & 0 & 0 & \frac{1}{\mu} \end{pmatrix}. \tag{136}$$

Equations (133) and (134) have been derived above from a purely phenomenological point of view. Alternatively, we can describe the fractured medium as a horizontally layered medium with fractures modelled as infinitely thin layers made of infinitely soft isotropic material. Consider a periodically layered medium of period H of layers of two types: thicker layers representing the background (medium 1, elastic constants λ_b and μ_b, thickness $h_b H$) and thinner layers representing fractures (medium 2, elastic

constants $\lambda_c \ll \lambda_b$ and $\mu_c \ll \mu_b$, thickness $h_c H$, $h_c \ll h_b$). According to Backus theory of thinly layered elastic media, (Mavko et al., 1998) for long waves such a medium will be equivalent to a transversely isotropic (TI) medium with a stiffness matrix $\mathbf{c} = \mathbf{s}^{-1}$

$$\mathbf{c} = \begin{pmatrix} a & b & f & 0 & 0 & 0 \\ b & a & f & 0 & 0 & 0 \\ f & f & c & 0 & 0 & 0 \\ 0 & 0 & 0 & d & 0 & 0 \\ 0 & 0 & 0 & 0 & d & 0 \\ 0 & 0 & 0 & 0 & 0 & m \end{pmatrix}, \tag{137}$$

where

$$c = \left\langle \frac{1}{L} \right\rangle^{-1},\ f = c\left\langle \frac{\lambda}{L} \right\rangle,\ b = \frac{f^2}{c} + \left\langle \frac{2\mu\lambda}{L} \right\rangle,\ a = b + \langle 2\mu \rangle,\ d = \left\langle \frac{1}{\mu} \right\rangle^{-1},\ m = \langle \mu \rangle\ . \tag{138}$$

Here brackets $\langle \bullet \rangle$ indicate thickness weighted average of the enclosed properties, e.g. $\langle q \rangle = h_b q_b + h_c q_c$. Inverting stiffness matrix $\mathbf{c}$ of layered medium gives compliance

matrix $\mathbf{s} = \mathbf{c}^{-1}$

$$\mathbf{s} = \begin{pmatrix} \frac{-ca+f^2}{(a-b)(-ca-cb+2f^2)} & -\frac{-cb+f^2}{(a-b)(-ca-cb+2f^2)} & \frac{f}{-ca-cb+2f^2} & 0\ 0\ 0 \\ -\frac{-cb+f^2}{(a-b)(-ca-cb+2f^2)} & \frac{-ca+f^2}{(a-b)(-ca-cb+2f^2)} & \frac{f}{-ca-cb+2f^2} & 0\ 0\ 0 \\ \frac{f}{-ca-cb+2f^2} & \frac{f}{-ca-cb+2f^2} & -\frac{a+b}{-ca-cb+2f^2} & 0\ 0\ 0 \\ 0 & 0 & 0 & \frac{1}{d}\ 0\ 0 \\ 0 & 0 & 0 & 0\ \frac{1}{d}\ 0 \\ 0 & 0 & 0 & 0\ 0\ \frac{1}{m} \end{pmatrix} \tag{139}$$

Calculating effective modulus m (shear velocity modulus parallel to the layering) for our particular model in the volume fractions limits $h_b \to 1,\ h_c \to 0$,and in the limit of shear and compressional velocity moduli of the layer representing fracture $\mu_c \to 0,\ L_c \to 0$, gives

$$m = \langle \mu \rangle = h_b \mu_b + h_c \mu_c \approx \mu_b.$$

It can be seen here that s_{66} element of TI compliance matrix is equal to s_{b66} element of isotropic compliance matrix (background), so this element is not affected by fractures (layering) $s_{66} - s_{b66} = 0$. Repeating the same procedure for d (shear velocity modulus normal to the layering) gives

$$\frac{1}{d} = \left\langle \frac{1}{\mu} \right\rangle = \frac{h_b}{\mu_b} + \frac{h_c}{\mu_c} \approx \frac{1}{\mu_b} + Z_T$$

where we have chosen ratio of h_c and μ_c (two quantities which go to zero together) to be Z_T, so, $\mathbf{s}_{55} - \mathbf{s}_{b55} = Z_T$. Now we calculate effective modulus c (compressional velocity modulus normal to the layering) and compare $\mathbf{s}_{33}$ with $\mathbf{s}_{b33}$.

$$\frac{1}{c} = \left\langle \frac{1}{L} \right\rangle = \frac{h_b}{L_b} + \frac{h_c}{L_c} \approx \frac{1}{L_b} + Z_N$$

where we have chosen ratio of h_c over modulus L_c (two quantities which go to zero together) to be Z_N. Then

$$c = \frac{L_b}{1 + L_b Z_N} \ .$$

In order to calculate $\mathbf{s}_{33} = (a+b) / (ca + cb - 2f^2)$, we need to know other effective moduli which are calculated below

$$f = c\left\langle \frac{\lambda}{L} \right\rangle = c\left(\frac{h_b \lambda_b}{L_b} + \frac{h_c \lambda_c}{L_c} \right) \approx c\left(\frac{\lambda_b}{L_b} + Z_N \lambda_c \right) \approx c\frac{\lambda_b}{L_b},$$

($\lambda_c \to 0$ for soft fracture material)

$$b = \frac{f^2}{c} + \left\langle \frac{2\mu\lambda}{L} \right\rangle = \frac{f^2}{c} + \left(\frac{h_b 2\mu_b \lambda_b}{L_b} + \frac{h_c 2\mu_c \lambda_c}{L_c} \right) \approx c\left(\frac{\lambda_b}{L_b} \right)^2 + \frac{2\mu_b \lambda_b}{L_b},$$

and finally

$$a = b + \langle 2\mu \rangle = b + (l_b 2\mu_b + l_c 2\mu_c) \approx c\left(\frac{\lambda_b}{L_b} \right)^2 + \frac{2\mu_b \lambda_b}{L_b} + 2\mu_b = b + 2\mu_b.$$

It is now easy to show that $\mathbf{s}_{33} - \mathbf{s}_{b33} = Z_N$, and for the rest of the moduli the differences between TI matrix elements and isotropic matrix elements will be zero. Summarizing the above results, one can see that the fractured medium modelled as a limiting case of a layered medium is described by the compliance matrix (134) with

$$Z_N \equiv \lim_{h_c \to 0} \frac{h_c}{L_c} \ , \text{ and } \quad Z_T \equiv \lim_{h_c \to 0} \frac{h_c}{\mu_c} \ ,$$

in the limit of thin layer representing fracture.

In the stiffness domain, equation (133) for the stiffness matrix corresponding to the compliance matrix $\mathbf{s}$ can be written in the form

$$\mathbf{c} = \begin{pmatrix} L\left[1-\left(\frac{\lambda}{L}\right)^2\Delta_N\right] & \lambda\left[1-\frac{\lambda}{L}\Delta_N\right] & \lambda(1-\Delta_N) & 0 & 0 & 0 \\ \lambda\left[1-\frac{\lambda}{L}\Delta_N\right] & L\left[1-\left(\frac{\lambda}{L}\right)^2\Delta_N\right] & \lambda(1-\Delta_N) & 0 & 0 & 0 \\ \lambda(1-\Delta_N) & \lambda(1-\Delta_N) & L(1-\Delta_N) & 0 & 0 & 0 \\ 0 & 0 & 0 & \mu(1-\Delta_T) & 0 & 0 \\ 0 & 0 & 0 & 0 & \mu(1-\Delta_T) & 0 \\ 0 & 0 & 0 & 0 & 0 & \mu \end{pmatrix}. \tag{140}$$

In equation (140) the effect of fractures is expressed through dimensionless *fracture weaknesses* (Hsu and Schoenberg, 1993b; Bakulin et al., 2000):

$$\Delta_N = \frac{(\lambda+2\mu)Z_N}{1+(\lambda+2\mu)Z_N}, \tag{141}$$

$$\Delta_T = \frac{\mu Z_T}{1+\mu Z_T}. \tag{142}$$

The two non-negative dimensionless fracture weaknesses $\mathbf{\Delta}_N$ and $\mathbf{\Delta}_T$ relate the fracture compliance to the total compliance of the fractured medium, separating the fracture induced anisotropy from (isotropic) the elastic properties of the background. The normal fracture weakness $\mathbf{\Delta}_N$ is the component of the strain ε_{33} that is a result of the normal fracture compliance divided by the total ε_{33}. The tangential fracture weakness $\mathbf{\Delta}_T$ is the component of total shear compliance that is a result of the vertical tangential fracture compliance.

Normal and tangential fracture weaknesses, $\mathbf{\Delta}_N$ and Δ_T, range from 0 to 1 and characterize the degree of fracturing. The fracture weaknesses are zero for a non-fractured medium, while a medium with a high degree of fracturing has larger fracture weak-

nesses close to unity. A non-zero normal fracture weakness $\mathbf{\Delta}_N$ implies the decreasing of the P-wave velocity normal to the fractures, while a non-zero tangential fracture weakness Δ_T implies the decreasing of the S-wave velocity across the fractures.

As described in Chapter 2.1.3, although general TI media are defined by five independent elastic parameters ($c_{11}, c_{33}, c_{13}, c_{66}, c_{55} = c_{44}$), the elastic properties of an isotropic medium with rotationally invariant parallel fractures is fully described by four parameters: two elastic constants of the host medium λ and μ, and two excess compliances Z_N and Z_T. Consequently, the stiffness matrix $\mathbf{c}$ represents a special case of the general compliance matrix for a TI medium in that the five elastic constants are not independent but are related by (Schoenberg and Sayers, 1995):

$$c_{11}c_{33} - (c_{13})^2 = 2c_{66}(c_{33} + c_{13}) \; . \tag{143}$$

4.2 Fractures in poroelastic media

4.2.1 Geometry of the model

We model a porous medium with aligned fractures as a periodic (with spatial period H) horizontally stratified system of relatively thick layers of a finite-porosity background material alternating with relatively thin layers of a high-porosity material composing the fractures, Figure 1. The background material is specified by porosity ϕ_b, permeability κ_b, dry (drained) bulk modulus K_b, shear modulus μ_b and thickness fraction h_b so that the thickness of a background layer is $h_b H$ (h_b is assumed to be close to 1). The material comprising the fractures is specified by porosity ϕ_c, permeability κ_c, dry bulk modulus K_c, shear modulus μ_c and thickness fraction $h_c = 1 - h_b \ll 1$ so that the thickness of a fracture is $h_c H$. Both background and fractures are assumed to

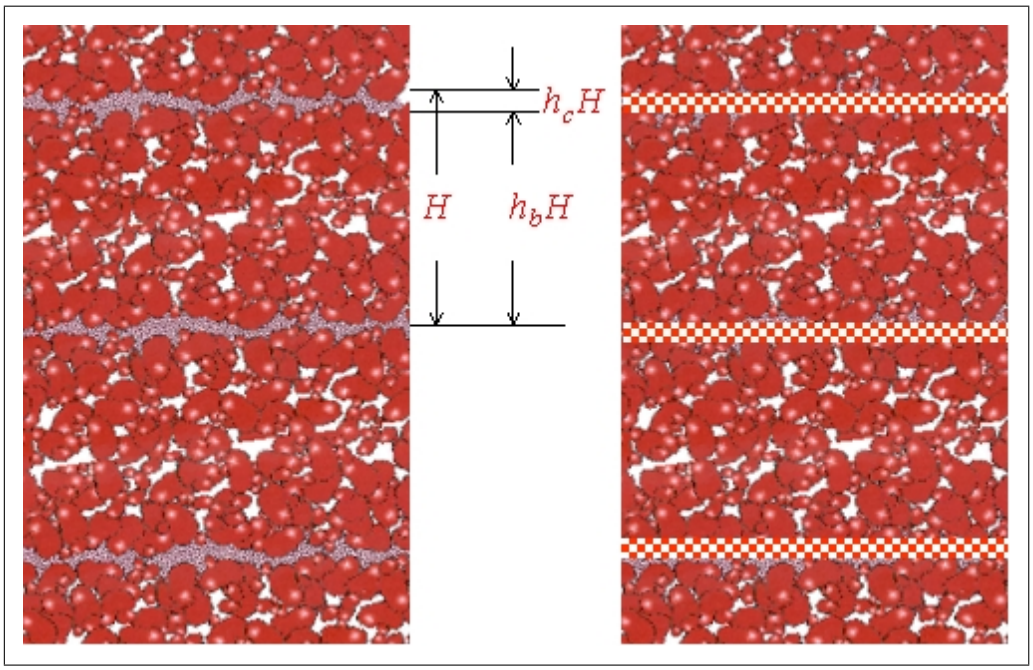

Fig. 1. *Poroelastic medium of a finite-porosity material of type b (background) and thin layers of a high-porosity material of type c.*

be made of the same isotropic grain material with bulk modulus K_g, shear modulus μ_g and density ρ_g, and to be saturated with the same fluid with bulk modulus K_f, density ρ_f and dynamic viscosity η. The aim of this section is to compute frequency dependent elastic wave velocities in such a system of layers in the limit $h_c \to 0$ and $\phi_c \to 1$.

Propagation of elastic waves in such a periodically layered and porous medium has been studied in Chapter 3. The results of Chapter 3 can now be used to relate overall elastic properties of the layered system to the properties of the background and fracture media. The properties of the fractured medium can then be established by taking the small fracture thickness limit $h_c \to 0$. The contribution of the fractures can only be significant in this limit if at the same time $K_c \to 0$, which is always the case when $\phi_c \to 1$. To understand the relationship between different fracture parameters and to relate those parameters to the commonly used fracture properties, we first consider the dry fractured medium.

4.2.2 Dry fractured porous rock

When the stratified medium is dry ($K_f = \rho_f = 0$), the layers behave as ideal elastic isotropic solids. Note that Lamé parameter λ is such that $\lambda + 2\mu = K + 4\mu/3 \equiv L$, and it is convenient for equivalent medium theory to define

$$\gamma \equiv \frac{\mu}{L} \,. \tag{144}$$

Physically, γ is the square of the ratio of shear wave speed to compressional wave speed, and as such it is always between 0 and 3/4 (and for positive Poisson ratio media, between 0 and 1/2). In the long wavelength limit, the system of horizontal layers perpendicular to x_3 axis is equivalent to a transversely isotropic elastic solid with stiffness matrix given by equations (137) and (138), which can be written in the form

$$\mathbf{c}^{dry} = \begin{pmatrix} \frac{(1-2\langle\gamma\rangle)^2}{\langle 1/L\rangle} + 4\langle\mu\rangle - 4\langle\gamma\mu\rangle & \frac{(1-2\langle\gamma\rangle)^2}{\langle 1/L\rangle} + 2\langle\mu\rangle - 4\langle\gamma\mu\rangle & \frac{1-2\langle\gamma\rangle}{\langle 1/L\rangle} & 0 & 0 & 0 \\ \frac{(1-2\langle\gamma\rangle)^2}{\langle 1/L\rangle} + 2\langle\mu\rangle - 4\langle\gamma\mu\rangle & \frac{(1-2\langle\gamma\rangle)^2}{\langle 1/L\rangle} + 4\langle\mu\rangle - 4\langle\gamma\mu\rangle & \frac{1-2\langle\gamma\rangle}{\langle 1/L\rangle} & 0 & 0 & 0 \\ \frac{1-2\langle\gamma\rangle}{\langle 1/L\rangle} & \frac{1-2\langle\gamma\rangle}{\langle 1/L\rangle} & \frac{1}{\langle 1/L\rangle} & 0 & 0 & 0 \\ 0 & 0 & 0 & \frac{1}{\langle 1/\mu\rangle} & 0 & 0 \\ 0 & 0 & 0 & 0 & \frac{1}{\langle 1/\mu\rangle} & 0 \\ 0 & 0 & 0 & 0 & 0 & \langle\mu\rangle \end{pmatrix} \tag{145}$$

where brackets $\langle\cdot\rangle$ indicate the thickness weighted average of the enclosed property, i.e. $\langle q\rangle = h_b q_b + h_c q_c = (1 - h_c)q_b + h_c q_c$. Inversion of stiffness matrix $\mathbf{c}^{dry}$ yields the

compliance matrix $\mathbf{s}^{dry} = \left(\mathbf{c}^{dry}\right)^{-1}$

$$\mathbf{s}^{dry} = \begin{pmatrix} \frac{1-\langle\gamma\mu\rangle/\langle\mu\rangle}{3\langle\mu\rangle-4\langle\gamma\mu\rangle} & -\frac{1-2\langle\gamma\mu\rangle/\langle\mu\rangle}{2(3\langle\mu\rangle-4\langle\gamma\mu\rangle)} & -\frac{1-2\langle\gamma\rangle}{2(3\langle\mu\rangle-4\langle\gamma\mu\rangle)} & 0 & 0 & 0 \\ -\frac{1-2\langle\gamma\mu\rangle/\langle\mu\rangle}{2(3\langle\mu\rangle-4\langle\gamma\mu\rangle)} & \frac{1-\langle\gamma\mu\rangle/\langle\mu\rangle}{3\langle\mu\rangle-4\langle\gamma\mu\rangle} & -\frac{1-2\langle\gamma\rangle}{2(3\langle\mu\rangle-4\langle\gamma\mu\rangle)} & 0 & 0 & 0 \\ -\frac{1-2\langle\gamma\rangle}{2(3\langle\mu\rangle-4\langle\gamma\mu\rangle)} & -\frac{1-2\langle\gamma\rangle}{2(3\langle\mu\rangle-4\langle\gamma\mu\rangle)} & \left\langle\frac{1}{L}\right\rangle + \frac{(1-2\langle\gamma\rangle)^2}{3\langle\mu\rangle-4\langle\gamma\mu\rangle} & 0 & 0 & 0 \\ 0 & 0 & 0 & \left\langle\frac{1}{\mu}\right\rangle & 0 & 0 \\ 0 & 0 & 0 & 0 & \left\langle\frac{1}{\mu}\right\rangle & 0 \\ 0 & 0 & 0 & 0 & 0 & \frac{1}{\langle\mu\rangle} \end{pmatrix}. \tag{146}$$

Taking the limit $h_c \to 0$ while $\mu_c, L_c \to 0$ (with the ratio between them γ_c remaining constant) gives the following results:

$$\begin{aligned} &\langle\mu\rangle \to \mu_b\ ,\ \ \langle\gamma\rangle \to \gamma_b\ ,\ \ \langle\gamma\mu\rangle \to \gamma_b\mu_b\ , \\ &\left\langle\frac{1}{\mu}\right\rangle \to \frac{1}{\mu_b} + \lim_{h_c\to 0}\frac{h_c}{\mu_c}\ ,\ \ \left\langle\frac{1}{L}\right\rangle \to \frac{1}{L_b} + \lim_{h_c\to 0}\frac{h_c}{L_c}\ . \end{aligned}$$

Substituting these results into equation (146), while noting that E_b (the dynamic Young's modulus) and ν_b (the dynamic Poisson's ratio) of the background medium are given in terms of μ_b and γ_b by

$$E_b = \frac{3-4\gamma_b}{1-\gamma_b}\mu_b,\ \ \nu_b = \frac{\frac{1}{2}-\gamma_b}{1-\gamma_b},$$

yields the compliance matrix of the dry fractured porous medium,

$$\mathbf{s}^{dry} \ \equiv\ \mathbf{s}_b^{dry} + \mathbf{s}_c^{dry} \tag{147}$$

where $\mathbf{s}_b^{dry}$ is compliance matrix of the dry background material,

$$\mathbf{s}_b^{dry} = \begin{pmatrix} \frac{1}{E_b} & -\frac{\nu_b}{E_b} & -\frac{\nu_b}{E_b} & 0 & 0 & 0 \\ -\frac{\nu_b}{E_b} & \frac{1}{E_b} & -\frac{\nu_b}{E_b} & 0 & 0 & 0 \\ -\frac{\nu_b}{E_b} & -\frac{\nu_b}{E_b} & \frac{1}{E_b} & 0 & 0 & 0 \\ 0 & 0 & 0 & \frac{1}{\mu_b} & 0 & 0 \\ 0 & 0 & 0 & 0 & \frac{1}{\mu_b} & 0 \\ 0 & 0 & 0 & 0 & 0 & \frac{1}{\mu_b} \end{pmatrix} \tag{148}$$

and the second matrix, $\mathbf{s}_c^{dry}$, is the excess compliance due to the dry fractures,

$$\mathbf{s}_c^{dry} = \lim_{h_c \to 0} \begin{pmatrix} 0 & 0 & 0 & 0 & 0 & 0 \\ 0 & 0 & 0 & 0 & 0 & 0 \\ 0 & 0 & \frac{h_c}{L_c} & 0 & 0 & 0 \\ 0 & 0 & 0 & \frac{h_c}{\mu_c} & 0 & 0 \\ 0 & 0 & 0 & 0 & \frac{h_c}{\mu_c} & 0 \\ 0 & 0 & 0 & 0 & 0 & 0 \end{pmatrix}.$$

Equation (147) is equivalent to the equation (133) for the compliance matrix of a fractured medium as given by linear slip deformation theory (Schoenberg and Douma, 1988; Schoenberg and Sayers, 1995), which stipulates that the compliance of an elastic medium with aligned rotationally symmetric (on average) fractures can be written as a sum of the compliance matrix of the background plus an excess compliance given

by

$$\mathbf{s}_e = \begin{pmatrix} 0 & 0 & 0 & 0 & 0 & 0 \\ 0 & 0 & 0 & 0 & 0 & 0 \\ 0 & 0 & Z_N & 0 & 0 & 0 \\ 0 & 0 & 0 & Z_T & 0 & 0 \\ 0 & 0 & 0 & 0 & Z_T & 0 \\ 0 & 0 & 0 & 0 & 0 & 0 \end{pmatrix} \tag{149}$$

Equivalence between $\mathbf{s}_c^{dry}$ and $\mathbf{s}_e$ can be established by assuming that shear modulus μ_c and longitudinal modulus $K_c + 4\mu_c/3$ are $\mathcal{O}(h_c)$ as $h_c \to 0$, and by defining

$$\lim_{h_c \to 0} \frac{h_c}{L_c} \equiv Z_N, \quad \lim_{h_c \to 0} \frac{h_c}{\mu_c} \equiv Z_T. \tag{150}$$

Equations (150) mean that the fractures in the dry porous background are modelled as very thin and very soft porous layers. The "softness" of the thin layer can be expressed through the parameter $\tilde{L} \equiv 1/Z_N$

$$L_c = \tilde{L} h_c \,, \tag{151}$$

showing that dry modulus of fracture skeleton $L_c \to 0$, as $h_c \to 0$. Using equations (150), the solutions of Biot's equations of poroelasticity for the fluid-saturated medium can be related to the excess fracture compliances Z_N and Z_T (Schoenberg and Sayers, 1995). These excess compliances can in turn be related to fracture density and aspect ratio for penny-shaped cracks (Schoenberg and Douma, 1988).

4.2.3 Fluid saturated fractured porous medium - asymptotic solution for the thin layer

In chapter 3, we have derived an expression for the compressional wave modulus c_{33}^{sat} of a periodically layered fluid-saturated porous medium composed of two constituents, b and c,

$$\frac{1}{c_{33}^{sat}} = \left\langle \frac{1}{C} \right\rangle + \frac{2}{\sqrt{i\omega\eta}H} \frac{\left(\frac{\alpha_b M_b}{C_b} - \frac{\alpha_c M_c}{C_c}\right)^2}{\sqrt{\frac{N_b}{\kappa_b}} \cot \sqrt{\frac{i\omega\eta}{\kappa_b N_b}} \frac{h_b H}{2} + \sqrt{\frac{N_c}{\kappa_c}} \cot \sqrt{\frac{i\omega\eta}{\kappa_c N_c}} \frac{h_c H}{2}} , \tag{152}$$

where N for each layer is given by

$$\frac{1}{N} = \frac{C}{ML} = \frac{1}{M} + \frac{\alpha^2}{L} . \tag{153}$$

Equation (152) is valid in the low frequency range, namely for frequencies much smaller than Biot's characteristic frequency $\omega_B = \eta\phi/\kappa\rho_f$, and also much smaller than the resonant frequency of the layering $\omega_R = V_p/H$. Physically, the quantity $\kappa N/\eta \equiv D$ in the denominator of the right hand side of equation (152) for each layer, is the diffusion coefficient appearing in the dispersion relation for Biot's slow wave, as discussed in Chapter 3.

The effective P-wave modulus of the fractured porous medium can now be obtained by taking the limit $h_c \to 0$ and setting h_b to 1 in equation (152), while at the same time assuming L_c and μ_c (and hence K_c) are $\mathcal{O}(h_c)$ as was done for the dry fractures. Note that this implies $\alpha_c \to 1$ and

$$\lim_{h_c \to 0} C_c = \lim_{h_c \to 0} M_c = \frac{1}{\frac{1-\phi_c}{K_g} + \frac{\phi_c}{K_f}} , \tag{154}$$

a finite value (close to K_f/ϕ_c if ϕ_c is not small and $K_g \gg K_f$), as $h_c \to 0$. From equation (154) $M_c/C_c \to 1$, implying $\alpha_c M_c/C_c \to 1$ and $N_c \to L_c$, so that N_c is also $\mathcal{O}(h_c)$. From (151) we can then write

$$N_c = \tilde{L} h_c , \tag{155}$$

which describes softness of the saturated fractures. In this limit, the first term of the right hand side of equation (152) becomes the high frequency (no fluid flow) background modulus

$$\left\langle \frac{1}{C} \right\rangle \rightarrow \frac{1}{C_b} \, .$$

The nominator in second term of equation (152) defines magnitude of difference in induced pore pressures between layers, which is the driving force for fluid diffusion.

The corresponding P-wave velocity along the symmetry axis x_3 is given by

$$V_{p3} = \sqrt{\frac{c_{33}^{sat}}{\rho_b}} \, , \tag{156}$$

where $\rho_b = \rho_g(1-\phi_b) + \rho_f \phi_b$ is mass density of the fluid-saturated background material. This velocity is complex and frequency dependent, indicating the presence of frequency dependent attenuation and velocity dispersion.

Taking into account the limit $h_c \rightarrow 0$ discussed above, equation (152) can be rewritten as

$$\frac{1}{c_{33}^{sat}} = \frac{1}{C_b} + \frac{(R_b - 1)^2}{\sqrt{\frac{i\omega\eta N_b}{\kappa_b}}\frac{H}{2}\cot\sqrt{\frac{i\omega\eta}{\kappa_b N_b}}\frac{H}{2} + \sqrt{\frac{i\omega\eta N_c}{\kappa_c}}\frac{H}{2}\cot\sqrt{\frac{i\omega\eta}{\kappa_c N_c}}\frac{H}{2}h_c} \, . \tag{157}$$

We can now analyze the second (fracture) term in the denominator, which is the only one depending on fracture "thickness" and fracture permeability. Dependence of permeability on thickness produces three different cases: fracture permeability much higher then permeability of the background, fracture permeability much lower then permeability of the background, and constant fracture permeability (independent of fracture thickness).

4.2.4 Permeability of fracture material is higher than in the background

Similarly to how proportionality constant $\tilde{L}$ was introduced in equation (155) to describe the softness of the fracture layer, for highly permeable fractures we can

write

$$\kappa_c = \frac{\tilde{\kappa}}{h_c}, \tag{158}$$

so as $h_c \to 0$, fracture permeability κ_c increases. Using relations (158) and (155), the second term in denominator of equation (157) can be rewritten in this limit as

$$\sqrt{\frac{i\omega\eta\tilde{L}}{\tilde{\kappa}}}\frac{H}{2}h_c \cot\sqrt{\frac{i\omega\eta}{\tilde{\kappa}\tilde{L}}}\frac{H}{2}h_c = \tilde{L}\sqrt{\frac{i\omega\eta}{\tilde{\kappa}\tilde{L}}}\frac{H}{2}h_c \cot\sqrt{\frac{i\omega\eta}{\tilde{\kappa}\tilde{L}}}\frac{H}{2}h_c \to \tilde{L}\ .$$

Thus as $h_c \to 0$, the argument of the trigonometric cotangent function relating to the fracture material is $\mathcal{O}(h_c)$. Using the property of the cotangent function $\lim_{x\to 0}\cot x = 1/x$ gives $\tilde{L}$ as the limiting value for the second term for all frequencies of interest. Then equation (157) is

$$\frac{1}{c_{33}^{sat}} = \frac{1}{C_b} + \frac{(R_b-1)^2}{\sqrt{\frac{i\omega\eta N_b}{\kappa_b}}\frac{H}{2}\cot\sqrt{\frac{i\omega\eta}{\kappa_b N_b}}\frac{H}{2} + \tilde{L}}\ , \tag{159}$$

where using equations (150) and (141) for $\tilde{L}$ gives

$$\tilde{L} = \frac{1}{Z_N} = \frac{L_b\,(1-\boldsymbol{\Delta}_N)}{\boldsymbol{\Delta}_N}\ . \tag{160}$$

Here we have used the definition of Z_N from equations (150). Note that $\sqrt{2\kappa_b N_b/\omega\eta}$ in the argument of the cotangent in equation (159) corresponds to fluid diffusion length in the background medium. Diffusion coefficient in fractures $D_c = \kappa_c N_c/\eta$ remains independent of h_c and cancels out, so that attenuation and dispersion for open highly permeable fractures is controlled by the diffusion length of the background and fracture weakness $\boldsymbol{\Delta}_N$.

Equation (159) gives the P-wave modulus for waves propagating normal to fractures as a function of frequency, background properties and normal fracture compliance

Z_N.

The results presented in this section are valid for the same frequency range as the original equation (152), i.e. for frequencies that satisfy the conditions $\omega \ll \omega_B$, which implies that the frequencies are sufficiently low that fluid flow in pore channels is Poiseuille flow, and $\omega \ll \omega_R$, which implies that the effective medium approximation is still valid and that without fluid flow the effective elastic moduli of the system would be given by Backus averaging.

It is important to note that, according to equation (152) within the conditions $\omega \ll \min(\omega_B, \omega_R)$, the wave velocity and attenuation will be frequency dependent due to the fluid flow between the fractures and the background (or between different layers). Consequently, under these conditions low and high frequencies can still be defined with respect to fluid flow. Low frequencies are those when pressure has enough time to equilibrate between layers within the wave cycle. This occurs when the diffusion length $\sqrt{2D_b/\omega}$ (or wavelength of Biot's slow wave) is much larger than the spatial period H,

$$\omega \ll D_b/H^2 \ .$$

High frequencies are those much higher than D_b/H^2 but still smaller than both ω_B and ω_R. In the next section, these results are analyzed in the limiting cases of low and high frequencies.

As can be seen from above, the normal elastic stiffnesses of the fractured medium can be very different for low and high frequencies. For instance, the P-wave modulus along the symmetry axis is given by equation (197) for low frequencies, while for high frequencies it is equal to C_b. This means that the stiffness matrix and corresponding elastic wave velocities are frequency dependent. Introducing dimensionless fracture

weakness $\boldsymbol{\Delta}_N$ (Hsu and Schoenberg, 1993a) defined as

$$\boldsymbol{\Delta}_N \equiv \frac{Z_N L_b}{1 + Z_N L_b} \, ,$$

the frequency dependence of P-wave modulus along the symmetry axis, given by equation (159), can be written in the form

$$\frac{1}{c_{33}^{sat}} = \frac{1}{C_b} + \frac{\boldsymbol{\Delta}_N \left(\frac{\alpha_b M_b}{C_b} - 1 \right)^2}{L_b \left[1 - \boldsymbol{\Delta}_N + \boldsymbol{\Delta}_N \sqrt{i\Omega} \cot \left(\frac{C_b}{M_b} \sqrt{i\Omega} \right) \right]} \, , \tag{161}$$

where Ω is a normalized frequency given by

$$\Omega = \omega \frac{H^2 \eta N_b}{4 \kappa_b L_b^2} = \omega \frac{H^2 \eta M_b}{4 \kappa_b C_b L_b} \, . \tag{162}$$

Equation (161) can be used to evaluate the frequency dependence of the P-wave phase slowness and attenuation for waves propagating perpendicular to the fractures. The P-wave phase slowness is the real part of the complex phase slowness V_{p3}^{-1}, where V_{p3} is given by equation (156)

$$V_p = \left[\mathrm{Re} \left(V_{p3}^{-1} \right) \right]^{-1} \, ,$$

and the attenuation Q^{-1} is given by half the ratio of the real part of the complex phase slowness to the imaginary part of the complex phase slowness

$$Q^{-1} = 2 V_p \, \mathrm{Im} \left(V_{p3}^{-1} \right) \, .$$

Figure 2 shows this P-wave velocity normalized by the high-frequency velocity $V_p^{high} = \sqrt{c_{33_{high}}/\rho}$, which is real (quasi-elastic case) because frequency is high enough to prevent fluid flow ($c_{33_{high}}$ is given by equation (200)). Figure 3 shows dimensionless attenuation Q^{-1} as a function of normalized frequency Ω. Both figures are for a water saturated, porous quartz grained sandstone ($K_g = 37$ GPa, $\mu_g = 44$ GPa, $\rho_g = 2.65$ g·cm^{-1}) with dry fracture weakness $\Delta_N = 0.05$ and different background porosity levels. Figures 4 and 5 show the results for the same rock but with higher fracture

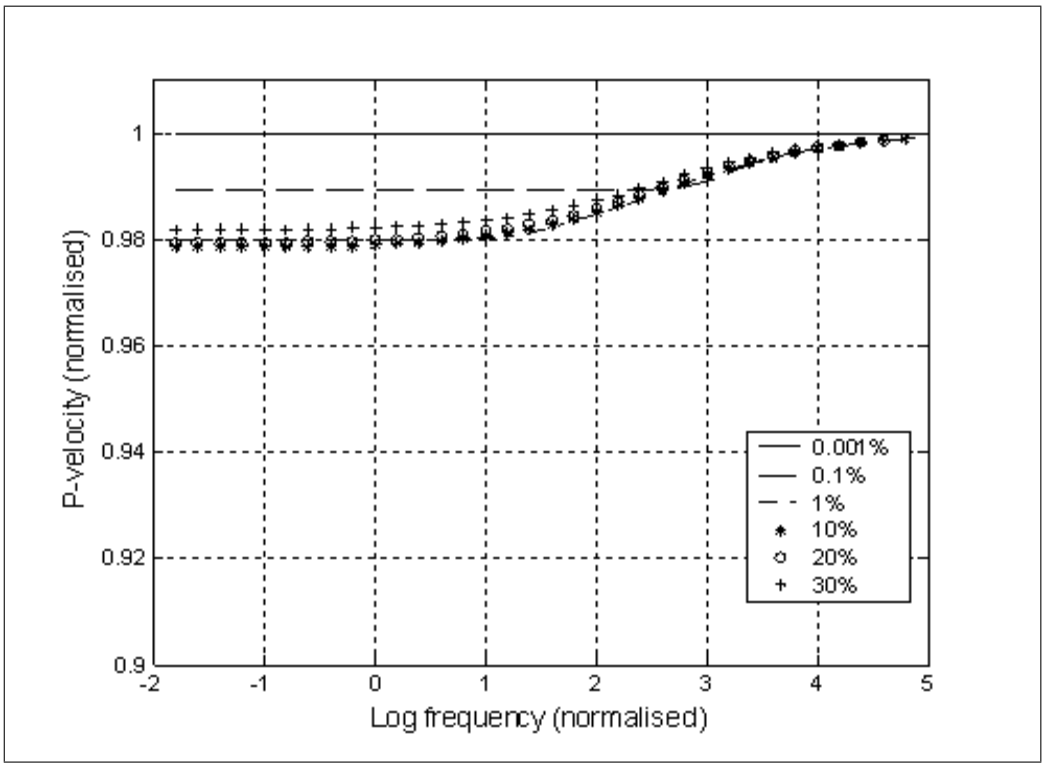

Fig. 2. *Normalized P-wave velocity vs circular frequency in fractured sandstone filled with water. Fracture weakness is fixed* $\Delta_N = 0.05$ *and porosity changes from 0.001% up to 30%.*

weakness $\Delta_N = 0.2$. The dependency of dry background bulk and shear moduli on porosity was assumed to follow the empirical model of Krief et al. (1990)

$$\frac{K_b}{K_g} = \frac{\mu_b}{\mu_g} = (1-\phi)^{3/(1-\phi)}. \tag{163}$$

Figures 2, 3, 4 and 5 show that velocity dispersion and attenuation have a shape typical for relaxation phenomena. For a given Δ_N, both attenuation and dispersion increase sharply with porosity up to a few per cent porosity, and have almost identical shapes for porosities higher than 10%. For zero porosity there is no attenuation as expected because there is no fluid flow.

The results for different values of $\boldsymbol{\Delta}_N$ are shown in more detail in Figures 6 and 7 for a typical reservoir background porosity of 20%. As expected, the dispersion and attenuation are proportional to the fracture weakness Δ_N. The normalized frequency for peak attenuation decreases with increasing fracture weakness Δ_N. It is also noted

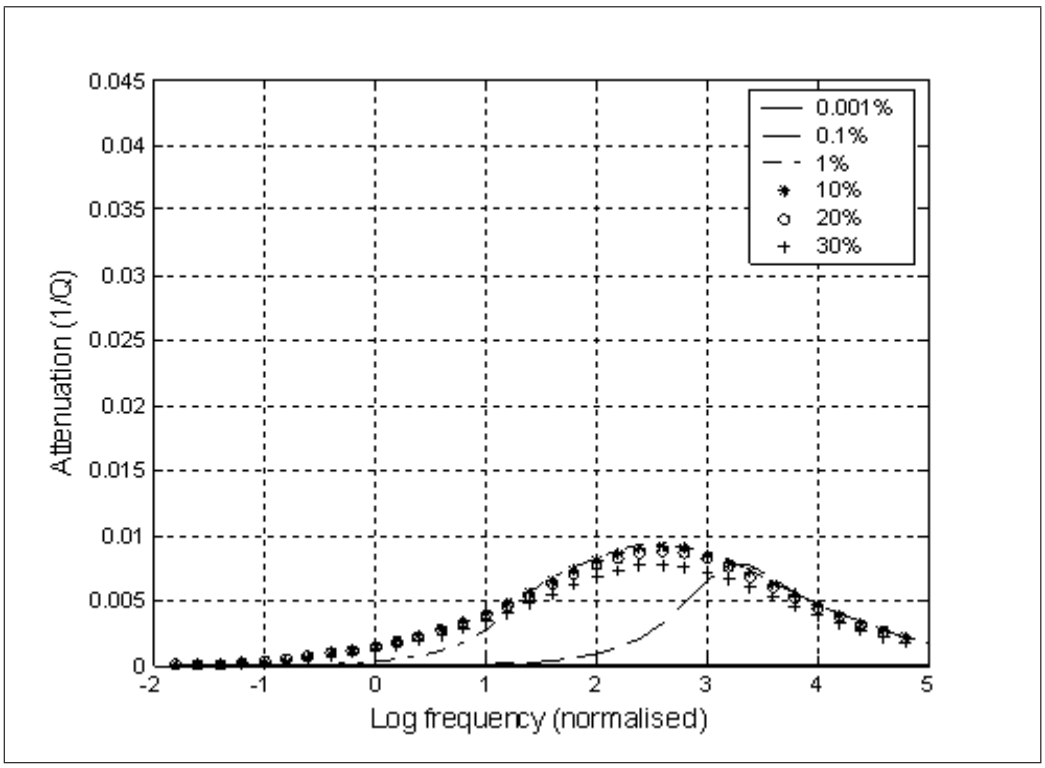

Fig. 3. *Attenuation vs circular frequency in fractured sandstone filled with water, with fracture weakness* $\Delta_N = 0.05$ *and porosity ranging from 0.001% up to 30%.*

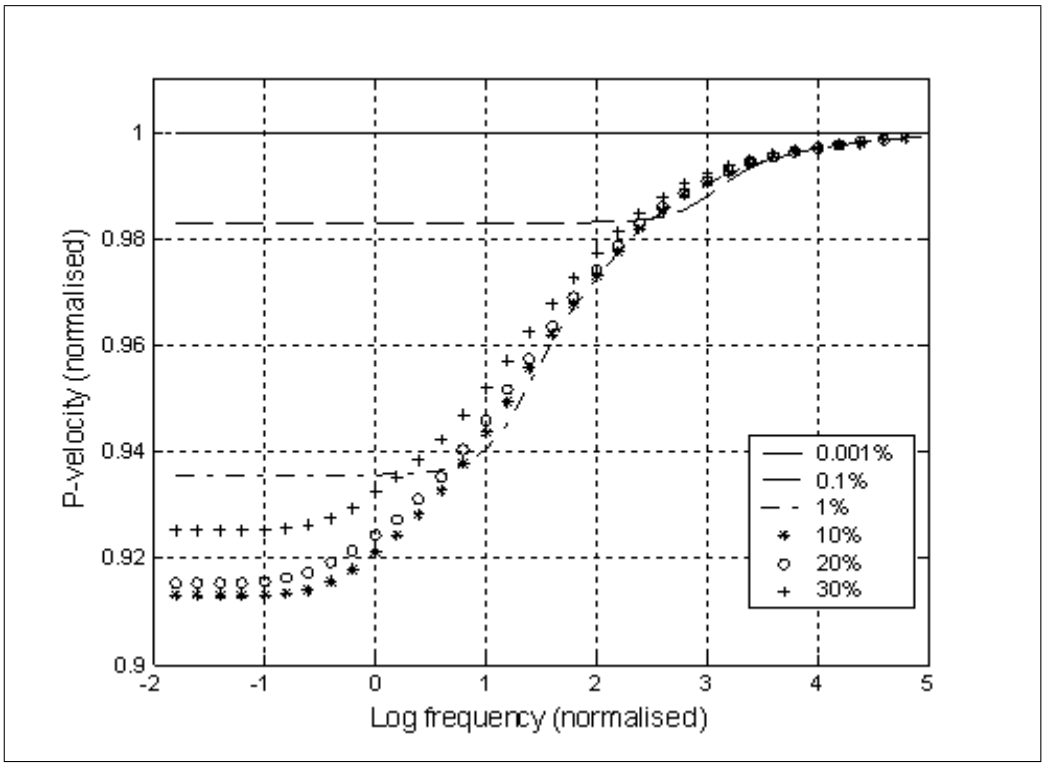

Fig. 4. *Normalized P-wave velocity vs circular frequency in sandstone filled with water. Fracture weakness is fixed* $\Delta_N = 0.2$ *and porosity changes from 0.001% up to 30%.*

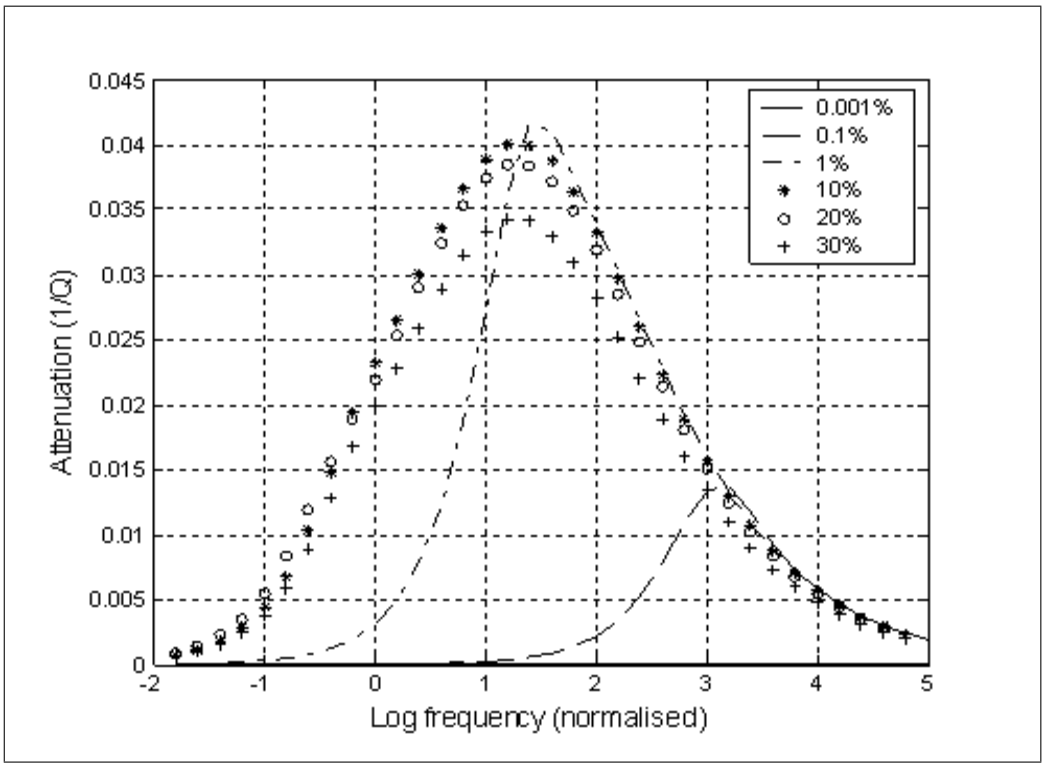

Fig. 5. *Attenuation vs circular frequency in fractured sandstone filled with water, with fracture weakness* $\Delta_N = 0.2$ *and porosity ranging from 0.001% up to 30%.*

that dispersion and attenuation are significant over a frequency range that spans at least two orders of magnitude.

In order to see the asymptotic dependence of attenuation on frequency, $\log(Q^{-1})$ is plotted versus $\log \omega$ in Figure 8.

In the high frequency limit the dependence of attenuation is $\mathcal{O}(\omega^{-1/2})$. In low frequency limit attenuation is proportional to frequency ω as expected. On the curve (marked with diamonds) for the case of lower fracture weakness, which intuitively corresponds to "thinner" fractures, we can clearly observe the transitional part of the curve proportional to $\omega^{1/2}$. Points P and M define crossover frequencies, which separate the curve into three regions with asymptotes given by ω to the power of $1, 1/2, -1/2$ respectively.

We will give now one possible interpretation of Figure 8. When we solved eigenvalue

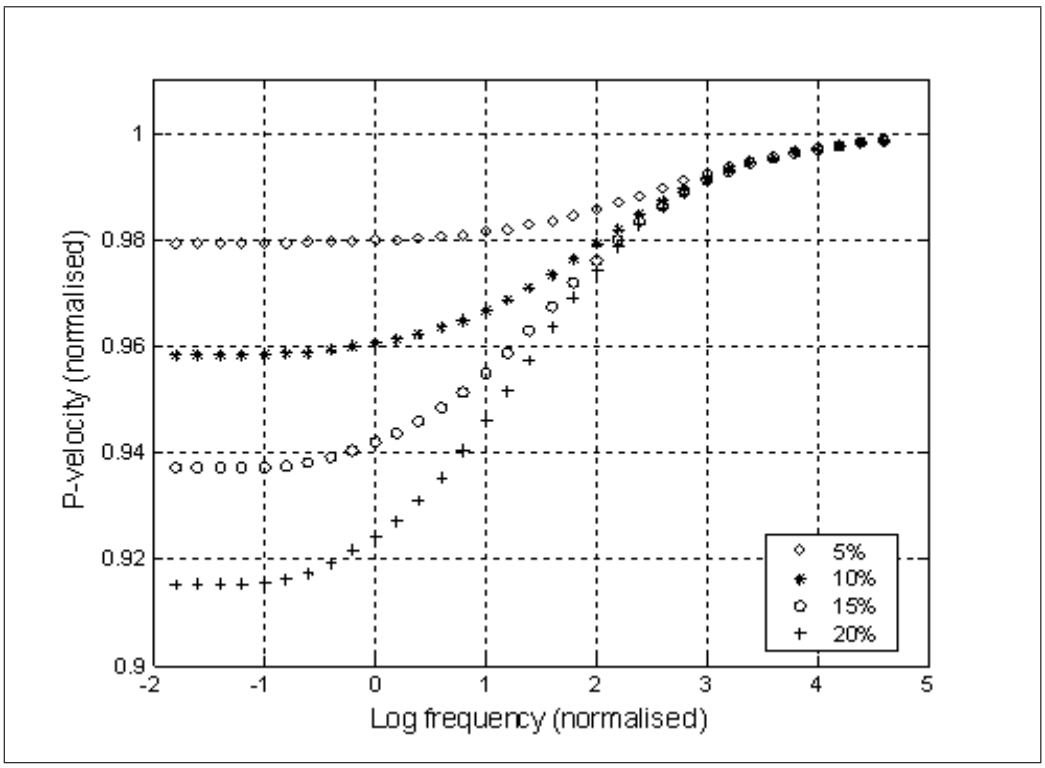

Fig. 6. *Normalized P-wave velocity vs circular frequency in fractured sandstone filled with water. Porosity is fixed* $\phi = 0.2$ *and fracture weakness* Δ_N *changes from 0.05 up to 0.2.*

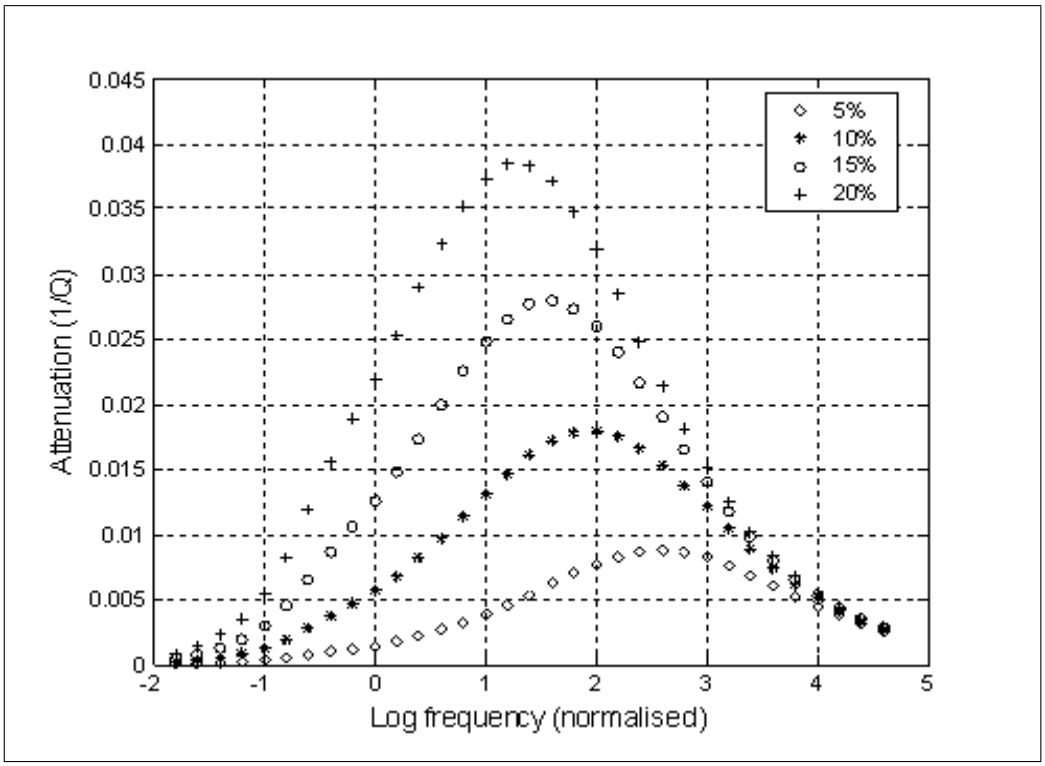

Fig. 7. *Attenuation vs circular frequency in fractured sandstone filled with water, with porosity* $\phi = 0.2$ *and fracture weakness* Δ_N *in range from 0.05 up to 0.2.*

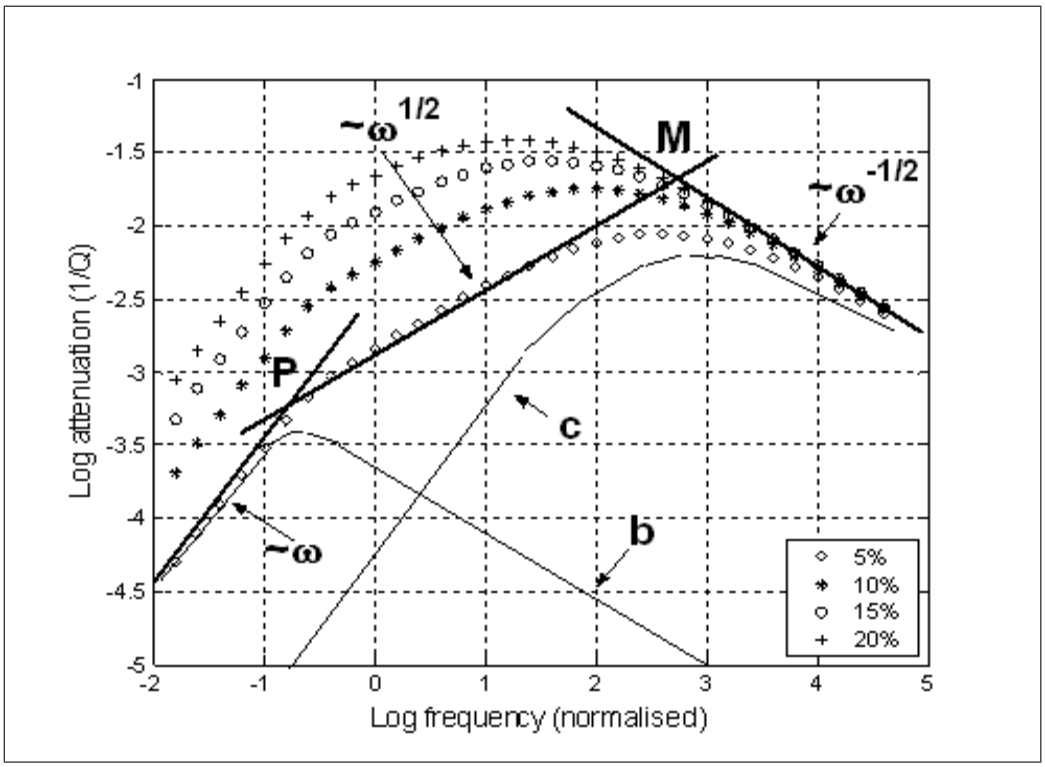

Fig. 8. *Log-log plot of attenuation versus circular frequency for the same material, with porosity* $\phi = 0.2$ *and fracture weakness* Δ_N *in range from 0.05 up to 0.2. Three different asymptotic parts of the attenuation curves are observed.*

problem for the equivalent propagator matrix $\exp(-i\omega H\mathbf{Q}^*)$ (for two layers together) in equations (86) (88) and (121), we have assumed implicitly that equivalent slowness of the Biot's slow wave s_d^* is a result of the interference between slownesses of each layer s_{d1} and s_{d2}. We can consider a system of two layers with different compliances and extremely different thicknesses under the normal loading (caused by the incident wave) as two "diffusional resonators" connected together. In Figure 8 they are represented by curves b and c. Although each layer alone does not produce any attenuation (because the layer is homogeneous), when connected together, attenuation takes place because a pore pressure gradient across the interface will be induced according to equation (117). To equilibrate pressure, fluid flow will occur between the background and fractures. This process is described by the diffusion equation with diffusion coefficients D_b and D_c for the background and fracture respectively. The condition of "diffusional resonance" for each layer is given by the equality of diffusion

length and half-thickness of the layer. The sum of these two resonant curves b and c will give the total attenuation curve for a given fracture weakness (in particular the case shown on Figure 8 marked with diamond) as a result of interference.

Apart from this intuitive interpretation, it would be instructive to derive analytical expressions for the crossover frequencies (points P and M) in order to investigate their dependence on fracture weakness. To do this we need to find asymptotic solution for imaginary parts of velocities normalized by the same real part from equation (161) and then equate expressions for real circular frequency to get values for the crossover frequency.

We can get the low-frequency asymptote by taking the zero frequency limit in equation (161)

$$\operatorname{Im}\frac{C_b}{c_{33}^{sat}} = \operatorname{Im}\left(1 + \frac{C_b\left(R_b-1\right)^2}{L_b}\frac{1}{\frac{1}{\boldsymbol{\Delta}_N} - 1 + \sqrt{i\Omega}\cot\left(\frac{C_b}{M_b}\sqrt{i\Omega}\right)}\right),$$

Keep multiplier $C_b\left(R_b-1\right)^2/L_b$ in mind as we will suppress it in the following derivations. Using the expansion for $\cot x$ for small x gives

$$\begin{aligned}\operatorname{Im}\frac{1}{\frac{1}{\boldsymbol{\Delta}_N} - 1 + \sqrt{i\Omega}\frac{M_b}{C_b}\frac{1}{\sqrt{i\Omega}}\left(1 - i\frac{\Omega C_b}{3M_b}\right)} &= \operatorname{Im}\frac{1}{\left(\frac{1}{\boldsymbol{\Delta}_N} - 1 + \frac{M_b}{C_b}\right) - i\frac{\Omega C_b}{3M_b}} \\ = \operatorname{Im}\frac{1}{B}\frac{1}{1 - i\frac{\Omega C_b}{3M_bB}} \approx \operatorname{Im}\frac{1}{B}\left(1 + i\frac{\Omega C_b}{3M_bB}\right) &= \frac{\Omega C_b}{3M_bB^2},\end{aligned}$$

where $B = \left(1/\boldsymbol{\Delta}_N + M_b/C_b - 1\right)$. Finally inserting the multiplier back into the equation

$$\operatorname{Im}\frac{1}{c_{33}^{sat}} = \frac{\Omega C_b\left(R_b-1\right)^2}{3M_bL_b\left(1/\boldsymbol{\Delta}_N + M_b/C_b - 1\right)^2}. \tag{164}$$

We see that the imaginary part of the modulus, and hence Q^{-1}, is proportional to Ω

or ω.

To find that the "middle" asymptote, first take the approximation for small $\mathbf{\Delta}_N$ in equation (161), and then take the limit as frequency goes to zero. For small $\mathbf{\Delta}_N$ we have

$$\operatorname{Im}\frac{C_b}{c_{33}^{sat}}\frac{L_b}{C_b\left(R_b-1\right)^2}=\operatorname{Im}\frac{\mathbf{\Delta}_N}{1-\left[\mathbf{\Delta}_N+\mathbf{\Delta}_N\sqrt{i\Omega}\cot\left(\frac{C_b}{M_b}\sqrt{i\Omega}\right)\right]}$$
$$=\operatorname{Im}\frac{\mathbf{\Delta}_N}{1-\mathbf{\Delta}_N+\mathbf{\Delta}_N F}\approx\operatorname{Im}\mathbf{\Delta}_N\left(1+\mathbf{\Delta}_N-\mathbf{\Delta}_N F\right)=\operatorname{Im}\mathbf{\Delta}_N^2 F=\mathbf{\Delta}_N^2\operatorname{Im}F\ . \quad (165)$$

Now we calculate $\operatorname{Im}F$, where $F=\sqrt{i\Omega}\cot\frac{C_b}{M_b}\sqrt{i\Omega}$. Representing cotangent of complex argument in exponential form we get

$$\begin{aligned}\operatorname{Im}F&=\operatorname{Im}\sqrt{i\Omega}i\frac{\exp i\frac{C_b}{M_b}\sqrt{i\Omega}+\exp -i\frac{C_b}{M_b}\sqrt{i\Omega}}{\exp i\frac{C_b}{M_b}\sqrt{i\Omega}-\exp -i\frac{C_b}{M_b}\sqrt{i\Omega}}=\\&=\operatorname{Im}\frac{i+1}{\sqrt{2}}i\sqrt{\Omega}\frac{\exp i\left(i+1\right)\frac{C_b\sqrt{\Omega}}{M_b\sqrt{2}}+\exp -i\left(i+1\right)\frac{C_b\sqrt{\Omega}}{M_b\sqrt{2}}}{\exp i\left(i+1\right)\frac{C_b\sqrt{\Omega}}{M_b\sqrt{2}}-\exp -i\left(i+1\right)\frac{C_b\sqrt{\Omega}}{M_b\sqrt{2}}}=\\&=\operatorname{Im}\left(i-1\right)\frac{\sqrt{\Omega}}{\sqrt{2}}\frac{\left(\cos P\cosh P-i\sin P\sinh P\right)^2}{\cos^2 P\cosh^2 P+\sin^2 P\sinh^2 P}=\\&=\frac{\sqrt{\Omega}\left(\cos^2 P\cosh^2 P-\sin^2 P\sinh^2 P+2\cos P\cosh P\sin P\sinh P\right)}{2\left(\cos^2 P\cosh^2 P+\sin^2 P\sinh^2 P\right)}\ ,\end{aligned} \quad (166)$$

where $P=\frac{C_b\sqrt{\Omega}}{M_b\sqrt{2}}$. As $P\to 0$ and $\sqrt{\Omega}\to 0$, the result from previous equation (166) is approximated by

$$\frac{\sqrt{\Omega}}{2}\left(1+\mathcal{O}(P^2)\right)\ .$$

Substitution of $\operatorname{Im}F$ into equation (165), gives

$$\operatorname{Im}\frac{1}{c_{33}^{sat}}=\mathbf{\Delta}_N^2\frac{\sqrt{\Omega}}{2}\frac{\left(R_b-1\right)^2}{L_b}\ . \quad (167)$$

Equation shows that in the limit of small fracture thickness Q^{-1} is proportional to $\omega^{1/2}$ as can be seen in Figure 8 (summation of curves b and c).

Equating right hand sides of equations (164) and (167)

$$\boldsymbol{\Delta}_N^2 \frac{\sqrt{\Omega}}{2} \frac{(R_b - 1)^2}{L_b} = \frac{\Omega C_b (R_b - 1)^2}{3 M_b L_b B^2} ,$$

yields

$$\boldsymbol{\Delta}_N^2 \frac{3 M_b B^2}{2 C_b} = \sqrt{\Omega} .$$

Substituting $B^2 \approx 1/\boldsymbol{\Delta}_N^2$ gives crossover frequency Ω_P for points P_i:

$$\Omega_P = \left(\frac{3 M_b}{2 C_b} \right)^2 . \tag{168}$$

Crossover frequency which positions point P for different $\boldsymbol{\Delta}_N$ on Figure 8 is constant, which means that the position of point P on the frequency axis depends only on diffusion length of background medium. This is logical since, as we already noted, the diffusion length in fracture for a given frequency is independent of volume fraction of fracture (that is small anyway), so for low frequencies resonance is dominated by the background.

To see what is the corresponding ω for the crossover frequency given by equation (168), from equation (162) for normalized frequency we can write

$$\frac{9 M_b^2}{4 C_b^2} = \omega \frac{H^2 \eta M_b}{4 \kappa_b C_b L_b} \Rightarrow \omega = \frac{9 M_b L_b \kappa_b}{H^2 C_b \eta} = \frac{9 D_b}{H^2} . \tag{169}$$

If it was possible for the resonator representing the background to exist alone, its diffusional resonant frequency would be defined by the equality of diffusion length

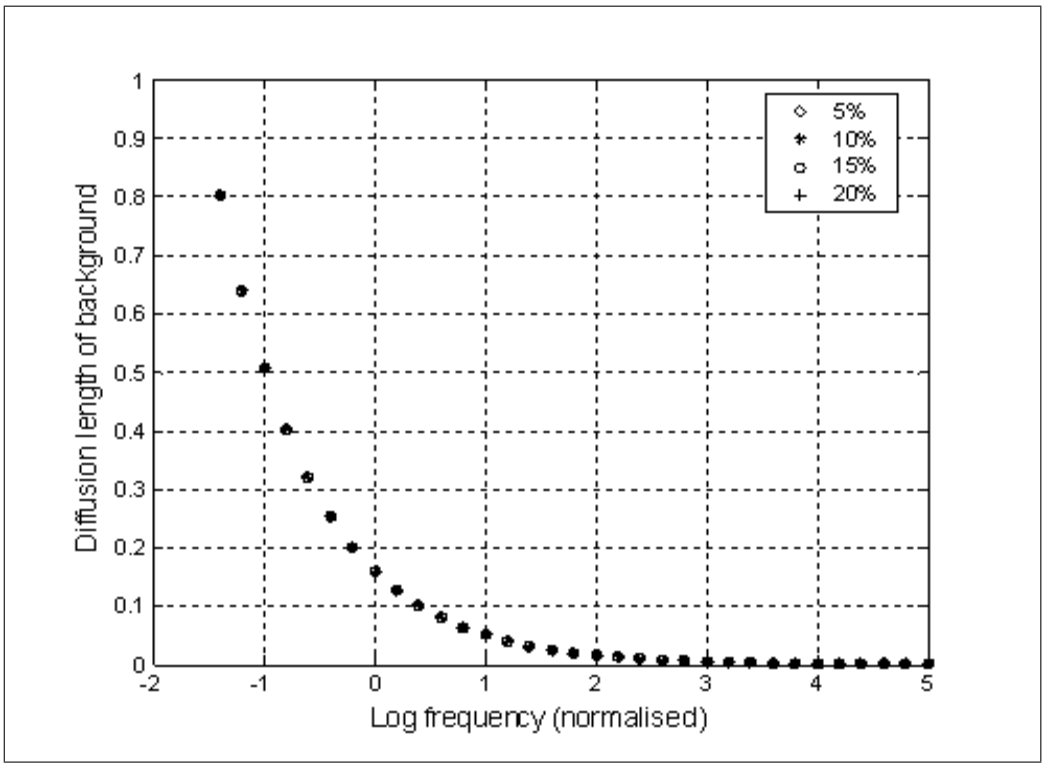

Fig. 9. *Diffusion lengths versus circular frequency for the same material with porosity* $\phi = 0.2$*, unity fracture distance and fractufracture weakness* Δ_N *in range from 0.05 up to 0.2.*

and its half-thickness so that

$$\sqrt{\frac{2D_b}{\omega}} = \frac{H}{2} \Rightarrow \omega = \frac{8D_b}{H^2} \ ,$$

which is very close to the crossover frequency in equation (169). Numerical results for the diffusion length of the background medium of unit length (spatial period) shown in Figure 9 confirm this fact.

In a similar way, the high frequency asymptote can be obtained. Writing the cotangent in exponential form gives

$$\operatorname{Im} \frac{C_b}{c_{33}^{sat}} \frac{L_b}{C_b \left(R_b - 1\right)^2} = \operatorname{Im} \frac{1}{\frac{1}{\mathbf{\Delta}_N} - 1 + \sqrt{i\Omega} i \frac{\exp P \exp -iP}{-\exp P \exp -iP}} \ ,$$

and when $P \to \infty$, we get

$$\operatorname{Im}\frac{1}{\frac{1}{\boldsymbol{\Delta}_N}-1-\frac{i-1}{\sqrt{2}}\sqrt{\Omega}}=\operatorname{Im}\frac{1}{\frac{1}{\boldsymbol{\Delta}_N}-1+\frac{\sqrt{\Omega}}{\sqrt{2}}-i\frac{\sqrt{\Omega}}{\sqrt{2}}}$$
$$=\operatorname{Im}\frac{\left(\frac{1}{\boldsymbol{\Delta}_N}-1-\frac{\sqrt{\Omega}}{\sqrt{2}}\right)+i\frac{\sqrt{\Omega}}{\sqrt{2}}}{\left(\frac{1}{\boldsymbol{\Delta}_N}-1-\frac{\sqrt{\Omega}}{\sqrt{2}}\right)^2+\frac{\Omega}{2}}\approx\frac{1}{\sqrt{2\Omega}}\,,$$

so finally

$$\operatorname{Im}\frac{1}{c_{33}^{sat}}=\frac{(R_b-1)^2}{\sqrt{2\Omega}L_b}\,. \tag{170}$$

Thus in the high frequencies Q^{-1} is proportional to $\omega^{-1/2}$.

Equating right hand sides of equations (170) and (167) gives the second crossover frequency Ω_M for the maxima (points M_i)

$$\frac{(R_b-1)^2}{\sqrt{2\Omega}L_b}=\boldsymbol{\Delta}_N^2\frac{\sqrt{\Omega}}{2}\frac{(R_b-1)^2}{L_b}\;\Rightarrow\frac{1}{\sqrt{2\Omega}}=\boldsymbol{\Delta}_N^2\frac{\sqrt{\Omega}}{2}, \tag{171}$$

$$\Omega_M=\frac{\sqrt{2}}{\boldsymbol{\Delta}_N^2}\,. \tag{172}$$

Substituting equation (172) into equation (171), shows that the magnitude of maximal attenuation is proportional to $\boldsymbol{\Delta}_N$

$$Q^{-1}=\frac{1}{\sqrt{2\frac{\sqrt{2}}{\boldsymbol{\Delta}_N^2}}}=\frac{\boldsymbol{\Delta}_N}{2^{3/4}}\,.$$

This fact can be confirmed numerically. Introduce another normalized frequency Ω'

$$\Omega'=\Omega\boldsymbol{\Delta}_N^2=\omega\frac{H^2\eta M_b\boldsymbol{\Delta}_N^2}{4\kappa_b C_b L_b}\,, \tag{173}$$

then from equation (161) we get,

$$\frac{1}{c_{33}^{sat}}=\frac{1}{C_b}+\frac{\boldsymbol{\Delta}_N\left(\frac{\alpha_b M_b}{C_b}-1\right)^2}{L_b\left[1-\boldsymbol{\Delta}_N+\sqrt{i\Omega'}\cot\left(\frac{C_b}{\boldsymbol{\Delta}_N M_b}\sqrt{i\Omega'}\right)\right]}\,. \tag{174}$$

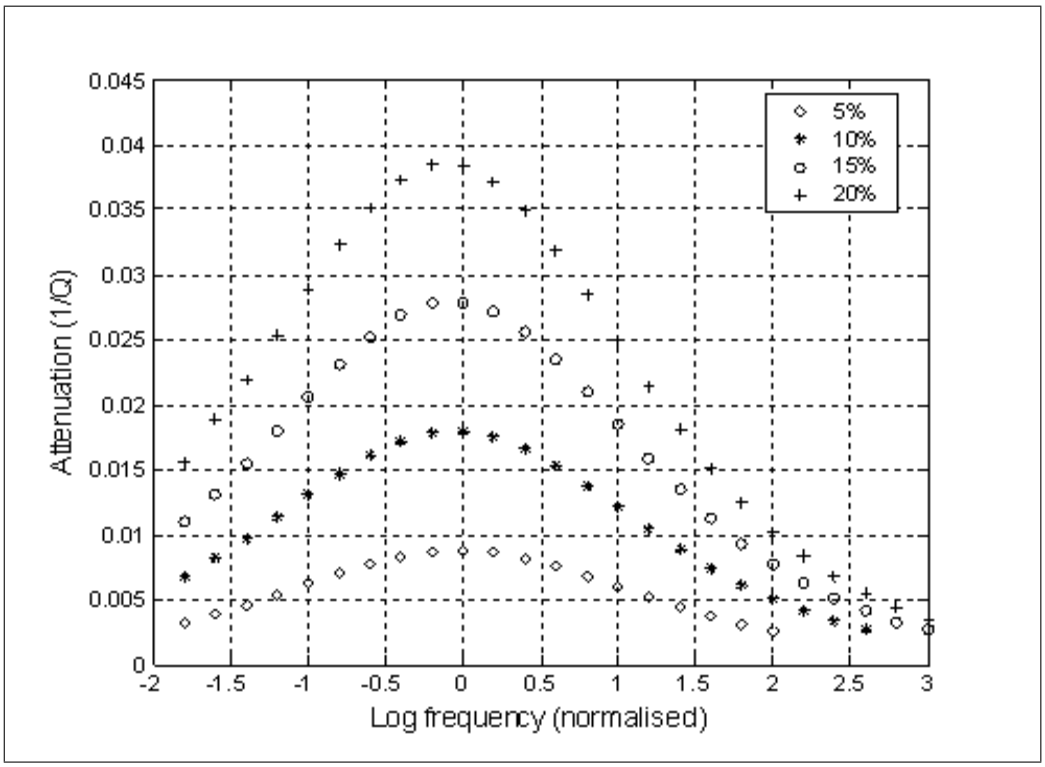

Fig. 10. *Attenuation vs circular frequency* Ω' *in fractured sandstone filled with water, with porosity* $\phi = 0.2$ *and fracture weakness* Δ_N *in range from 0.05 up to 0.2.*

Figure 10 shows attenuation versus Ω'. The maximal attenuation is at the zero position on logaritmic scale and for constant steps of changing Δ_N the maxima are equidistant. Thus by measuring the magnitude of attenuation we can estimate some of the parameters like permeability of the background or fracture weakness.

Rewriting equation (172) in real circular frequency for the maximum gives

$$\omega_M \frac{H^2 \eta M_b}{4\kappa_b C_b L_b} = \frac{\sqrt{2}}{\boldsymbol{\Delta}_N^2} \Rightarrow \omega_M = \frac{\sqrt{2} 4\kappa_b C_b L_b}{\boldsymbol{\Delta}_N^2 H^2 \eta M_b} = \frac{4\sqrt{2} D_b}{H^2} \left(\frac{C_b}{M_b \boldsymbol{\Delta}_N} \right)^2 ,$$

and substituting $\boldsymbol{\Delta}_N$ from equation (160) for small $\boldsymbol{\Delta}_N$ gives

$$\frac{1}{Z_N} = \frac{L_c}{h_c} = \frac{L_b}{\boldsymbol{\Delta}_N}$$

$$\omega_M = \frac{4\sqrt{2}D_b}{H^2}\left(\frac{C_b L_c}{M_b L_b h_c}\right)^2 = \frac{4\sqrt{2}D_b}{N_b^2}\left(\frac{L_c}{h_c H}\right)^2 \ ,$$

where $h_c H$ is the thickness of the fracture. For the unit spatial period H, thickness of the background is of the order $\mathcal{O}(1-h_c)$ while thickness of the fracture is of the order $\mathcal{O}(h_c)$. Therefore, the frequency for peak attenuation corresponding to points M_i is dominated by resonance in the fracture (curve c), because the attenuation curve of the background b (see Figure 8 is monotonically decreasing in this frequency range. The magnitude of the attenuation is defined by both diffusion lengths, meaning that the diffusion length of the background shows the depth of penetration of the fluid into the background while the diffusion length of the fracture shows the depth in fracture fluid can penetrate. Combination these two conditions creates the maximum.

4.2.5 Permeability of fracture material is lower than in the background

In this case (opposite to the previous one), we still assume that the fracture is made of soft material so that relation (155) holds. Let however the fracture permeability be now a different function of h_c:

$$\kappa_c = \tilde{\kappa} h_c, \tag{175}$$

where $\tilde{\kappa}$ is an estimator for fracture permeability, so as $h_c \to 0$, fracture permeability κ_c decreases and becomes lower than permeability of background, which is taken to be $\kappa_b = 10^{-13} m^2$ for modeling purposes. Using relations (158) and (155), the second term in denominator of equation (157) can be rewritten as

$$\sqrt{\frac{i\omega\eta N_c}{\kappa_c}}\frac{H}{2}\cot\sqrt{\frac{i\omega\eta}{\kappa_c N_c}}\frac{H}{2}h_c = \sqrt{\frac{i\omega\eta\tilde{L}}{\tilde{\kappa}}}\frac{H}{2}\cot\sqrt{\frac{i\omega\eta}{\tilde{\kappa}\tilde{L}}}\frac{H}{2} = \tilde{L}\sqrt{\frac{i\omega\eta}{\tilde{\kappa}\tilde{L}}}\frac{H}{2}\cot\sqrt{\frac{i\omega\eta}{\tilde{\kappa}\tilde{L}}}\frac{H}{2} \ . \tag{176}$$

Here note that h_c is no longer a factor in the argument of the cotangent so the argument is small only for frequencies much lower than in the previous case although the limit of the expression (176) is also $\tilde{L}$ when

$$\tan \sqrt{\frac{i\omega\eta}{\tilde{\kappa}\tilde{L}}} \frac{H}{2} \rightarrow 0 \, .$$

Figures 11 and 12 show the dispersion and the comparison of frequency peaks between high and low permeability of fractures of the same softness. Curve "hp" denotes case when the permeability of fractures is of the same order of magnitude as that of the background, while curves "lp2" and "lp1" denote cases of fracture permeability being lower than that of the background by one and two order of magnitudes, respectively. There is strong shift of the maximum of attenuation towards lower frequencies for less and less permeable fractures. The diffusion coefficient in the fracture $D_c = \kappa_c N_c/\eta$ is then of the order $O(h_c^2)$ so it is necessary to go to $\sqrt{\omega}$ very small in order to have a peak of attenuation. This case is only for very low fracture permeability. This case also confirms the fact that the maximum is dominated by the diffusion length of the fracture, because whatever the diffusion length of the background, conservation of mass of fluid moving across the interface must be satisfied, so amount of fluid which can flow and produce attenuation is given by the diffusion length of fracture ($D_c < D_b$).

4.2.6 Permeability of fractures is independent of h_c

In this case relation (155) is also valid. Fracture permeability is independent of h_c, so as $h_c \rightarrow 0$, fracture permeability κ_c remains the same. Using relation (155), the second term in the denominator of equation (157) can be rewritten as

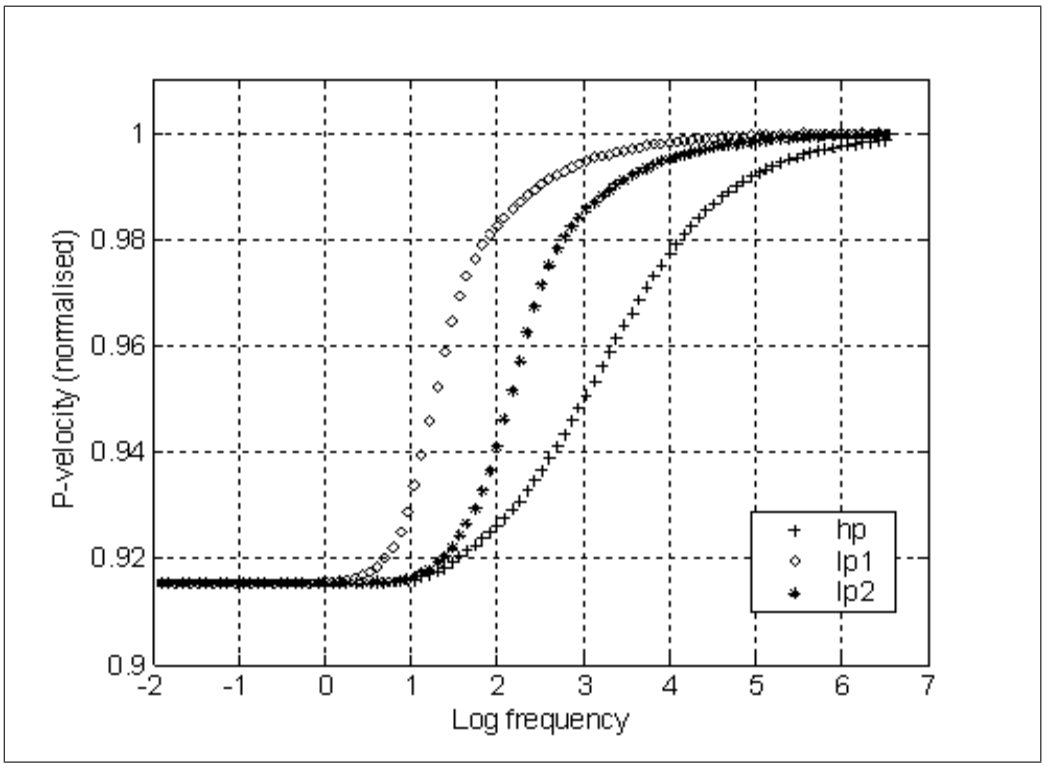

Fig. 11. *Normalized P-wave velocity vs circular frequency for different fracture permeability (curve "hp" denotes case when the permeability of fractures is of the same order of magnitude as that of the background, while curves "lp2" and "lp1" denote cases of fracture permeability being lower than that of the background by one and two order of magnitudes, respectively.*

$$\sqrt{\frac{i\omega\eta N_c}{\kappa_c}}\frac{H}{2}\cot\sqrt{\frac{i\omega\eta}{\kappa_c N_c}}\frac{H}{2}h_c = \tilde{L}\sqrt{\frac{i\omega\eta}{\kappa_c\tilde{L}}}\frac{H}{2}\sqrt{h_c}\cot\sqrt{\frac{i\omega\eta}{\kappa_c\tilde{L}}}\frac{H}{2}\sqrt{h_c}\,. \qquad (177)$$

As $\sqrt{h_c} \to 0$ (instead of $h_c \to 0$ like in the first case), the argument of the trigonometric cotangent function becomes small enough to give the same limiting value for the second term $\tilde{L}$. This case has to be investigated carefully to see at which frequency limit $\tilde{L}$ will be reached. In order to demonstrate frequency behavior we will show graphs of varying fracture permeability and h_c. The limit of the expression (177) is also $\tilde{L}$ but is reached only at much smaller frequencies when

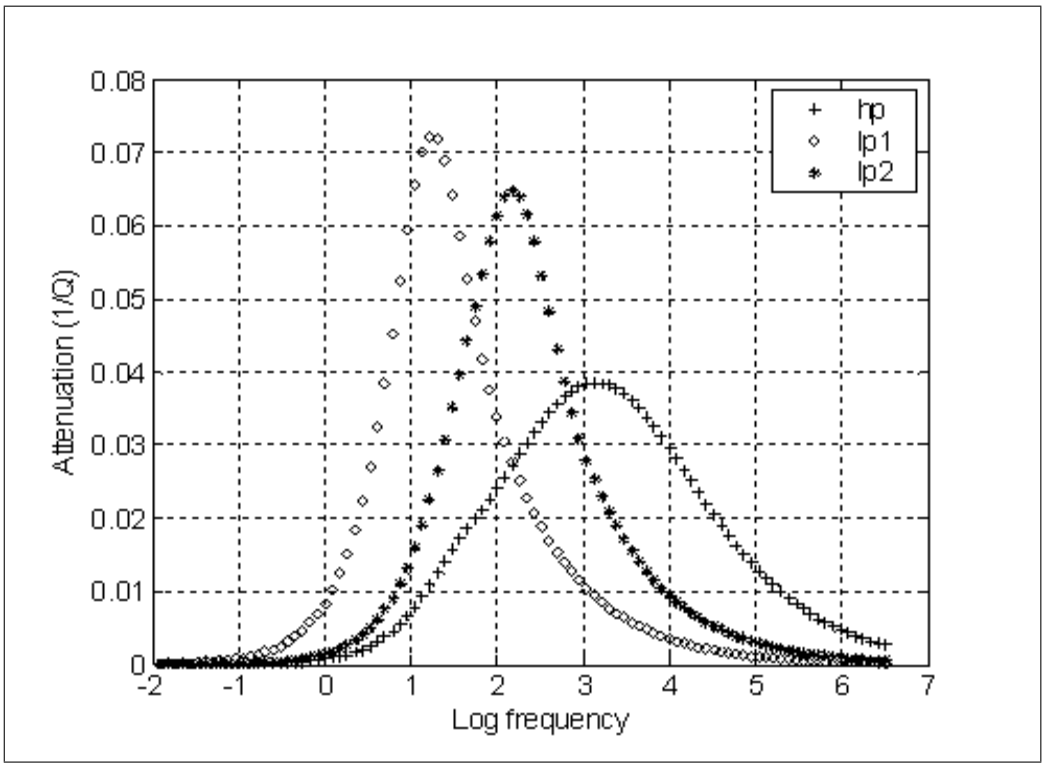

Fig. 12. *Attenuation vs circular frequency for different fracture permeability (curve "hp" denotes case when the permeability of fractures is of the same order of magnitude as that of the background, while curves "lp2" and "lp1" denote cases of fracture permeability being lower than that of the background by one and two order of magnitudes, respectively.*

$$\tan \sqrt{\frac{i\omega\eta}{\kappa_c \tilde{L}}} \frac{H}{2} \sqrt{h_c} \to 0 \, .$$

The diffusion coefficient in the fracture $D_c = \kappa_c N_c/\eta$ is then of the order $O(h_c)$. In this case fracture permeability can be higher or lower than the permeability of the background, and the attenuation peak occurs at different frequencies. The attenuation mechanism is explained by the ratio of the diffusion length and fracture "thickness". Figures 13 and 14 show dispersion curves and the comparison in attenuation peak between high and low permeability of fractures of the same softness.

Figures 15 and 16 show dispersion curves and the attenuation peak for the fractures of same permeability but different thickness. Here we see how much attenuation peak is affected by the ratio of diffusion length and thickness of fracture. In Figure 17

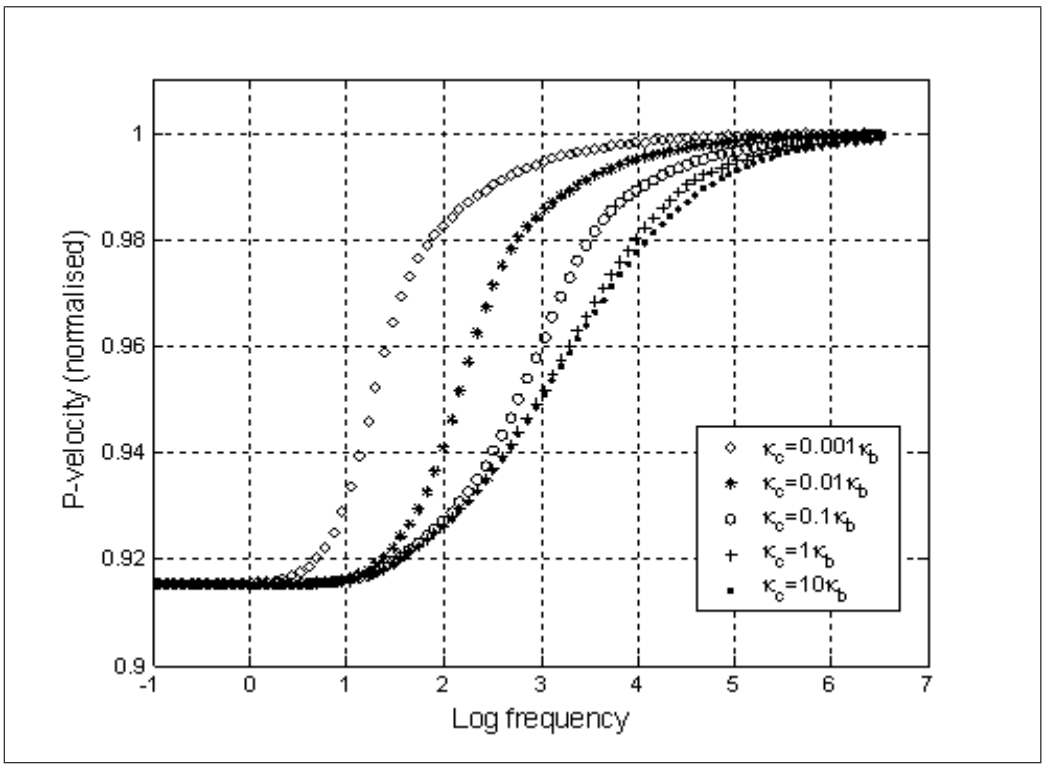

Fig. 13. *Normalized P-wave velocity vs circular frequency for the constant fracture thickness* $h_c = 0.01h_b$ *and varying fracture permeability* κ_c.

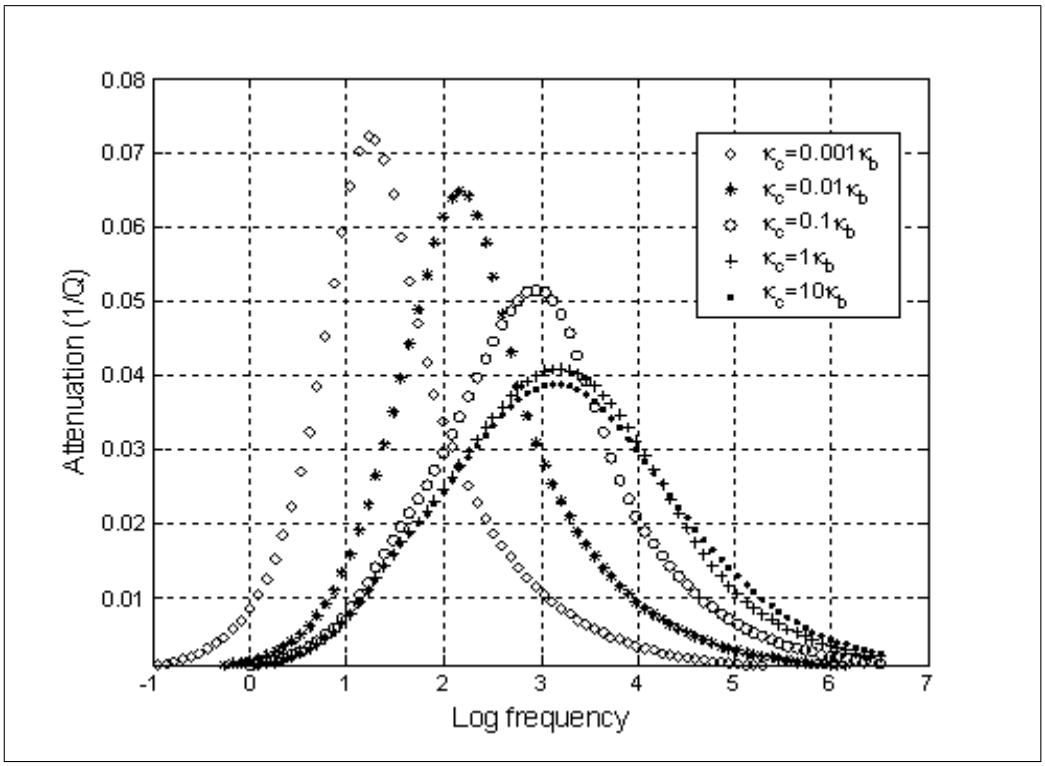

Fig. 14. *Attenuation curves for the constant fracture thickness* $h_c = 0.01h_b$ *and varying fracture permeability* κ_c *with respect to constant background permeability* κ_b.

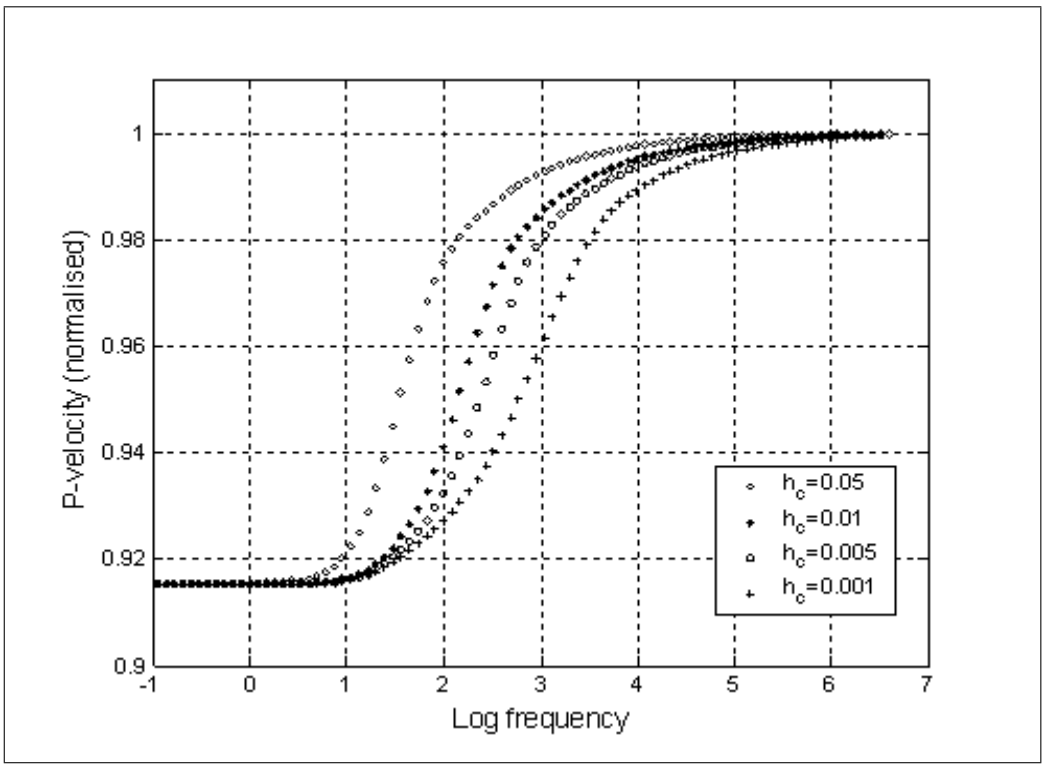

Fig. 15. *Normalized P-wave velocity vs circular frequency for the constant fracture permeability* $\kappa_c = 0.01\kappa_b$ *and varying fracture thickness* h_c.

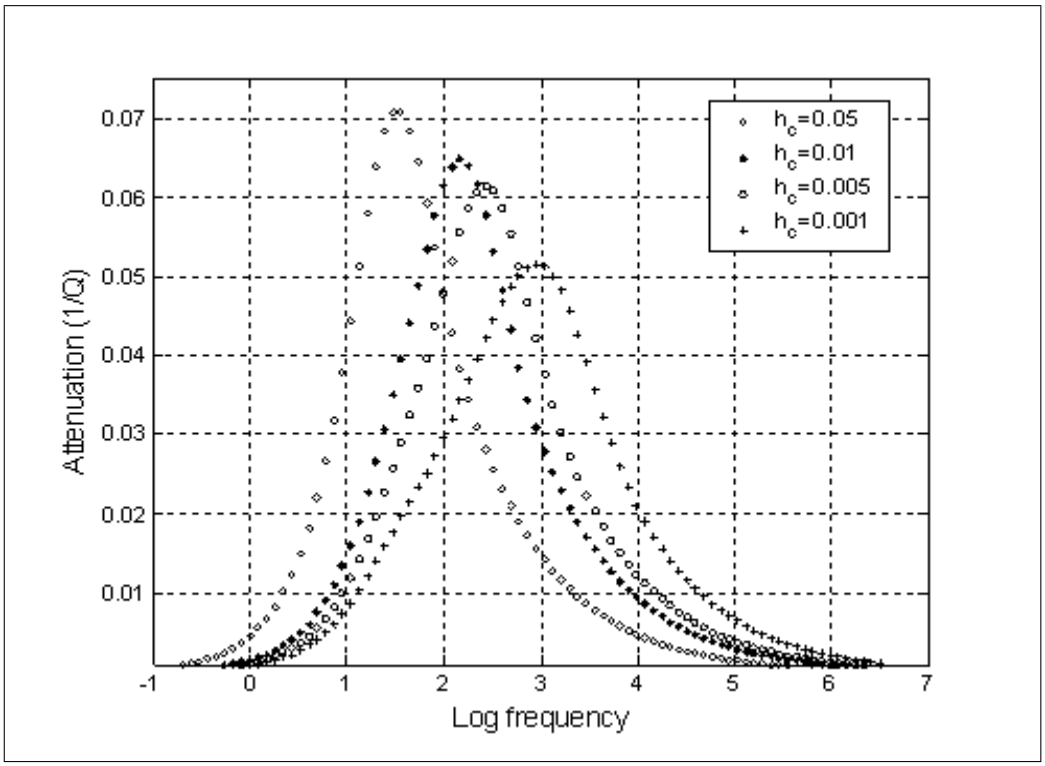

Fig. 16. *Attenuation vs frequecny for the constant fracture permeability* $\kappa_c = 0.01\kappa_b$ *and varying fracture thickness* h_c.

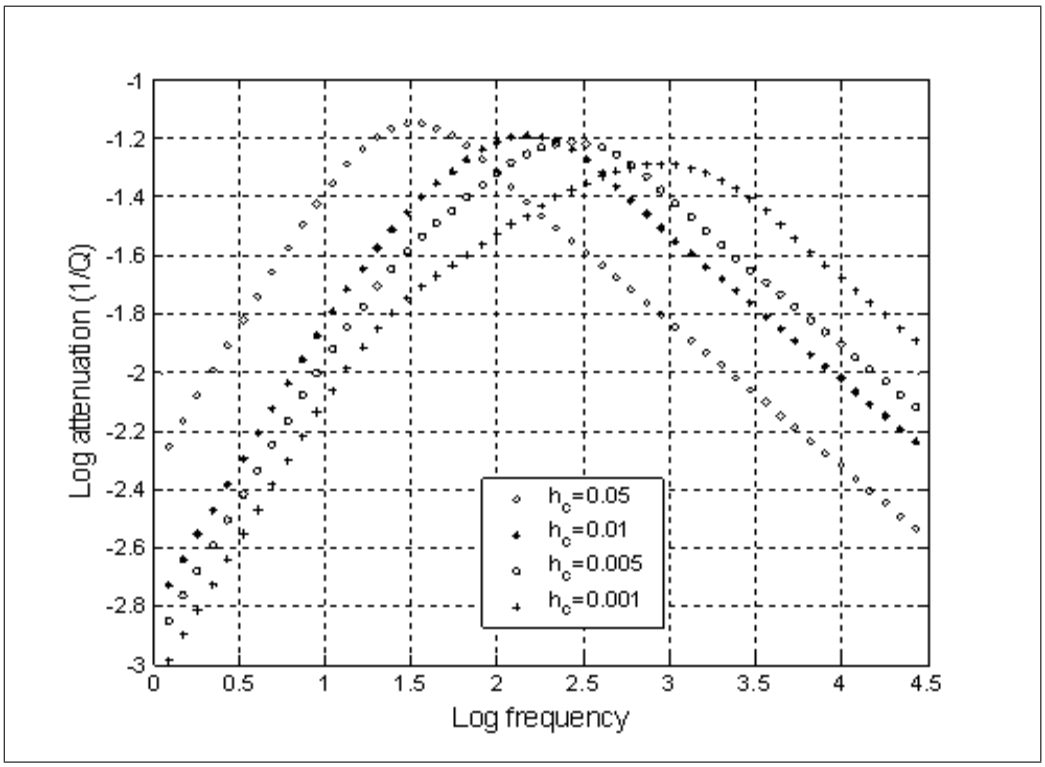

Fig. 17. *Bilogarithmic plot of attenuation vs frequency for the constant fracture permeability* $\kappa_c = 0.01\kappa_b$ *and varying fracture thickness* h_c.

the separation of background and fracture parts of the attenuation curves is shown, and as fracture thickness decreases, this separation becomes stronger and transitional part of the curve where attenuation scales with $\omega^{1/2}$ is more apparent.

5 Fractured porous media - low and high frequency moduli

5.1 Iso-stress moduli for layered media

In this section we will derive low frequency moduli without referring to the frequency dependent solution, but directly from iso-stress condition in z direction (Norris, 1993). Again, using definitions of P-wave moduli for dry L saturated modulus $L_s = C$ respectively,

$$L = \lambda + 2\mu = K + \frac{4}{3}\mu,\ L_s = C = \lambda_s + 2\mu = K_s + \frac{4}{3}\mu,$$

and the relation between them (Gassmann relation):

$$K_s = K + \alpha^2 M,\ C = L + \alpha^2 M \tag{178}$$

we can rewrite constitutive relations (57) in the following form:

$$\boldsymbol{\sigma} = (\mathbf{L} + \alpha^2 M)\boldsymbol{\varepsilon} - \alpha M \left(\frac{p}{M} + \alpha\varepsilon\right)\mathbf{I} = \mathbf{L}\boldsymbol{\varepsilon} - \alpha p\mathbf{I}, \tag{179}$$

where $\mathbf{L}$ is the stiffness tensor for the dry rock. Note here that shear modulus μ is not affected by fluid, so dry and saturated shear moduli are equal.

Low frequency limit means that pore pressure is constant (there is enough time for pressure to equilibrate throughout the stack) and average increase of fluid in stack is zero

$$p = const,\ \langle\xi\rangle = 0\ .$$

Therefore, by averaging constitutive relations (179) over the stack of layers we get:

$$\begin{aligned} 0 &= \langle\xi\rangle = \langle\alpha\varepsilon\rangle + \left\langle M^{-1}\right\rangle p, \\ \boldsymbol{\sigma} &= \mathbf{L}\boldsymbol{\varepsilon} + \alpha\left\langle M^{-1}\right\rangle^{-1}\langle\alpha\varepsilon\rangle\,\mathbf{I} \end{aligned} \tag{180}$$

Furthermore, as discussed in Chapter 3, in a horizontally stratified medium with $x_3 =$

z being axis of symmetry, the displacements u_1, u_2, u_3 and stresses $\sigma_{13}, \sigma_{23}, \sigma_{33}$ are continuous across the interfaces. Recalling the linear relationship (5) between stain and displacement, we note that variables $(\varepsilon_{11}, \varepsilon_{22}, \varepsilon_{12}, \sigma_{13}, \sigma_{23}, \sigma_{33})$ are constant across the interfaces. Thus we can express a set of "jumping" variables (those which can change on the interface) $(\varepsilon_{33}, \varepsilon_{13}, \varepsilon_{23}, \sigma_{11}, \sigma_{22}, \sigma_{12})$ as a function of "constant" variables $(\varepsilon_{11}, \varepsilon_{22}, \varepsilon_{12}, \sigma_{13}, \sigma_{23}, \sigma_{33})$, then we will average these "jumping" variables. First, we can find ε_{33} from equation (179):

$$\sigma_{33} = c_{31}\varepsilon_{11} + c_{32}\varepsilon_{22} + c_{33}\varepsilon_{33} - \alpha p = \lambda(\varepsilon_{11} + \varepsilon_{22}) + (\lambda + 2\mu)\varepsilon_{33} - \alpha p$$

$$\varepsilon_{33} = \frac{1}{L}\left[\sigma_{33} - \lambda(\varepsilon_{11} + \varepsilon_{22}) + \alpha p\right]$$

Expressing ξ in terms of "constants":

$$\begin{aligned}\xi &= \frac{p}{M} + \alpha(\varepsilon_{11} + \varepsilon_{22}) + \frac{\alpha}{L}\left[\sigma_{33} - \lambda(\varepsilon_{11} + \varepsilon_{22}) + \alpha p\right] \\ &= \alpha(\varepsilon_{11} + \varepsilon_{22})\left(1 - \frac{\lambda}{L}\right) + \frac{\alpha}{L}\sigma_{33} + p\left[\frac{1}{M} - \frac{\alpha^2}{L}\right]\end{aligned}$$

then using identities:

$$1 - \frac{\lambda}{L} = \frac{L - \lambda}{L} = \frac{\lambda + 2\mu - \lambda}{L} = \frac{2\mu}{L}$$

ξ can be rewritten as:

$$\xi = 2\mu\frac{\alpha}{L}(\varepsilon_{11} + \varepsilon_{22}) + \frac{\alpha}{L}\sigma_{33} + \left(\frac{1}{M} - \frac{\alpha^2}{L}\right)p.$$

Averaging through layers and applying the low-frequency condition $\langle\xi\rangle = 0$, we get:

$$0 = \langle\xi\rangle = \left\langle 2\mu\frac{\alpha}{L}\right\rangle(\varepsilon_{11} + \varepsilon_{22}) + \left\langle\frac{\alpha}{L}\right\rangle\sigma_{33} + \left\langle\frac{1}{M} + \frac{\alpha^2}{L}\right\rangle p$$

Expressing p as a function of "constants" we have

$$p = -A(\varepsilon_{11} + \varepsilon_{22}) - B\sigma_{33} \tag{181}$$

where

$$A = \left\langle \frac{1}{M} + \frac{\alpha^2}{L} \right\rangle^{-1} \left\langle 2\mu \frac{\alpha}{L} \right\rangle, \; B = \left\langle \frac{1}{M} + \frac{\alpha^2}{L} \right\rangle^{-1} \left\langle \frac{\alpha}{L} \right\rangle. \tag{182a}$$

Substituting p from (181) into (179) we can obtain the vector of the "jumping" variables as a linear function of the continuous variables.

Focusing our attention on compressional wave only, we can reduce the set of "constant" variables to $(\varepsilon_{11}, \varepsilon_{22}, \sigma_{33})$. First, calculating σ_{11} in terms of $(\varepsilon_{11}, \varepsilon_{22}, \sigma_{33})$ for any isotropic layer, we get

$$\sigma_{11} = (\lambda + 2\mu)\,\varepsilon_{11} + \lambda\varepsilon_{22} + \lambda\varepsilon_{33} - \alpha p = (\lambda + 2\mu)\,\varepsilon_{11} + \lambda\varepsilon_{22} + \lambda\varepsilon_{33} + \alpha A\varepsilon_{11} + \alpha A\varepsilon_{22} + \alpha B\sigma_{33}$$

$$\begin{aligned}
\sigma_{11} = {} & \frac{1}{\lambda + 2\mu} \left[(\lambda + 2\mu)^2 + (\lambda + 2\mu)\,\alpha A - \lambda^2 - \lambda\alpha A \right] \varepsilon_{11} + \\
& + \frac{1}{\lambda + 2\mu} \left[\lambda\,(\lambda + 2\mu) + (\lambda + 2\mu)\,\alpha A - \lambda^2 - \lambda\alpha A \right] \varepsilon_{22} + \\
& + \frac{1}{\lambda + 2\mu} \left[(\lambda + 2\mu)\alpha B + \lambda - \lambda\alpha B \right] \sigma_{33},
\end{aligned}$$

so that:

$$\sigma_{11} = \frac{1}{\lambda + 2\mu} \left[2\mu\,(2\lambda + 2\mu + \alpha A)\,\varepsilon_{11} + 2\mu\,(\lambda + \alpha A)\,\varepsilon_{22} + (\lambda + 2\mu\alpha B)\,\sigma_{33} \right]. \tag{183}$$

In the same way expressions for σ_{22} and ε_{33} can be calculated:

$$\sigma_{22} = \frac{1}{\lambda + 2\mu} \left[2\mu\,(\lambda + \alpha A)\,\varepsilon_{11} + 2\mu\,(2\lambda + 2\mu + \alpha A)\,\varepsilon_{22} + (\lambda + 2\mu\alpha B)\,\sigma_{33} \right], \tag{184}$$

$$\varepsilon_{33} = \frac{1}{L} \left[-(\lambda + \alpha A)\,\varepsilon_{11} - (\lambda + \alpha A)\,\varepsilon_{22} + (1 - \alpha B)\,\sigma_{33} \right] \tag{185}$$

Combining the last three expressions yields

$$\begin{bmatrix} \sigma_{11} \\ \sigma_{22} \\ \varepsilon_{33} \end{bmatrix} = \frac{1}{\lambda + 2\mu} \begin{bmatrix} 2\mu(2\lambda + 2\mu + \alpha A) & 2\mu(\lambda + \alpha A) & \lambda + 2\mu\alpha B \\ 2\mu(\lambda + \alpha A) & 2\mu(2\lambda + 2\mu + \alpha A) & \lambda + 2\mu\alpha B \\ -(\lambda + \alpha A) & -(\lambda + \alpha A) & 1 - \alpha B \end{bmatrix} \begin{bmatrix} \varepsilon_{11} \\ \varepsilon_{22} \\ \sigma_{33} \end{bmatrix}$$

From this expression we will be able to calculate effective elastic moduli. Solving equation (185) for σ_{33}, we can write

$$\sigma_{33} = \frac{\lambda + \alpha A}{1 - \alpha B}\left(\varepsilon_{11} + \varepsilon_{22}\right) + \frac{L}{1 - \alpha B}\varepsilon_{33} = \frac{\lambda + \alpha A}{L}\frac{L}{1 - \alpha B}\left(\varepsilon_{11} + \varepsilon_{22}\right) + \frac{L}{1 - \alpha B}\varepsilon_{33},$$

or

$$\frac{1 - \alpha B}{L}\sigma_{33} = \frac{\lambda + \alpha A}{L}\left(\varepsilon_{11} + \varepsilon_{22}\right) + \varepsilon_{33}.$$

Averaging through all layers whilst keeping in mind that ε_{11}, ε_{22}, and σ_{33} are continuous, we have

$$\left\langle \frac{1 - \alpha B}{L} \right\rangle \sigma_{33} = \left\langle \frac{\lambda + \alpha A}{L} \right\rangle \left(\varepsilon_{11} + \varepsilon_{22}\right) + \left\langle \varepsilon_{33} \right\rangle$$

$$\sigma_{33} = \left\langle \frac{\lambda + \alpha A}{L} \right\rangle \left\langle \frac{1 - \alpha B}{L} \right\rangle^{-1} \left(\varepsilon_{11} + \varepsilon_{22}\right) + \left\langle \frac{1 - \alpha B}{L} \right\rangle^{-1} \left\langle \varepsilon_{33} \right\rangle \tag{186}$$

Equation (186) is our first stress-average strain relation for the layered porous medium. Comparison with the general stiffness matrix for a TI medium yields low frequency equivalent elastic moduli $c_{33_0}^{sat}$ and $c_{13_0}^{sat}$ (with subscript 0 indicating low frequency limit).

$$c_{33_0}^{sat} = \left\langle \frac{1 - \alpha B}{L} \right\rangle^{-1} \tag{187}$$

$$c_{13_0}^{sat} = c_{33_0}^{sat} \left\langle \frac{\lambda + \alpha A}{L} \right\rangle \tag{188}$$

In order to calculate $c_{11_0}^{sat}$, we average (183):

$$\begin{aligned} \left\langle \sigma_{11} \right\rangle &= \left\langle \frac{2\mu\left(2\lambda + 2\mu + \alpha A\right)}{L} \right\rangle \varepsilon_{11} + \left\langle \frac{2\mu\left(\lambda + \alpha A\right)}{L} \right\rangle \varepsilon_{22} + \left\langle \frac{\lambda + 2\mu\alpha B}{L} \right\rangle \sigma_{33} \\ &= \left\langle \frac{2\mu\left(2\lambda + 2\mu + \alpha A\right)}{L} \right\rangle \varepsilon_{11} + \left\langle \frac{\lambda + 2\mu\alpha B}{L} \right\rangle c_{13_0}^{sat}\varepsilon_{11} + \\ &+ \left\langle \frac{2\mu\left(\lambda + \alpha A\right)}{L} \right\rangle \varepsilon_{22} + \left\langle \frac{\lambda + 2\mu\alpha B}{L} \right\rangle c_{13_0}^{sat}\varepsilon_{22} + \left\langle \frac{\lambda + 2\mu\alpha B}{L} \right\rangle c_{33_0}^{sat} \left\langle \varepsilon_{33} \right\rangle \end{aligned} \tag{189}$$

Taking just coefficients connected with ε_{11} in (189), we have:

$$\left\langle \frac{2\mu\left(2\lambda + 2\mu + \alpha A\right)}{L} \right\rangle = \left\langle \frac{2\mu\left(\lambda + \alpha A + L\right)}{L} \right\rangle = \left\langle \frac{2\mu\left(\lambda + \alpha A\right)}{L} \right\rangle + \left\langle 2\mu \right\rangle$$

$$\left\langle \frac{\lambda + 2\mu\alpha B}{L} \right\rangle c_{13_0}^{sat} = c_{13_0}^{sat} \left[\left\langle \frac{\lambda}{L} \right\rangle + \left\langle \frac{2\mu\alpha}{L} \right\rangle B \right] . \tag{190}$$

From equations (182a), the relation between quantities A and B is

$$B = \left\langle \frac{1}{M} + \frac{\alpha^2}{L} \right\rangle^{-1} \left\langle \frac{\alpha}{L} \right\rangle = A \frac{\left\langle \frac{\alpha}{L} \right\rangle}{\left\langle \frac{2\mu\alpha}{L} \right\rangle}, \qquad \left\langle \frac{2\mu\alpha}{L} \right\rangle B = A \left\langle \frac{\alpha}{L} \right\rangle ,$$

which we substitute in equation (190) to get

$$\left\langle \frac{\lambda + 2\mu\alpha B}{L} \right\rangle c_{13_0}^{sat} = c_{13_0}^{sat} \left[\left\langle \frac{\lambda}{L} \right\rangle + \left\langle \frac{\alpha}{L} \right\rangle A \right] = c_{13_0}^{sat} \left\langle \frac{\lambda + \alpha A}{L} \right\rangle = \frac{\left(c_{13_0}^{sat} \right)^2}{c_{33_0}^{sat}} ,$$

and finally

$$c_{11_0}^{sat} = \frac{\left(c_{13_0}^{sat} \right)^2}{c_{33_0}^{sat}} + \left\langle \frac{2\mu \left(\lambda + \alpha A \right)}{L} \right\rangle + \langle 2\mu \rangle \tag{191}$$

Similarly, taking just coefficients connected with ε_{22} in equation (189), we get the remaining stiffness coefficient:

$$c_{12_0}^{sat} = \frac{\left(c_{13_0}^{sat} \right)^2}{c_{33_0}^{sat}} + \left\langle \frac{2\mu \left(\lambda + \alpha A \right)}{L} \right\rangle \tag{192}$$

Equations (187), (188), (191), and (192) give the effective stiffness coefficients which are needed to fully describe compressional wave propagation in the layered medium in the low-frequency limit.

In order to compare the results of this section with the frequency dependent solution (152), we rewrite equation (187) in the form

$$\frac{1}{c_{33_0}^{sat}} = \left\langle \frac{1}{L} \right\rangle - \frac{\left\langle \frac{\alpha}{L} \right\rangle^2}{\left\langle \frac{1}{N} \right\rangle} . \tag{193}$$

Noting that from equation

$$\frac{1}{N} = \frac{C}{ML} = \frac{1}{M} + \frac{\alpha^2}{L} ,$$

for each layer, from identity $ML/NC \equiv 1$, and from relation $L = C - \alpha^2 M$, it can be shown that for a two-layer periodic system, equation (193) yields

$$
\begin{aligned}
\frac{1}{c_{33_0}^{sat}} &= \frac{h_b M_b}{C_b N_b} + \frac{h_c M_c}{C_c N_c} - \frac{\left(\frac{h_b \alpha_b M_b}{N_b C_b} + \frac{h_c \alpha_c M_c}{N_c C_c}\right)^2}{\frac{h_b}{N_b} + \frac{h_c}{N_c}} \\
&= \frac{h_b M_b}{C_b N_b} + \frac{h_c M_c}{C_c N_c} - \frac{\left(\frac{h_b \alpha_b M_b}{N_b C_b}\right)^2 + \left(\frac{h_c \alpha_c M_c}{N_c C_c}\right)^2 + 2 h_b h_c \alpha_b \alpha_c \frac{M_b M_c}{C_b C_c N_b N_c}}{\frac{h_b h_c}{N_b N_c}\left[\frac{N_b}{h_b} + \frac{N_c}{h_c}\right]} \\
&= \frac{h_b}{C_b} \underbrace{\frac{M_b \left(C_b - \alpha_b^2 M_b\right)}{C_b N_b}}_{M_b L_b / C_b N_b \equiv 1} + \frac{h_c}{C_c} \underbrace{\frac{M_c \left(C_c - \alpha_c^2 M_c\right)}{C_c N_c}}_{M_c L_c / C_c N_c \equiv 1} + \frac{\left(\frac{\alpha_b M_b}{C_b} - \frac{\alpha_c M_c}{C_c}\right)^2}{\frac{N_b}{h_b} + \frac{N_c}{h_c}} \\
&= \left\langle \frac{1}{C} \right\rangle + \frac{\left(\frac{\alpha_b M_b}{C_b} - \frac{\alpha_c M_c}{C_c}\right)^2}{\frac{N_b}{h_b} + \frac{N_c}{h_c}} \,,
\end{aligned}
$$

which is precisely the zero frequency limit of equation (152).

Substituting parameter γ (144) into equations (188) and (191) for other the moduli we find:

$$
c_{13_0}^{sat} = c_{33_0}^{sat} \left(1 - 2\langle\gamma\rangle + 2\left\langle\frac{\alpha}{L}\right\rangle \frac{\langle\alpha\gamma\rangle}{\left\langle\frac{1}{N}\right\rangle}\right) \,, \quad c_{11_0}^{sat} = \frac{\left(c_{13_0}^{sat}\right)^2}{c_{33_0}^{sat}} + 4\left(\langle\mu\rangle - \langle\gamma\mu\rangle + \frac{\langle\alpha\gamma\rangle^2}{\left\langle\frac{1}{N}\right\rangle}\right), \tag{194}
$$

where

$$
\left\langle\frac{1}{N}\right\rangle = \left\langle\frac{C}{ML}\right\rangle = \left\langle\frac{1}{M} + \frac{\alpha^2}{L}\right\rangle = \frac{\langle\alpha\rangle}{K_g} + \left(\frac{1}{K_f} - \frac{1}{K_g}\right)\langle\phi\rangle + \left\langle\frac{\alpha^2}{L}\right\rangle \,.
$$

Shear stiffnesses are unaffected by the fluid, they are exactly the same as in elastic media (Backus, 1962):

$$
c_{55_0}^{sat} = c_{55_0}^{dry} = \left\langle\frac{1}{\mu}\right\rangle^{-1} \,, \quad c_{66_0}^{sat} = c_{66_0}^{dry} = \langle\mu\rangle \,. \tag{195}
$$

Substituting γ into equation (44) we get

$$
\alpha_j = 1 - \frac{(1 - \frac{4}{3}\gamma_j) L_j}{K_g} \,,
$$

then

$$
\langle\alpha\rangle = 1 - \frac{\langle L\rangle - \frac{4}{3}\langle\mu\rangle}{K_g} \,, \; \langle\alpha\gamma\rangle = \langle\gamma\rangle - \frac{\langle\mu\rangle - \frac{4}{3}\langle\gamma\mu\rangle}{K_g} \,, \; \left\langle\frac{\alpha}{L}\right\rangle = \left\langle\frac{1}{L}\right\rangle - \frac{1 - \frac{4}{3}\langle\gamma\rangle}{K_g} \,,
$$

and

$$\left\langle \frac{\alpha^2}{L} \right\rangle = \left\langle \frac{1}{L} \right\rangle - 2\frac{1 - \frac{4}{3}\langle\gamma\rangle}{K_g} + \frac{\left\langle \frac{1}{L} \right\rangle - \frac{8}{3}\langle\mu\rangle + \frac{16}{9}\langle\gamma\mu\rangle}{K_g^2} \ .$$

5.2 Iso-stress moduli for fractured media

As with the frequency dependent P-wave modulus, the low-frequency stiffnesses for the fractured medium can be obtained by taking the small thickness ratio limit $h_c \to 0$. Remembering that L_c and μ_c are required to be $\mathcal{O}(h_c)$, we can write

$$\langle\alpha\rangle \to \alpha_b \ , \ \langle\alpha\gamma\rangle \to \alpha_b\gamma_b \ , \ \left\langle \frac{\alpha}{L} \right\rangle \to \frac{\alpha_b}{L_b} + Z_N \ , \ \left\langle \frac{\alpha^2}{L} \right\rangle \to \frac{\alpha_b^2}{L_b} + Z_N \ ,$$

so that

$$\left\langle \frac{1}{N} \right\rangle \to \frac{1}{N_b} + Z_N \ .$$

Equation (193) then gives,

$$\begin{aligned} \frac{1}{c_{33_0}^{sat}} &= \frac{1}{L_b} + Z_N - \frac{\left(\frac{\alpha_b}{L_b} + Z_N\right)^2}{\frac{1}{N_b} + Z_N} = \frac{1}{C_b} + \frac{\alpha_b^2 N_b}{L_b^2} + Z_N - \frac{\left(\frac{\alpha_b}{L_b} + Z_N\right)^2}{\frac{1}{N_b} + Z_N} \\ &= \frac{1}{C_b} + \frac{Z_N\left(\frac{\alpha_b^2 N_b}{L_b^2} + \frac{1}{N_b} - 2\frac{\alpha_b}{L_b}\right)}{\frac{1}{N_b} + Z_N} = \frac{1}{C_b} + \frac{Z_N\left(\frac{\alpha_b N_b}{L_b} - 1\right)^2}{1 + Z_N N_b} \\ &= \frac{1}{C_b}\left[1 + \frac{Z_N(\alpha_b M_b - C_b)^2}{C_b(1 + Z_N N_b)}\right] \ . \end{aligned} \tag{196}$$

It is interesting to compare this result with the low-frequency limit of the frequency dependent solution (159). In this limit, the cotangent function in equation (159) can be replaced by the inverse of its argument, and this equation reduces to

$$\frac{1}{c_{33_0}^{sat}} = \frac{1}{C_b} + \frac{\left(\frac{\alpha_b M_b}{C_b} - 1\right)^2}{N_b + \frac{1}{Z_N}} = \frac{1}{C_b}\left[1 + \frac{Z_N(\alpha_b M_b - C_b)^2}{C_b(1 + Z_N N_b)}\right] \ . \tag{197}$$

which is identical to equation (196), as expected. Equation (197) provides an expression for the P-wave modulus of waves propagating normal to the fractures at low

frequencies, i.e. for frequencies low enough to allow equilibration of the fluid pressure p between fractures and the background during the period of the wave.

Taking into account that $(L_b/N_b)(1+Z_N N_b) \equiv \alpha_b^2 + L_b/M_b + Z_N L_b$, the small thickness ratio limit $h_c \to 0$ in the first and second of equations (194) gives,

$$c_{13_0}^{sat} = c_{33_0}^{sat}\left[1 - 2\gamma_b + 2\alpha_b\gamma_b\frac{N_b}{L_b}\,\frac{\alpha_b + Z_N L_b}{1 + Z_N N_b}\right] , \tag{198}$$
$$c_{11_0}^{sat} = \frac{\left(c_{13_0}^{sat}\right)^2}{c_{33_0}^{sat}} + 4\left[(1-\gamma_b)\mu_b + \frac{\alpha_b^2\gamma_b^2 N_b}{1 + Z_N N_b}\right] .$$

The shear moduli, independent of the fluid, are given from (195) by

$$c_{55_0} = \frac{1}{\mu_b} + Z_T , \quad c_{66_0} = \mu_b . \tag{199}$$

Equations (197), (198) and (199) provide exact explicit analytical expressions for low-frequency elastic moduli of a fractured medium as a function of the properties of the background, fractures, and fluid bulk modulus. Using simple algebra one can show that these equations are exactly equivalent to the equations of the anisotropic Gassmann model for fluid substitution in a porous medium with aligned fractures (Gurevich, 2002). This equivalence demonstrates that the model of wave propagation in fractured media proposed in this work is consistent with the fundamental equations of anisotropic poroelasticity (Gassmann, 1951; Brown and Korringa, 1975), which are exact in the low frequency limit. These equations can be used for fluid substitution in fractured porous rocks. More detailed analysis of the effects of background porosity and fluid properties on the low frequency anisotropy of fractured rocks can be found in Gurevich (2002) and Cardona (2002).

The results for high frequencies can be obtained by taking the limit $\omega \to \infty$ in equation (152), while still assuming ω to be less than ω_B and ω_R. For this reason, the subscript $_{high}$ will be used instead of subscript $_\infty$. Noting that $\lim_{\omega\to\infty} \cot\sqrt{i\omega}B = -i$, taking this limit gives

$$\frac{1}{c^{sat}_{33_{high}}} = \left\langle \frac{1}{C} \right\rangle = \frac{h_b}{C_b} + \frac{h_c}{C_c} \,. \tag{200}$$

This result, that at high frequencies the P-wave elastic modulus is the weighted harmonic average of the saturated moduli of the two media (computed using isotropic Gassmann equations), is to be expected. Indeed, at high frequencies the fluid has no time to move from pores in the background into the medium representing the fractures, or vice versa. No flow between the media means the interfaces can be considered impermeable, and the whole layered continuum can be considered as a stack of elastic layers. The properties of the stack can therefore be determined by Backus averaging the saturated Gassmann moduli C and μ. Equation (200) is consistent with this approach.

As $h_c \to 0$, recall that although L_c is $\mathcal{O}(h_c)$, the Gassmann modulus C_c remains finite (154). Thus, the moduli obtained as $h_c \to 0$ are:

$$\begin{aligned}
\frac{1}{c^{sat}_{33_{high}}} &= \left\langle \frac{1}{C} \right\rangle \to \frac{1}{C_b} \,, \\
c^{sat}_{13_{high}} &= c^{sat}_{33_{high}} \left(1 - 2\left\langle \frac{\mu}{C} \right\rangle\right) \to c^{sat}_{33_{high}} \left(1 - 2\frac{\mu_b}{C_b}\right) \,, \\
c^{sat}_{11_{high}} &= \frac{\left(c^{sat}_{13_{high}}\right)^2}{c^{sat}_{33_{high}}} + 4\left(\langle\mu\rangle - \left\langle \frac{\mu^2}{C} \right\rangle\right) \to \frac{\left(c^{sat}_{13_{high}}\right)^2}{c^{sat}_{33_{high}}} + 4\mu_b\left(1 - \frac{\mu_b}{C_b}\right) = C_b \,,
\end{aligned} \tag{201}$$

which are equivalent to the moduli as if there were no fractures. Note that the first and third of equations (201) show that $c^{sat}_{33_{high}} = C_b = c^{sat}_{11_{high}}$, i.e. at high frequencies P-wave velocities for waves propagating parallel and perpendicular to layering are

equal. This effect is caused by the liquid stiffening the otherwise very compliant fractures, and is a well known result for elastic fractured (non-porous) media when $Z_N \to 0$ (Hudson, 1980; Schoenberg and Douma, 1988; Thomsen, 1995).

The shear moduli as $h_c \to 0$ are given by

$$c_{55_{high}} = \frac{1}{\mu_b} + Z_T = c_{55_0} \ , \qquad c_{66_{high}} = \mu_b = c_{55_0} \ , \tag{202}$$

which indicates that these fluid independent moduli are unchanged over the entire frequency range, as expected.

5 Fractured porous media - low and high frequency moduli

5.1 Iso-stress moduli for layered media

In this section we will derive low frequency moduli without referring to the frequency dependent solution, but directly from iso-stress condition in z direction (Norris, 1993). Again, using definitions of P-wave moduli for dry L saturated modulus $L_s = C$ respectively,

$$L = \lambda + 2\mu = K + \frac{4}{3}\mu,\ L_s = C = \lambda_s + 2\mu = K_s + \frac{4}{3}\mu,$$

and the relation between them (Gassmann relation):

$$K_s = K + \alpha^2 M,\ C = L + \alpha^2 M \tag{178}$$

we can rewrite constitutive relations (57) in the following form:

$$\boldsymbol{\sigma} = (\mathbf{L} + \alpha^2 M)\boldsymbol{\varepsilon} - \alpha M \left(\frac{p}{M} + \alpha\varepsilon\right)\mathbf{I} = \mathbf{L}\boldsymbol{\varepsilon} - \alpha p\mathbf{I}, \tag{179}$$

where $\mathbf{L}$ is the stiffness tensor for the dry rock. Note here that shear modulus μ is not affected by fluid, so dry and saturated shear moduli are equal.

Low frequency limit means that pore pressure is constant (there is enough time for pressure to equilibrate throughout the stack) and average increase of fluid in stack is zero

$$p = const,\ \langle\xi\rangle = 0\ .$$

Therefore, by averaging constitutive relations (179) over the stack of layers we get:

$$\begin{aligned} 0 &= \langle\xi\rangle = \langle\alpha\varepsilon\rangle + \left\langle M^{-1}\right\rangle p, \\ \boldsymbol{\sigma} &= \mathbf{L}\boldsymbol{\varepsilon} + \alpha\left\langle M^{-1}\right\rangle^{-1}\langle\alpha\varepsilon\rangle\,\mathbf{I} \end{aligned} \tag{180}$$

Furthermore, as discussed in Chapter 3, in a horizontally stratified medium with $x_3 =$

z being axis of symmetry, the displacements u_1, u_2, u_3 and stresses $\sigma_{13}, \sigma_{23}, \sigma_{33}$ are continuous across the interfaces. Recalling the linear relationship (5) between stain and displacement, we note that variables $(\varepsilon_{11}, \varepsilon_{22}, \varepsilon_{12}, \sigma_{13}, \sigma_{23}, \sigma_{33})$ are constant across the interfaces. Thus we can express a set of "jumping" variables (those which can change on the interface) $(\varepsilon_{33}, \varepsilon_{13}, \varepsilon_{23}, \sigma_{11}, \sigma_{22}, \sigma_{12})$ as a function of "constant" variables $(\varepsilon_{11}, \varepsilon_{22}, \varepsilon_{12}, \sigma_{13}, \sigma_{23}, \sigma_{33})$, then we will average these "jumping" variables. First, we can find ε_{33} from equation (179):

$$\sigma_{33} = c_{31}\varepsilon_{11} + c_{32}\varepsilon_{22} + c_{33}\varepsilon_{33} - \alpha p = \lambda(\varepsilon_{11} + \varepsilon_{22}) + (\lambda + 2\mu)\varepsilon_{33} - \alpha p$$

$$\varepsilon_{33} = \frac{1}{L}\left[\sigma_{33} - \lambda(\varepsilon_{11} + \varepsilon_{22}) + \alpha p\right]$$

Expressing ξ in terms of "constants":

$$\begin{aligned}\xi &= \frac{p}{M} + \alpha(\varepsilon_{11} + \varepsilon_{22}) + \frac{\alpha}{L}\left[\sigma_{33} - \lambda(\varepsilon_{11} + \varepsilon_{22}) + \alpha p\right] \\ &= \alpha(\varepsilon_{11} + \varepsilon_{22})\left(1 - \frac{\lambda}{L}\right) + \frac{\alpha}{L}\sigma_{33} + p\left[\frac{1}{M} - \frac{\alpha^2}{L}\right]\end{aligned}$$

then using identities:

$$1 - \frac{\lambda}{L} = \frac{L - \lambda}{L} = \frac{\lambda + 2\mu - \lambda}{L} = \frac{2\mu}{L}$$

ξ can be rewritten as:

$$\xi = 2\mu\frac{\alpha}{L}(\varepsilon_{11} + \varepsilon_{22}) + \frac{\alpha}{L}\sigma_{33} + \left(\frac{1}{M} - \frac{\alpha^2}{L}\right)p.$$

Averaging through layers and applying the low-frequency condition $\langle\xi\rangle = 0$, we get:

$$0 = \langle\xi\rangle = \left\langle 2\mu\frac{\alpha}{L}\right\rangle(\varepsilon_{11} + \varepsilon_{22}) + \left\langle\frac{\alpha}{L}\right\rangle\sigma_{33} + \left\langle\frac{1}{M} + \frac{\alpha^2}{L}\right\rangle p$$

Expressing p as a function of "constants" we have

$$p = -A(\varepsilon_{11} + \varepsilon_{22}) - B\sigma_{33} \tag{181}$$

where

$$A = \left\langle \frac{1}{M} + \frac{\alpha^2}{L} \right\rangle^{-1} \left\langle 2\mu \frac{\alpha}{L} \right\rangle, \; B = \left\langle \frac{1}{M} + \frac{\alpha^2}{L} \right\rangle^{-1} \left\langle \frac{\alpha}{L} \right\rangle. \tag{182a}$$

Substituting p from (181) into (179) we can obtain the vector of the "jumping" variables as a linear function of the continuous variables.

Focusing our attention on compressional wave only, we can reduce the set of "constant" variables to $(\varepsilon_{11}, \varepsilon_{22}, \sigma_{33})$. First, calculating σ_{11} in terms of $(\varepsilon_{11}, \varepsilon_{22}, \sigma_{33})$ for any isotropic layer, we get

$$\sigma_{11} = (\lambda + 2\mu)\,\varepsilon_{11} + \lambda\varepsilon_{22} + \lambda\varepsilon_{33} - \alpha p = (\lambda + 2\mu)\,\varepsilon_{11} + \lambda\varepsilon_{22} + \lambda\varepsilon_{33} + \alpha A\varepsilon_{11} + \alpha A\varepsilon_{22} + \alpha B\sigma_{33}$$

$$\begin{aligned}
\sigma_{11} = {} & \frac{1}{\lambda + 2\mu} \left[(\lambda + 2\mu)^2 + (\lambda + 2\mu)\,\alpha A - \lambda^2 - \lambda\alpha A \right] \varepsilon_{11} + \\
& + \frac{1}{\lambda + 2\mu} \left[\lambda\,(\lambda + 2\mu) + (\lambda + 2\mu)\,\alpha A - \lambda^2 - \lambda\alpha A \right] \varepsilon_{22} + \\
& + \frac{1}{\lambda + 2\mu} \left[(\lambda + 2\mu)\alpha B + \lambda - \lambda\alpha B \right] \sigma_{33},
\end{aligned}$$

so that:

$$\sigma_{11} = \frac{1}{\lambda + 2\mu} \left[2\mu\,(2\lambda + 2\mu + \alpha A)\,\varepsilon_{11} + 2\mu\,(\lambda + \alpha A)\,\varepsilon_{22} + (\lambda + 2\mu\alpha B)\,\sigma_{33} \right]. \tag{183}$$

In the same way expressions for σ_{22} and ε_{33} can be calculated:

$$\sigma_{22} = \frac{1}{\lambda + 2\mu} \left[2\mu\,(\lambda + \alpha A)\,\varepsilon_{11} + 2\mu\,(2\lambda + 2\mu + \alpha A)\,\varepsilon_{22} + (\lambda + 2\mu\alpha B)\,\sigma_{33} \right], \tag{184}$$

$$\varepsilon_{33} = \frac{1}{L} \left[-(\lambda + \alpha A)\,\varepsilon_{11} - (\lambda + \alpha A)\,\varepsilon_{22} + (1 - \alpha B)\,\sigma_{33} \right] \tag{185}$$

Combining the last three expressions yields

$$\begin{bmatrix} \sigma_{11} \\ \sigma_{22} \\ \varepsilon_{33} \end{bmatrix} = \frac{1}{\lambda + 2\mu} \begin{bmatrix} 2\mu(2\lambda + 2\mu + \alpha A) & 2\mu(\lambda + \alpha A) & \lambda + 2\mu\alpha B \\ 2\mu(\lambda + \alpha A) & 2\mu(2\lambda + 2\mu + \alpha A) & \lambda + 2\mu\alpha B \\ -(\lambda + \alpha A) & -(\lambda + \alpha A) & 1 - \alpha B \end{bmatrix} \begin{bmatrix} \varepsilon_{11} \\ \varepsilon_{22} \\ \sigma_{33} \end{bmatrix}$$

From this expression we will be able to calculate effective elastic moduli. Solving equation (185) for σ_{33}, we can write

$$\sigma_{33} = \frac{\lambda + \alpha A}{1 - \alpha B}\left(\varepsilon_{11} + \varepsilon_{22}\right) + \frac{L}{1 - \alpha B}\varepsilon_{33} = \frac{\lambda + \alpha A}{L}\frac{L}{1 - \alpha B}\left(\varepsilon_{11} + \varepsilon_{22}\right) + \frac{L}{1 - \alpha B}\varepsilon_{33},$$

or

$$\frac{1 - \alpha B}{L}\sigma_{33} = \frac{\lambda + \alpha A}{L}\left(\varepsilon_{11} + \varepsilon_{22}\right) + \varepsilon_{33}.$$

Averaging through all layers whilst keeping in mind that ε_{11}, ε_{22}, and σ_{33} are continuous, we have

$$\left\langle \frac{1 - \alpha B}{L} \right\rangle \sigma_{33} = \left\langle \frac{\lambda + \alpha A}{L} \right\rangle \left(\varepsilon_{11} + \varepsilon_{22}\right) + \left\langle \varepsilon_{33} \right\rangle$$

$$\sigma_{33} = \left\langle \frac{\lambda + \alpha A}{L} \right\rangle \left\langle \frac{1 - \alpha B}{L} \right\rangle^{-1} \left(\varepsilon_{11} + \varepsilon_{22}\right) + \left\langle \frac{1 - \alpha B}{L} \right\rangle^{-1} \left\langle \varepsilon_{33} \right\rangle \tag{186}$$

Equation (186) is our first stress-average strain relation for the layered porous medium. Comparison with the general stiffness matrix for a TI medium yields low frequency equivalent elastic moduli $c_{33_0}^{sat}$ and $c_{13_0}^{sat}$ (with subscript 0 indicating low frequency limit).

$$c_{33_0}^{sat} = \left\langle \frac{1 - \alpha B}{L} \right\rangle^{-1} \tag{187}$$

$$c_{13_0}^{sat} = c_{33_0}^{sat} \left\langle \frac{\lambda + \alpha A}{L} \right\rangle \tag{188}$$

In order to calculate $c_{11_0}^{sat}$, we average (183):

$$\begin{aligned} \left\langle \sigma_{11} \right\rangle &= \left\langle \frac{2\mu\left(2\lambda + 2\mu + \alpha A\right)}{L} \right\rangle \varepsilon_{11} + \left\langle \frac{2\mu\left(\lambda + \alpha A\right)}{L} \right\rangle \varepsilon_{22} + \left\langle \frac{\lambda + 2\mu\alpha B}{L} \right\rangle \sigma_{33} \\ &= \left\langle \frac{2\mu\left(2\lambda + 2\mu + \alpha A\right)}{L} \right\rangle \varepsilon_{11} + \left\langle \frac{\lambda + 2\mu\alpha B}{L} \right\rangle c_{13_0}^{sat}\varepsilon_{11} + \\ &+ \left\langle \frac{2\mu\left(\lambda + \alpha A\right)}{L} \right\rangle \varepsilon_{22} + \left\langle \frac{\lambda + 2\mu\alpha B}{L} \right\rangle c_{13_0}^{sat}\varepsilon_{22} + \left\langle \frac{\lambda + 2\mu\alpha B}{L} \right\rangle c_{33_0}^{sat} \left\langle \varepsilon_{33} \right\rangle \end{aligned} \tag{189}$$

Taking just coefficients connected with ε_{11} in (189), we have:

$$\left\langle \frac{2\mu\left(2\lambda + 2\mu + \alpha A\right)}{L} \right\rangle = \left\langle \frac{2\mu\left(\lambda + \alpha A + L\right)}{L} \right\rangle = \left\langle \frac{2\mu\left(\lambda + \alpha A\right)}{L} \right\rangle + \left\langle 2\mu \right\rangle$$

$$\left\langle \frac{\lambda + 2\mu\alpha B}{L} \right\rangle c_{13_0}^{sat} = c_{13_0}^{sat} \left[\left\langle \frac{\lambda}{L} \right\rangle + \left\langle \frac{2\mu\alpha}{L} \right\rangle B \right] . \tag{190}$$

From equations (182a), the relation between quantities A and B is

$$B = \left\langle \frac{1}{M} + \frac{\alpha^2}{L} \right\rangle^{-1} \left\langle \frac{\alpha}{L} \right\rangle = A \frac{\left\langle \frac{\alpha}{L} \right\rangle}{\left\langle \frac{2\mu\alpha}{L} \right\rangle}, \qquad \left\langle \frac{2\mu\alpha}{L} \right\rangle B = A \left\langle \frac{\alpha}{L} \right\rangle ,$$

which we substitute in equation (190) to get

$$\left\langle \frac{\lambda + 2\mu\alpha B}{L} \right\rangle c_{13_0}^{sat} = c_{13_0}^{sat} \left[\left\langle \frac{\lambda}{L} \right\rangle + \left\langle \frac{\alpha}{L} \right\rangle A \right] = c_{13_0}^{sat} \left\langle \frac{\lambda + \alpha A}{L} \right\rangle = \frac{\left(c_{13_0}^{sat} \right)^2}{c_{33_0}^{sat}} ,$$

and finally

$$c_{11_0}^{sat} = \frac{\left(c_{13_0}^{sat} \right)^2}{c_{33_0}^{sat}} + \left\langle \frac{2\mu \left(\lambda + \alpha A \right)}{L} \right\rangle + \langle 2\mu \rangle \tag{191}$$

Similarly, taking just coefficients connected with ε_{22} in equation (189), we get the remaining stiffness coefficient:

$$c_{12_0}^{sat} = \frac{\left(c_{13_0}^{sat} \right)^2}{c_{33_0}^{sat}} + \left\langle \frac{2\mu \left(\lambda + \alpha A \right)}{L} \right\rangle \tag{192}$$

Equations (187), (188), (191), and (192) give the effective stiffness coefficients which are needed to fully describe compressional wave propagation in the layered medium in the low-frequency limit.

In order to compare the results of this section with the frequency dependent solution (152), we rewrite equation (187) in the form

$$\frac{1}{c_{33_0}^{sat}} = \left\langle \frac{1}{L} \right\rangle - \frac{\left\langle \frac{\alpha}{L} \right\rangle^2}{\left\langle \frac{1}{N} \right\rangle} . \tag{193}$$

Noting that from equation

$$\frac{1}{N} = \frac{C}{ML} = \frac{1}{M} + \frac{\alpha^2}{L} ,$$

for each layer, from identity $ML/NC \equiv 1$, and from relation $L = C - \alpha^2 M$, it can be shown that for a two-layer periodic system, equation (193) yields

$$
\begin{aligned}
\frac{1}{c_{33_0}^{sat}} &= \frac{h_b M_b}{C_b N_b} + \frac{h_c M_c}{C_c N_c} - \frac{\left(\frac{h_b \alpha_b M_b}{N_b C_b} + \frac{h_c \alpha_c M_c}{N_c C_c}\right)^2}{\frac{h_b}{N_b} + \frac{h_c}{N_c}} \\
&= \frac{h_b M_b}{C_b N_b} + \frac{h_c M_c}{C_c N_c} - \frac{\left(\frac{h_b \alpha_b M_b}{N_b C_b}\right)^2 + \left(\frac{h_c \alpha_c M_c}{N_c C_c}\right)^2 + 2 h_b h_c \alpha_b \alpha_c \frac{M_b M_c}{C_b C_c N_b N_c}}{\frac{h_b h_c}{N_b N_c}\left[\frac{N_b}{h_b} + \frac{N_c}{h_c}\right]} \\
&= \frac{h_b}{C_b} \underbrace{\frac{M_b \left(C_b - \alpha_b^2 M_b\right)}{C_b N_b}}_{M_b L_b / C_b N_b \equiv 1} + \frac{h_c}{C_c} \underbrace{\frac{M_c \left(C_c - \alpha_c^2 M_c\right)}{C_c N_c}}_{M_c L_c / C_c N_c \equiv 1} + \frac{\left(\frac{\alpha_b M_b}{C_b} - \frac{\alpha_c M_c}{C_c}\right)^2}{\frac{N_b}{h_b} + \frac{N_c}{h_c}} \\
&= \left\langle \frac{1}{C} \right\rangle + \frac{\left(\frac{\alpha_b M_b}{C_b} - \frac{\alpha_c M_c}{C_c}\right)^2}{\frac{N_b}{h_b} + \frac{N_c}{h_c}} \,,
\end{aligned}
$$

which is precisely the zero frequency limit of equation (152).

Substituting parameter γ (144) into equations (188) and (191) for other the moduli we find:

$$
c_{13_0}^{sat} = c_{33_0}^{sat} \left(1 - 2\langle\gamma\rangle + 2\left\langle\frac{\alpha}{L}\right\rangle \frac{\langle\alpha\gamma\rangle}{\left\langle\frac{1}{N}\right\rangle}\right) \,, \quad c_{11_0}^{sat} = \frac{\left(c_{13_0}^{sat}\right)^2}{c_{33_0}^{sat}} + 4\left(\langle\mu\rangle - \langle\gamma\mu\rangle + \frac{\langle\alpha\gamma\rangle^2}{\left\langle\frac{1}{N}\right\rangle}\right), \tag{194}
$$

where

$$
\left\langle\frac{1}{N}\right\rangle = \left\langle\frac{C}{ML}\right\rangle = \left\langle\frac{1}{M} + \frac{\alpha^2}{L}\right\rangle = \frac{\langle\alpha\rangle}{K_g} + \left(\frac{1}{K_f} - \frac{1}{K_g}\right)\langle\phi\rangle + \left\langle\frac{\alpha^2}{L}\right\rangle \,.
$$

Shear stiffnesses are unaffected by the fluid, they are exactly the same as in elastic media (Backus, 1962):

$$
c_{55_0}^{sat} = c_{55_0}^{dry} = \left\langle\frac{1}{\mu}\right\rangle^{-1} \,, \quad c_{66_0}^{sat} = c_{66_0}^{dry} = \langle\mu\rangle \,. \tag{195}
$$

Substituting γ into equation (44) we get

$$
\alpha_j = 1 - \frac{(1 - \frac{4}{3}\gamma_j) L_j}{K_g} \,,
$$

then

$$
\langle\alpha\rangle = 1 - \frac{\langle L\rangle - \frac{4}{3}\langle\mu\rangle}{K_g} \,, \; \langle\alpha\gamma\rangle = \langle\gamma\rangle - \frac{\langle\mu\rangle - \frac{4}{3}\langle\gamma\mu\rangle}{K_g} \,, \; \left\langle\frac{\alpha}{L}\right\rangle = \left\langle\frac{1}{L}\right\rangle - \frac{1 - \frac{4}{3}\langle\gamma\rangle}{K_g} \,,
$$

and

$$\left\langle \frac{\alpha^2}{L} \right\rangle = \left\langle \frac{1}{L} \right\rangle - 2\frac{1 - \frac{4}{3}\langle\gamma\rangle}{K_g} + \frac{\left\langle \frac{1}{L} \right\rangle - \frac{8}{3}\langle\mu\rangle + \frac{16}{9}\langle\gamma\mu\rangle}{K_g^2} \ .$$

5.2 Iso-stress moduli for fractured media

As with the frequency dependent P-wave modulus, the low-frequency stiffnesses for the fractured medium can be obtained by taking the small thickness ratio limit $h_c \to 0$. Remembering that L_c and μ_c are required to be $\mathcal{O}(h_c)$, we can write

$$\langle\alpha\rangle \to \alpha_b \ , \ \langle\alpha\gamma\rangle \to \alpha_b\gamma_b \ , \ \left\langle \frac{\alpha}{L} \right\rangle \to \frac{\alpha_b}{L_b} + Z_N \ , \ \left\langle \frac{\alpha^2}{L} \right\rangle \to \frac{\alpha_b^2}{L_b} + Z_N \ ,$$

so that

$$\left\langle \frac{1}{N} \right\rangle \to \frac{1}{N_b} + Z_N \ .$$

Equation (193) then gives,

$$\begin{aligned} \frac{1}{c_{33_0}^{sat}} &= \frac{1}{L_b} + Z_N - \frac{\left(\frac{\alpha_b}{L_b} + Z_N\right)^2}{\frac{1}{N_b} + Z_N} = \frac{1}{C_b} + \frac{\alpha_b^2 N_b}{L_b^2} + Z_N - \frac{\left(\frac{\alpha_b}{L_b} + Z_N\right)^2}{\frac{1}{N_b} + Z_N} \\ &= \frac{1}{C_b} + \frac{Z_N\left(\frac{\alpha_b^2 N_b}{L_b^2} + \frac{1}{N_b} - 2\frac{\alpha_b}{L_b}\right)}{\frac{1}{N_b} + Z_N} = \frac{1}{C_b} + \frac{Z_N\left(\frac{\alpha_b N_b}{L_b} - 1\right)^2}{1 + Z_N N_b} \\ &= \frac{1}{C_b}\left[1 + \frac{Z_N(\alpha_b M_b - C_b)^2}{C_b(1 + Z_N N_b)}\right] \ . \end{aligned} \tag{196}$$

It is interesting to compare this result with the low-frequency limit of the frequency dependent solution (159). In this limit, the cotangent function in equation (159) can be replaced by the inverse of its argument, and this equation reduces to

$$\frac{1}{c_{33_0}^{sat}} = \frac{1}{C_b} + \frac{\left(\frac{\alpha_b M_b}{C_b} - 1\right)^2}{N_b + \frac{1}{Z_N}} = \frac{1}{C_b}\left[1 + \frac{Z_N(\alpha_b M_b - C_b)^2}{C_b(1 + Z_N N_b)}\right] \ . \tag{197}$$

which is identical to equation (196), as expected. Equation (197) provides an expression for the P-wave modulus of waves propagating normal to the fractures at low

frequencies, i.e. for frequencies low enough to allow equilibration of the fluid pressure p between fractures and the background during the period of the wave.

Taking into account that $(L_b/N_b)(1+Z_N N_b) \equiv \alpha_b^2 + L_b/M_b + Z_N L_b$, the small thickness ratio limit $h_c \to 0$ in the first and second of equations (194) gives,

$$c_{13_0}^{sat} = c_{33_0}^{sat}\left[1 - 2\gamma_b + 2\alpha_b\gamma_b\frac{N_b}{L_b}\,\frac{\alpha_b + Z_N L_b}{1 + Z_N N_b}\right] , \tag{198}$$
$$c_{11_0}^{sat} = \frac{\left(c_{13_0}^{sat}\right)^2}{c_{33_0}^{sat}} + 4\left[(1-\gamma_b)\mu_b + \frac{\alpha_b^2\gamma_b^2 N_b}{1 + Z_N N_b}\right] .$$

The shear moduli, independent of the fluid, are given from (195) by

$$c_{55_0} = \frac{1}{\mu_b} + Z_T , \quad c_{66_0} = \mu_b . \tag{199}$$

Equations (197), (198) and (199) provide exact explicit analytical expressions for low-frequency elastic moduli of a fractured medium as a function of the properties of the background, fractures, and fluid bulk modulus. Using simple algebra one can show that these equations are exactly equivalent to the equations of the anisotropic Gassmann model for fluid substitution in a porous medium with aligned fractures (Gurevich, 2002). This equivalence demonstrates that the model of wave propagation in fractured media proposed in this work is consistent with the fundamental equations of anisotropic poroelasticity (Gassmann, 1951; Brown and Korringa, 1975), which are exact in the low frequency limit. These equations can be used for fluid substitution in fractured porous rocks. More detailed analysis of the effects of background porosity and fluid properties on the low frequency anisotropy of fractured rocks can be found in Gurevich (2002) and Cardona (2002).

The results for high frequencies can be obtained by taking the limit $\omega \to \infty$ in equation (152), while still assuming ω to be less than ω_B and ω_R. For this reason, the subscript $_{high}$ will be used instead of subscript $_\infty$. Noting that $\lim_{\omega\to\infty} \cot\sqrt{i\omega}B = -i$, taking this limit gives

$$\frac{1}{c^{sat}_{33_{high}}} = \left\langle \frac{1}{C} \right\rangle = \frac{h_b}{C_b} + \frac{h_c}{C_c} \,. \tag{200}$$

This result, that at high frequencies the P-wave elastic modulus is the weighted harmonic average of the saturated moduli of the two media (computed using isotropic Gassmann equations), is to be expected. Indeed, at high frequencies the fluid has no time to move from pores in the background into the medium representing the fractures, or vice versa. No flow between the media means the interfaces can be considered impermeable, and the whole layered continuum can be considered as a stack of elastic layers. The properties of the stack can therefore be determined by Backus averaging the saturated Gassmann moduli C and μ. Equation (200) is consistent with this approach.

As $h_c \to 0$, recall that although L_c is $\mathcal{O}(h_c)$, the Gassmann modulus C_c remains finite (154). Thus, the moduli obtained as $h_c \to 0$ are:

$$\begin{aligned}
\frac{1}{c^{sat}_{33_{high}}} &= \left\langle \frac{1}{C} \right\rangle \to \frac{1}{C_b} \,, \\
c^{sat}_{13_{high}} &= c^{sat}_{33_{high}} \left(1 - 2\left\langle \frac{\mu}{C} \right\rangle\right) \to c^{sat}_{33_{high}} \left(1 - 2\frac{\mu_b}{C_b}\right) \,, \\
c^{sat}_{11_{high}} &= \frac{\left(c^{sat}_{13_{high}}\right)^2}{c^{sat}_{33_{high}}} + 4\left(\langle\mu\rangle - \left\langle \frac{\mu^2}{C} \right\rangle\right) \to \frac{\left(c^{sat}_{13_{high}}\right)^2}{c^{sat}_{33_{high}}} + 4\mu_b\left(1 - \frac{\mu_b}{C_b}\right) = C_b \,,
\end{aligned} \tag{201}$$

which are equivalent to the moduli as if there were no fractures. Note that the first and third of equations (201) show that $c^{sat}_{33_{high}} = C_b = c^{sat}_{11_{high}}$, i.e. at high frequencies P-wave velocities for waves propagating parallel and perpendicular to layering are

equal. This effect is caused by the liquid stiffening the otherwise very compliant fractures, and is a well known result for elastic fractured (non-porous) media when $Z_N \to 0$ (Hudson, 1980; Schoenberg and Douma, 1988; Thomsen, 1995).

The shear moduli as $h_c \to 0$ are given by

$$c_{55_{high}} = \frac{1}{\mu_b} + Z_T = c_{55_0} \ , \qquad c_{66_{high}} = \mu_b = c_{55_0} \ , \tag{202}$$

which indicates that these fluid independent moduli are unchanged over the entire frequency range, as expected.

6 Fractured porous media - numerical modeling

6.1 Methodology

In this chapter, the dispersion and the attenuation curves given by equation (174) with respect to the normalized frequency Ω' (173) are compared with a numerical solution for porous media with fractures modelled as high porosity layers of small but finite thickness. The numerical solution is obtained using independent reflectivity method for layered porous media, utilizing OASES (Ocean Acoustics and Seismic Exploration Synthesis) software developed at MIT (Schmidt and Tango, 1986). OASES is a general purpose computer code for modelling seismo-acoustic propagation in horizontally stratified waveguides using wavenumber integration in combination with the Direct Global Matrix solution technique. The software package is advanced implementation of 1.5D elastic reflectivity algorithm that can compute plane wave reflection-transmition coefficients taking into account all the effects occurring in horizontally layered media. Also, OASES can handle fluid and anisotropic media and frequency dependent attenuation, and has been extended to handle poroelastic layers (taking into account Biot's slow wave) with proper boundary conditions.

Figure 18 shows model with horizontal lines showing the position of thin soft layers representing fractures. Models like this are created using a MATLAB code for a given set of properties of the background and fracture materials, fractures thickness and fracture spacing and then utilized in OASES. Using OASES code we obtain plane wave complex transmission coefficients for this layered system (Figure 19). These coefficients can then be used to calculate effective complex velocity v and attenuation Q^{-1} in an equivalent homogeneous medium. The normal incidence transmission coefficient T for such an equivalent medium can be written as

$$T = \exp(-\alpha z)\exp(ikz). \tag{203}$$

where z is the overall thickness of the layered system, α is the effective coefficient of attenuation and $k = \omega/v$ is the wavenumber of the transmitted wave. Taking absolute values of left and right hand sides of equation (203) yields

$$|T| = \exp(-\alpha z) \tag{204}$$

or

$$\alpha = -\frac{\ln|T|}{z}$$

Attenuation coefficient α is related to inverse quality factor Q^{-1} by (White, 1983)

$$Q^{-1} = \frac{2\alpha v}{\omega} = -\frac{2v}{z\omega}\ln|T| \ . \tag{205}$$

Equation (205) can be used to compute inverse quality factor from absolute values of transmission coefficients obtained from OASES. Phase velocity can be obtained from the phase of the transmission coefficient. For this the phase (right pane of Figure 19) has to be unwrapped. This can be done in MATLAB using a standard *unwrap* function.

6.2 Periodic system of fractures

Figure 20 shows results for the periodic distribution of fractures. We observe excellent agreement between numerical experiment (dashed line) and theoretical solution (solid line). On the numerical curve at high frequencies we observe stopping and passing bands for frequencies satisfying resonance conditions

$$n\frac{\lambda}{2} = H \ ,$$

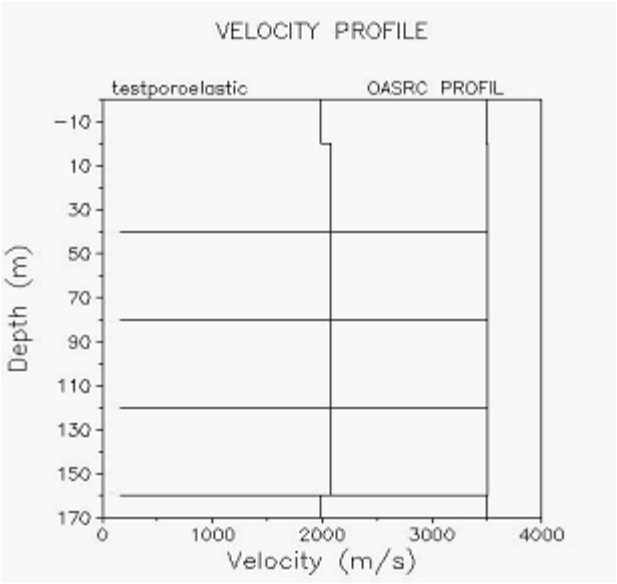

Fig. 18. *Simple model showing periodic fractures. P-wave velocity is represented on the right with S-wave velocity shown on the left.*

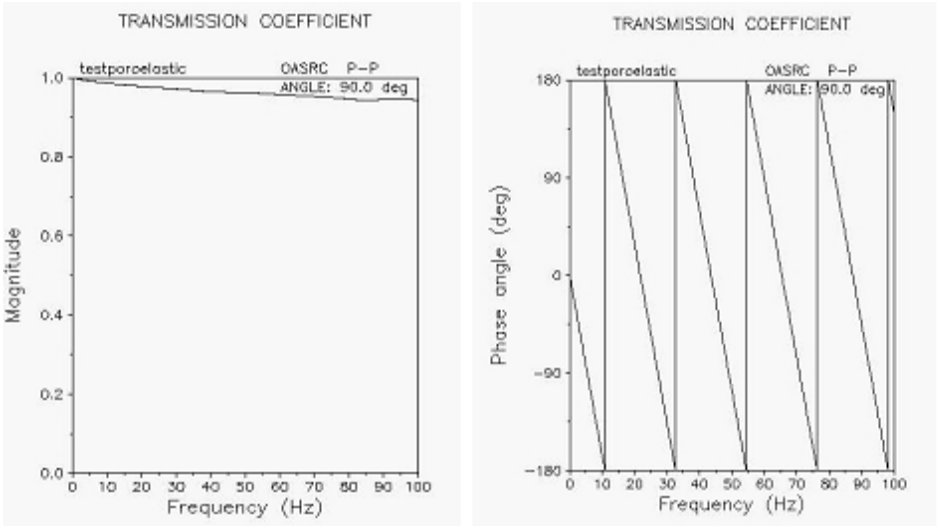

Fig. 19. *Resultant transmission coefficients and phase relationships for model shown in Figure 18.*

where λ is the wavelength, n is an integer and H is spatial period. Such an effect is not observed in our theoretical curve (solid line) because we have assumed low frequency range ($\lambda < 2H/n$) for the effective medium theory.

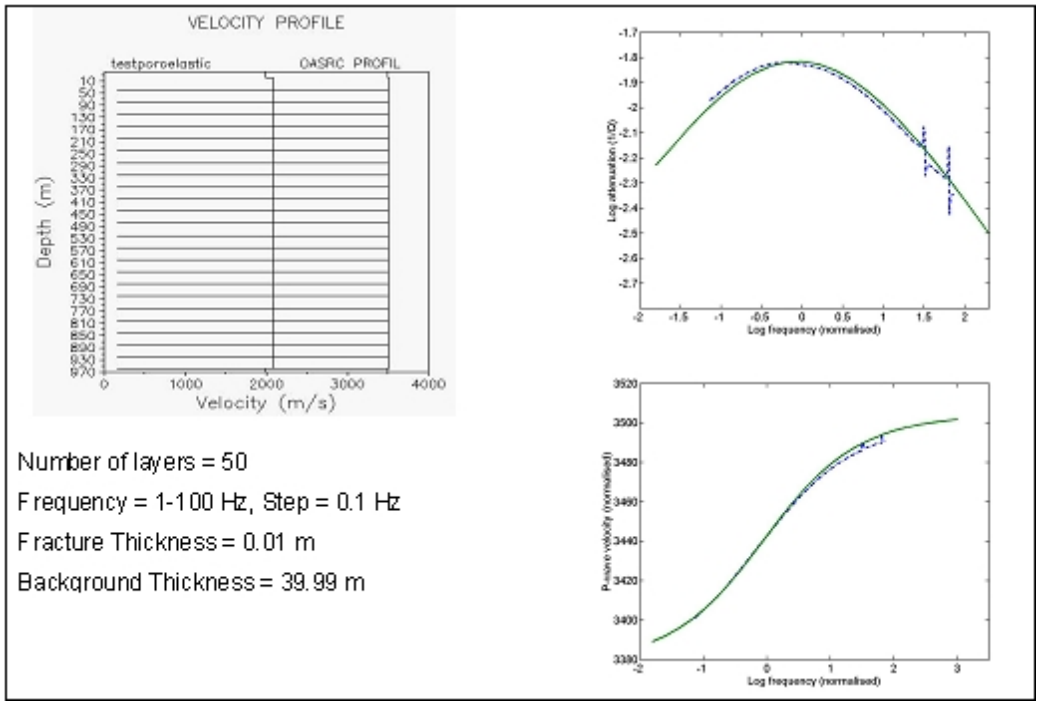

Fig. 20. *Comparison of numerical (dashed lines) and theoretical (solid lines) results for the periodic distribution of fractures.*

6.3 Random system of fractures

Having validated results for periodic system of fractures, the models were then expanded to incorporate:

a) Model A - Random fracture distribution with constant fracture thickness

b) Model B - Random fracture distribution with random thickness

These numerical results were then compared with the theoretical solution which as before represents periodic distribution of fractures. For the Model A little variation is seen between the theoretical and numerical results, with similar attenuation and P-wave velocity curves obtained (Figure 21). However, significant variation between theoretical and numerical results is observed when fracture thickness was varied in conjunction with fracture distribution (Figure 22). From these results it can be deduced that fracture distribution, as a stand alone variable, will not greatly influence

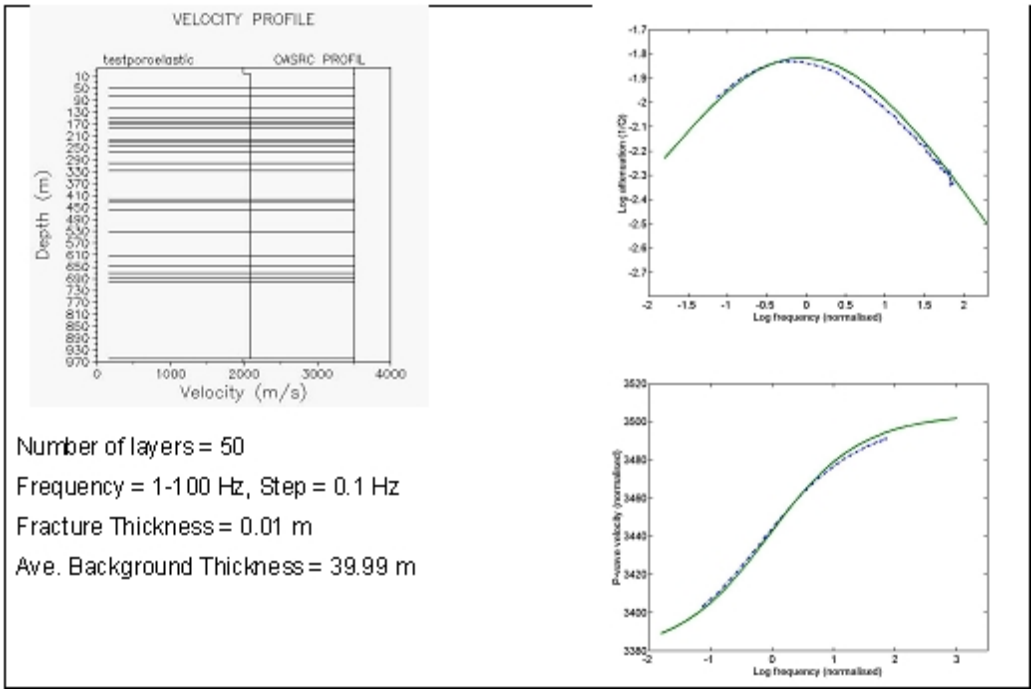

Fig. 21. *Model A - Random fracture distribution with constant fracture thickness; Comparison of numerical (dashed lines) and theoretical (solid lines) results.*

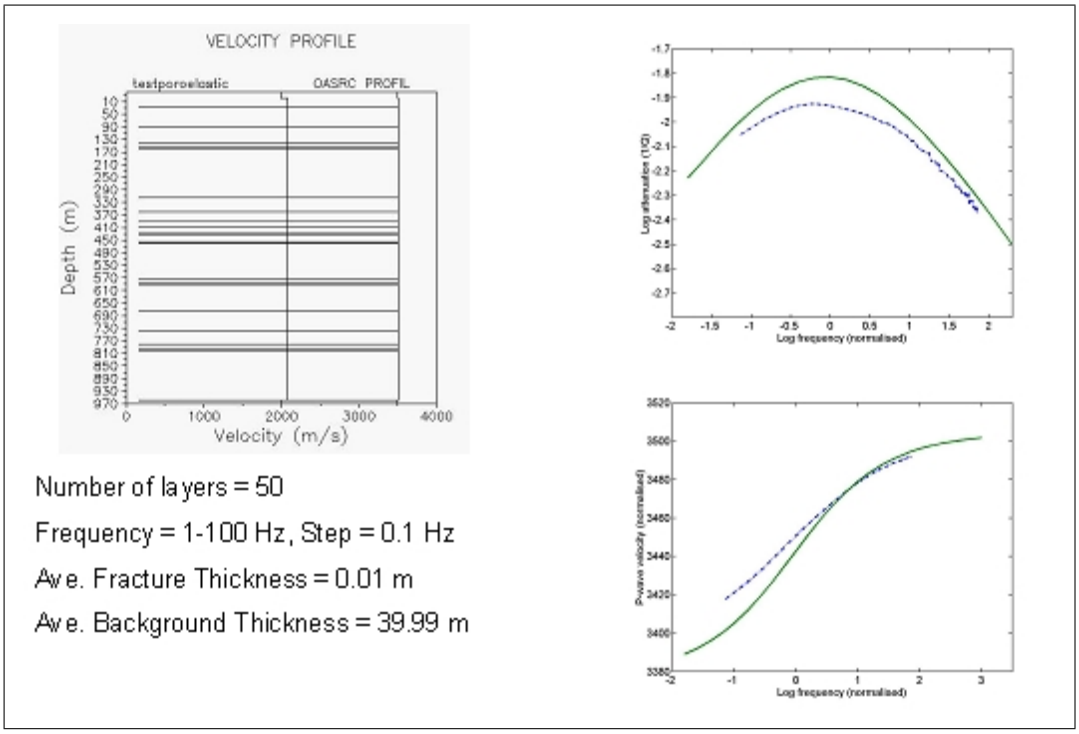

Fig. 22. *Model B - Random fracture distribution with random fracture thickness; Comparison of numerical (dashed lines) and theoretical (solid lines) results.*

attenuation or P-wave velocity in a saturated fractured medium.

Model A was created with random fracture distribution (average background thickness of 39.99 m) and constant fracture thickness of 0.01 m. The random distribution of fractures was created by generating uniformly distributed random numbers in the interval (0, H) and using them as coordinates of fracture locations. Results obtained from Model A were also found to agree very well with the theoretical results for periodic fracturing.

Model B was created using random fracture location combined with random (uniformly distributed) fracture thickness (average background and fracture thickness of 39.99 m and 0.01 m respectively). The simulation involving Model B resulted in velocity and attenuation curves that markedly varied from the theoretical results. The attenuation and P-wave velocity is influenced by fracture thickness not distribution.

6.4 Possibilities of experimental validation of the model

Practical application of the model of frequency dependent anisotropy, attenuation and dispersion developed in this work requires validation by comparison with experimental data. This however is not an easy task. The principal difficulty lies in the fact that each of the seismic and acoustic technologies - reflection seismology, sonic logging, ultrasonic measurements - cover a relatively narrow frequency band. Thus these technologies are not adequate for measuring the frequency dependencies of attenuation or velocity, which require measurements in a wide frequency range, see figures 2-8. Interpretation of narrow band attenuation measurements is ambiguous, as attenuation may be caused by other mechanisms, such as scattering.

One promising possibility is comparison with repeated seismic measurements known as time-lapse seismic. If for example a gas reservoir is subjected to water injection, water will replace gas. This makes possible identification of changes in seismic veloc-

ity and attenuation due to fluid effect (as well as pressure). However, for a fractured medium studied in this work, multi-azimuth and/or multicomponent data will probably be required to characterise anisotropy and identify fracture effects. Multi-azimuth is almost never recorded offshore (and certainly not in time-lapse mode due to the current marine acquisition technology). Time lapse multicomponent data (so called 4D-9C) is also rare. Multicomponent and multi-azimuth data are sometimes recorded on land, but land time lapse is rare because of repeatability problems and economic factors.

One specific phenomenon which opens some opportunity for controlled comparison is shear wave splitting. If a medium is, say, fractured, shear waves propagating parallel or at an angle to fractures will split into two waves: one polarised parallel to fractures and another polarised in the plane perpendicular to fractures. Shear wave splitting is an excellent indicator of seismic anisotropy. For vertical and sub-vertical fractures shear wave splitting can be measured by multicomponent seismic at small offsets and single azimuth. If fractures are rotationally invariant and vertical, shear wave splitting must be independent of the fluid fill.

Recently, Guest et al. (1998) and van der Kolk et al. (2001) presented experimental evidence demonstrating that in the Natih field in Oman shear waves are sensitive to fluid type in fractured media. Sayers (2002) suggested that if the fractures are not perfectly vertical, the shear-wave splitting also varies with the normal compliance of the fractures. If the fracture contains a fluid, the normal compliance of the fracture decreases with increasing fluid bulk modulus and is sensitive to the interconnectivity of the fracture network and the permeability of the background medium and to whether the fracture is fully or partially saturated. This results in a decrease in shear-wave splitting and an increase in shear-wave velocity with increasing fluid bulk modulus. The expressions for the limiting low and high-frequency moduli derived in

this work suggest that the magnitude of this effect will be the largest, if fractures are fully saturated and frequency is in the high-frequency range. Given that background permeability in Natih is low, probably less than 1 milidarcy (as background porosity is only a few per cent), seismic waves are indeed likely to fall into the high frequency range. This suggests that Natih observations are consistent with the model developed in this work. More detailed comparison of our results with Natih observations require knowledge of all reservoir parameters (such as permeability, fracture spacing and distribution) which have not been published.

Generally speaking, comparison of our model with experimental data will require well controlled condition. The only experiments that can satisfy this condition are laboratory experiments. Such experiments are planned for the near future.

7 Conclusions

Fractures in the porous rock can be modelled as very thin and highly porous layers in a porous background. When both pores and fractures are dry, such material is equivalent to a transversely isotropic dry elastic porous material with linear-slip interfaces. When saturated with a liquid this material exhibits significant attenuation and velocity dispersion due to wave induced fluid flow between pores and fractures. At low frequencies the material properties are equal to those obtained by anisotropic Gassmann theory applied to a porous material with linear-slip interfaces (Gassmann, 1951; Brown and Korringa, 1975). At high frequencies the results are equivalent to those for fractures with vanishingly small normal slip in a solid (non-porous) background (Schoenberg and Douma, 1988). The characteristic frequency of the attenuation and dispersion depends on the background permeability, fluid viscosity, as well as fracture density and spacing.

The wave induced fluid flow between pores and fractures considered in this paper has exactly the same physical nature as so-called squirt flow, which is widely believed to by a major cause of seismic attenuation (Mavko and Nur, 1975; O'Connell and Budiansky, 1977; Jones, 1986). Hence, the present model can be viewed as a new model of squirt-flow attenuation, consistent with Biot's theory of poroelasticity. This model can be extended to multiple fracture sets using the method of added compliances (Sayers and Kachanov, 1995).

The present work is limited to the derivation of the P-wave modulus along the symmetry axis. Derivation of other moduli of the periodically fractured medium would require the solution for the compressional and shear waves of arbitrary incidence in a layered poroelastic medium. This will be done in separate study.

The theoretical results of this work are also limited by the assumption of periodic distribution of fractures. In reality fractures may be distributed in a random fashion. Sensitivity of our results to the violation of the periodicity assumption was examined numerically using reflectivity modelling for layered poroelastic media. Numerical experiments for a random distribution of fractures of the same thickness still show surprisingly good agreement with theoretical results obtained for periodic fractures. However this agreement may break down if fracture properties are allowed to vary from fracture to fracture.

The results of this thesis show how to compute frequency dependences of attenuation and velocity caused by wave induced fluid flow between pores and fractures. These results can be used to obtain important parameters of fractured reservoirs, such as permeability and fracture weakness, from attenuation measurements. The major requirement for the success of such an approach is that measurements must be made in over a relatively broad frequency range.

References

Aguilera, R., 1998. Geologic aspects of naturally fractured reservoirs. The Leading Edge 17, 1667–1670.

Aki, K., Richards, P. G., 1980. Quantitative Seismology: Theory and Methods. W. H. Freeman and Co., San Francisco.

Backus, A. E., 1962. Long-wave elastic anisotropy produced by horizontal layering. J. Geophys. Res. 67, 4427–4460.

Bakulin, A., Grechka, V., Tsvankin, I., 2000. Estimation of fracture parameters from reflection seismic data – Part I: HTI model due to a single fracture set. Geophysics 65, 1788–1802.

Biot, M. A., 1956a. Theory of propagation of elastic waves in a fluid-saturated porous solid. I. Low-frequency range. J. Acoust. Soc. Amer. 28, 168–178.

Biot, M. A., 1956b. Theory of propagation of elastic waves in a fluid-saturated porous solid. II. Higher frequency range. J. Acoust. Soc. Amer. 28, 179–191.

Biot, M. A., 1956a. Theory of propagation of elastic waves in a fluid-saturated porous solid. I. Low-frequency range. J. Acoust. Soc. Amer. 28, 168–178.

Biot, M. A., 1956b. Theory of propagation of elastic waves in a fluid-saturated porous solid. II. Higher frequency range. J. Acoust. Soc. Amer. 28, 179–191.

Biot, M. A., 1962. Mechanics of deformation and acoustic propagation in porous media. J. Appl. Phys. 33, 1482–1498.

Biot, M. A., Willis, D. G., 1957. The elastic coefficients of the theory of consolidation. J. Appl. Mech. 24, 594–601.

Bourbié, T., Coussy, O., Zinszner, B., 1987. Acoustics of Porous Media. Technip, Paris.

Brekhovskikh, L. M., 1981. Waves in Layered Media. Academic Press.

Brillouin, L., 1963. Wave Propagation in Periodic Structures. McGraw-Hill Book Co. (Div. of McGraw-Hill, Inc.).

Brown, R. J. S., Korringa, J., 1975. On the dependence of the elastic properties of a porous rock on the compressibility of the pore fluid. Geophysics 40, 608–616.

Cardona, R., 2002. Two theories for fluid substitution in porous rocks with aligned cracks. Submitted to Journal of Applied Geophysics .

Crampin, S., 1984. Effective anisotropic elastic constants for wave propagation through cracked solids. Geophys. J. Roy. Astr. Soc. 76, 135–145.

Deresiewicz, H., Skalak, R., 1963. On uniqueness in dynamic poroelasicity. Bull. Seismol. Soc. Amer. 53, 783–788.

Ewing, W. M., 1957. Elastic Waves in Layered Media. McGraw Hill.

Frenkel, J., 1944. On the theory of seismic and seismoelectric phenomena in moist soil. J. Phys. 8, 230–241.

Gassmann, F., 1951. Über die elastizität poröser medien. Viertel. Naturforsch. Ges. Zürich 96, 1–23.

Gelinsky, S., Shapiro, S., Müller, T., Gurevich, B., 1998. Dynamic poroelasticity of thinly layered structures. Internat. J. Solids Structures. 35, 4739–4752.

Guest, S., van der Kolk, C., Peters, H., 1998. The effect of fracture filling liquids on shear-wave propagation. SEG Expanded Abstracts , 948–951.

Gurevich, B., 2002. Elastic properties of saturated porous rocks with aligned fractures. Submitted to Journal of Applied Geophysics .

Gurevich, B., Lopatnikov, S. L., 1995. Velocity and attenuation of elastic waves in finely layered porous rocks. Geophys. J. Internat. 121, 933–947.

Gurevich, B., Schoenberg, M., 1999. Interface conditions for biot's equations of poroelasticity. J. Acoust. Soc. Amer. 105, 2585–2589.

Hsu, C., Schoenberg, M., 1993a. Elastic waves through a simulated fractured medium.

Geophysics 58, 964–977.

Hsu, C.-J., Schoenberg, M., 1993b. Elastic waves through a simulated fractured medium. Geophysics 58, 964–977.

Hudson, J. A., 1980. Overall properties of a cracked solid. Math. Proc. Camb. Phil. Soc. 88, 371–384.

Hudson, J. A., 1981. Wave speeds and attenuation of elastic waves in material containing cracks. Geophys. J. Roy. Astr. Soc. 64, 133–150.

Jones, T., 1986. Pore fluids and frequency dependent wave propagation in rocks. Geophysics 51, 1939–1953.

Kosten, C. W., Zwikker, C., 1941. Extended theory of the absorbtion of sound by compressible wall-coverings. Physica 8, 968–978.

Krief, M., Garat, J., Stellingwerff, J., Ventre, J., 1990. A petrophysical interpretation using the velocities of P and S waves (Full-Wave Sonic). The Log Analyst 5, 355–369.

Lancaster, P., 1969. Theory of Matrices. Academic Press, New York - London.

Landau, L., Lifshitz, E., 1976. Mechanics. Permagon.

Landau, L., Lifshitz, E., 1986. Theory of Elasticity. Permagon.

Landau, L., Lifshitz, E., 1987. Fluid Mechanics. Permagon.

Mavko, G., Mukerji, T., Dvorkin, J., 1998. The Rock Physics Handbook: Tools for Seismic Analysis in Porous Media. Cambridge University Press.

Mavko, G., Nur, A., 1975. Melt squirt in the aesthenosphere. J. Geophys. Res. 80, 1444–1448.

Murphy, W. F. I., Winkler, K. W., Kleinberg, R. L., 1986. Acoustic relaxation in sedimentary rocks: Dependence on grain contacts and fluid saturation. Geophysics 51, 757–766.

Nelson, R. A., 2001. Geologic analysis of naturally fractured reservoirs. Gulf Professional Publishing, Boston.

Nishizawa, O., 1982. Seismic velocity anisotropy in a medium containing oriented cracks – Transversely isotropic case. Journal of the Physics of the Earth 30, 435–446.

Norris, A. N., 1993. Low-frequency dispersion and attenuation in partially saturated rocks. J. Acoust. Soc. Amer. 94, 359–370.

O'Connell, R. J., Budiansky, B., 1977. Viscoelastic properties of fluid-saturated cracked solids. J. Geophys. Res. 82, 5719–5740.

Pride, S. R., Gangi, A. F., Morgan, F. D., 1992. Deriving the equations of motion for porous isotropic media. J. Acoust. Soc. Amer. 92, 3278–3290.

Rytov, S. M., 1956. Acoustical properties of a thinly laminated medium. Sov. Phys. Acoust. 2, 68–80.

Sayers, C. M., 1990. Stress-induced fluid flow anisotropy in fractured rock. Transport in Porous Media 5, 287–297.

Sayers, C. M., 2002. Fluid-dependent shear-wave splitting in fractured media. Geophysical Prospecting 50, 393–401.

Sayers, C. M., Kachanov, M., 1991. A simple technique for finding effective elastic constants of cracked solids for arbitrary crack orientation statistics. Int. J. Solids and Structures 27, 671–680.

Sayers, C. M., Kachanov, M., 1995. Microcrack-induced elastic wave anisotropy of brittle rocks. Journal of Geophysical Research B 100, 4149–4156.

Schmidt, H., Tango, G., 1986. Efficient global matrix approach to the computation of synthetic seismograms. Geophys. J. R. Astr. Soc. 84, 331–359.

Schoenberg, M., 1980. Elastic wave behavior across linear slip interfaces. J. Acoust. Soc. Amer. 68, 1516–1521.

Schoenberg, M., Douma, J., 1988. Elastic-wave propagation in media with parallel fractures and aligned cracks. Geophys. Prosp. 36, 571–590.

Schoenberg, M., Sayers, C. M., 1995. Seismic anisotropy of fractured rock. Geophysics

60, 204–211.

Shapiro, S. A., Müller, T., 1999. Seismic signatures of permeability in heterogeneous porous media. Geophysics 64, 99–103.

Thomsen, L., 1995. Elastic anisotropy due to aligned cracks in porous rock. Geophysical Prospecting 43, 805–829.

van der Kolk, C., Guest, W. S., Potters, J. H. H. M., 2001. The 3d shear experiment over the natih field in oman: the effect of fracture-filling fluids on shear propagation. Geophysical Prospecting 49, 179–197.

White, J. E., 1983. Underground Sound: Application of Seismic Waves. Elsevier, Amsterdam.

White, J. E., Mikhaylova, N. G., Lyakhovitsky, F. M., 1975. Low-frequency seismic waves in fluid saturated layered rocks. Izvestija Academy of Sciences USSR, Phys. Solid Earth 11 (10), 654–659.